OPTIMIZATION APPROACHES FOR OPTIMAL POWER FLOW PROBLEMS IN RENEWABLE ENERGY GRIDS

by

ABDULLAH MOHAMMED A ALZAHRANI

A dissertation submitted in partial fulfillment of the
requirements for the degree of

DOCTOR OF PHILOSOPHY IN ELECTRICAL AND COMPUTER ENGINEERING

2021

Oakland University
Rochester, Michigan

Doctoral Advisory Committee:

Mohamed A. Zohdy, Ph.D., Chair
Shadi Alawneh, Ph.D.
Ryan Monroe, Ph.D.
Suzan ElSayed, Ph.D.

© Copyright by Abdullah Mohammed A Alzahrani, 2021
All rights reserved

This dissertation is dedicated to my dear father, who has been nicely my supporter until my research was fully finished, and my beloved mother who, for months past, has encouraged me attentively with her fullest and truest attention to accomplish my work with truthful self-confidence.

This dissertation is also dedicated to my wife who encouraged me to pursue my dreams and finish my dissertation.

ACKNOWLEDGMENTS

I would like to give my most sincere gratitude to **Prof. Mohamed A. Zohdy** for his expertise, understanding, patience, and conscientious guidance during my PhD studies. Thank you very much for offering me the chance to study at Oakland University (OU), encouraging my research interests and helping me to develop. I appreciate your vast knowledge and skill and your advice has been invaluable in helping me complete my project in a very timely manner.

A very special thanks goes out to my dissertation committee, **Dr. Shadi Alawneh**, **Dr. Ryan Monroe**, and **Dr. Suzan ElSayed**, for giving me precious advice in my research. Your guidance has been extremely valuable to me and will continue to be helpful in my future career and life. I sincerely appreciate your efforts in sharing your knowledge and experience during the research of my dissertation.

I would also like to thank my family for the support they provided me throughout my entire life, and during my dissertation in particular. Many thanks to my friends for their kind help during my doctoral studies as well. Thanks to all of you for bringing me a productive studying atmosphere and assisting me through those extremely tough days.

I would like to thank all the professors and staff members from the Dept of Electrical and Computer Engineering at OU for their extended cooperation and guidance. I also take this opportunity to give thanks to all others who have given me support for the dissertation or in other aspects of my studies at OU.

Abdullah Mohammed A Alzahrani

ABSTRACT

OPTIMIZATION APPROACHES FOR OPTIMAL POWER FLOW PROBLEMS IN RENEWABLE ENERGY GRIDS

by

ABDULLAH M. ALZAHRANI

Adviser: Mohamed A. Zohdy, Ph.D.

In recent years, the global energy crisis confronting humanity is attributable to a deficiency in classical energy sources whereas the energy demands are widespread growth. In overcoming this crisis, increasing the efficiency of energy and sustainability are becoming significantly crucial. Therefore, the integration of various renewable energy resources into the traditional electrical grid is quite a challenging issue due to their intermittent nature. In this dissertation, the main focus is on the operational stage optimization problem considering the optimal power flow (OPF) problem to economically meet time-varying consumer demands. This brings a new level of complexity to the OPF problem that needs to be addressed by new and more performant optimization algorithms. One promising area of research that will be followed in this work is the use of heuristic optimization algorithms. These have been used both alone, or in hybrid combinations of two optimization algorithms to compensate for the weaknesses of each.

Due to nonlinearity introduced by alternating current power flow equations, this research focuses on improving the non-linear of the OPF problem for an electrical power grid that includes different energy sources along with thermal plants as energy generators. This dissertation illustrates how to improve the numerical stability of the proposed optimization approach by considering different variables to

avoid ill-conditioned numerical operations. The proposed optimization approach, on the other hand, is able to deal with non-convex problems with multiple local optima, and also it is able to deal with the additional complexity of the hybrid power grid.

This dissertation aimed at improving the use of stand-alone and hybrid AC/DC microgrid systems by minimizing some issues, e.g., global warming emissions and the increasing cost of power systems and losses during the entire time horizon. In this work, some assumptions have been made by considering line constraints on the network to theoretically prove that the performance of the polynomial optimization problem relaxation can satisfy the original power flow equations.

Finally, the performance of the proposed algorithm has been examined on different electrical power networks with various power system sizes, such as IEEE 5, 14, and 30 bus. The outcomes of the experiments proved the adaptability of the algorithm when considering large-scale electrical power networks. In addition, this proposed algorithm has been compared with some exiting optimization algorithms given in the literature for similar power systems, where it shows the effectiveness of this proposed method. This achievement will strengthen the use of this convexification approach in its applications on large-scale systems to reduce energy expenses and network system losses.

TABLE OF CONTENTS

ACKNOWLEDGMENTS iv

ABSTRACT v

LIST OF TABLES xiii

LIST OF FIGURES xvi

LIST OF ABBREVIATIONS xix

CHAPTER ONE
INTRODUCTION 1

1.1. Motivation 4

1.2. Dissertation Outline 5

CHAPTER TWO
BACKGROUND AND STATE-OF-THE-ART 8

2.1. Demand Response 8

2.2. OPF Problem Formulations 14

2.3. Classical Optimization Methods 17

2.4. Heuristic Optimization Methods 18

2.5. Hybrid Optimization Methods and the OPF 22

2.6. Discussion 23

CHAPTER THREE
OPTIMAL POWER FLOW PROBLEM FORMULATION 24

3.1. Notation 24

3.2. Mathematical Model and Problem Formulation 25

3.2.1. The Optimal Power Flow in the Absence of Energy Storage 25

3.2.2. The Optimal Power Flow with Energy Storage 28

CHAPTER FOUR
POLYNOMIAL OPTIMIZATION PROBLEM 31

4.1. Introduction 31

4.2. Application 31

4.3. The Polynomial Optimization Problem (POP) 33

4.3.1. Solution Report and Analysis 34

4.3.2. Result Summary 35

4.4. The Proposed Research Problem 35

4.5. Model Description and Problem Formulation 37

4.6. Numerical Experiments and Discussions 44

4.7. Conclusion 49

4.8. Future Work 49

CHAPTER FIVE
AN OVERVIEW OF OPTIMIZATION APPROACHES FOR OPERATION OF HYBRID DISTRIBUTED ENERGY SYSTEMS WITH PHOTOVOLTAIC AND DIESEL TURBINE GENERATOR 53

5.1. Introduction 53

5.2. Optimization Formulation Framework for Hybrid Power Systems 58

5.2.1. The Standard Formulation for the Optimization 58

5.3. Types and Approaches of Optimization in Power System Operations 71

5.3.1. Types of Optimization 71

5.3.2. Optimization Approaches 74

5.4. Conclusion 83

CHAPTER SIX
OPTIMAL POWER FLOW WITH ENERGY STORAGE 85

6.1. Notation 85

6.2. The Optimal Power Flow with Energy Storage 85

6.2.1. Optimal Power Flow with Line Constraints 89

6.2.2. Modeling the Energy Storage 91

CHAPTER SEVEN
DEMONSTRATION AND ASSESSMENT OF THE PROPOSED OPF APPROACH INCLUDING ENERGY STORAGE 93

7.1. CASE STUDIES 93

7.1.1. The DC Microgrid Power System Test Case 93

7.1.2. The Parameters and Results of the First Case Scenario-I 93

7.1.3. Demonstration of the First Case Scenario-I 95

7.1.4. The Load Data of the First Case Scenario-I 99

7.1.5. The Power Generation Data of the First Case Scenario-I 100

7.1.6. The State-of-Charge (SOC) and Battery Rate (r) of Case Scenario-I 101

7.1.7. The Voltages Profile of the First Case Scenario-I 103

7.1.8. The Parameters and Results of the Second Case Scenario-II 105

7.1.9. Demonstration of the Second Case Scenario-II 107

7.1.10. The Load Data of the Second Case Scenario-II 110

7.1.11. The Power Generation Data of the Second Case Scenario-II 111

7.1.12. The State-of-Charge (SOC) and Battery Rate (r) for Case Scenario-II 112

7.1.13. The Voltages Profile of the Second Case Scenario-II 115

7.1.14. Analysis of Results 117

CHAPTER EIGHT
HYBRID AC-DC POWER GRIDS 119

8.1. Introduction: 119

8.2. System Model and the Proposed Hybrid AC/DC OPF Formulation 122

8.2.1. The Model of Hybrid AC-DC Power Grids 123

8.2.2. The Model of the Voltage Source Converter (VSC) 124

8.2.3. Objective Function 126

8.2.4. Constraints 127

8.3. Performance Evaluation 133

8.3.1. Hybrid AC/DC Power Grid of IEEE 5 Bus Case Study 134

8.3.2. Hybrid AC/DC Power Grid of IEEE 14 Bus Case Study 136

8.3.3. Hybrid AC/DC Power Grid of IEEE 30 Bus Case Study 138

8.4. Analysis of Simulation Results 140

CHAPTER NINE
CONCLUSION AND FUTURE WORK 144

9.1. Conclusions 144

9.2. Future Work 145

9.2.1. Other Possible Topics for Future Research 146

APPENDICES 150

A. APPENDIX

Power Load Data of the First Scenario 151

B. APPENDIX

Power Load Data of the Second Scenario 155

C. APPENDIX

Power Load Data for the IEEE 5 Bus Power System 159

D. APPENDIX
Power Load Data for the IEEE 14 Bus Power System 162

E. APPENDIX
Power Load Data for the IEEE 30 Bus Power System 169

REFERENCES 172

Publications 190

LIST OF TABLES

Table 2.1	This table depicts the demand response advantages.	13
Table 4.1	This table depicts the results of the IEEE 6 bus power system.	34
Table 4.2	The objective values obtained from the Matlab-SparsePOP programming solver.	35
Table 5.1	A synopsis of the cost objective functions and their equivalent formulation.	60
Table 5.2	A synopsis of the reliability objective functions and their equivalent formulation.	62
Table 5.3	A synopsis of the advantages and disadvantages of deterministic and stochastic optimization methods.	81
Table 7.1	The lower and upper bounds of the constraint parameters.	94
Table 7.2	The power capacity bounds of the constraint parameters.	95
Table 7.3	The result of the first case scenario-I.	98
Table 7.4	The lower and upper bounds of the constraint parameters.	106
Table 7.5	The power capacity bounds of the constraint parameters.	107
Table 7.6	The result of the second case scenario-II.	110
Table 8.1	The result of the hybrid AC/DC power grid of the IEEE 5 bus.	135
Table 8.2	The result of the hybrid AC/DC power grid of the IEEE 14 bus.	138
Table 8.3	The result of the hybrid AC/DC power grid of the IEEE 30 bus.	140

Table 8.4	The result of the IEEE 30 test system including the DC converters.	142
Table 8.5	The result of the IEEE 30 test system including the DC converters rated at 100 MVA.	143
Table 8.6	The result of the IEEE 30 test system including the DC converters rated at 100 MVA.	143
Table A.1	The power load data of the first case scenario-I.	151
Table A.2	The power generation data of the first case scenario-I.	152
Table A.3	The power load data and the battery charging rate for the first case scenario-I.	153
Table B.1	The power load data for the second case scenario-II.	155
Table B.2	The power generation data for the second case scenario-II.	156
Table B.3	The power load data and the battery charging rate for the second case scenario-II.	157
Table C.1	The data profile for the IEEE 5 bus power system.	159
Table C.2	The optimal power flow results of the IEEE 5 bus power system.	160
Table D.1	The data profile for the IEEE 14 bus of AC power system.	162
Table D.2	The data profile for the IEEE 14 bus of AC power system.	163
Table D.3	The data profile for the IEEE 14 bus of DC power system.	164

Table D.4	The power flow results of the IEEE 14 bus of AC power system.	165
Table D.5	The power flow results for the IEEE 14 bus of AC power system.	166
Table D.6	The power flow results for the IEEE 14 bus of DC power system	167
Table E.1	The data profile of the AC generators and buses for the IEEE 30 bus power system.	169
Table E.2	The data profile of the AC branches and buses for the IEEE 30 bus power system.	170
Table E.3	The data profile of the DC power system for the IEEE 30 bus power system.	171

LIST OF FIGURES

Figure 1.1	The flowchart of the dissertation outline.	7
Figure 2.1	This figure depicts the effect of demand response on electricity market price [1].	9
Figure 2.2	This figure depicts a schematic diagram for the demand response strategies [2].	11
Figure 3.1	Summary of the power system notation.	24
Figure 3.2	This figure depicts a diagram of a three bus power system.	25
Figure 4.1	This figure depicts a schematic diagram for a 30 bus MG system.	38
Figure 4.2	This figure depicts the results of the IEEE 30 bus test system.	45
Figure 4.3	This figure depicts the power injection profiles.	46
Figure 4.4	This figure depicts the results of the IEEE 30 bus test system	47
Figure 4.5	This figure depicts the nodal voltage profiles.	48
Figure 4.6	This figure depicts a partial power network failure.	51
Figure 5.1	Schematic of PV-Battery-Diesel Microgrid systems.	56
Figure 5.2	Diversity of Optimization Approaches.	75
Figure 7.1	The first scenario-I: fourteen bus power system with energy storage units.	96
Figure 7.2	The power load profiles.	99

Figure 7.3	The hourly economic schedule of power generation.	100
Figure 7.4	The hourly economic schedule for state-of-charge.	101
Figure 7.5	The hourly economic schedule for the battery units.	103
Figure 7.6	The voltage profile of the IEEE 14 bus system.	104
Figure 7.7	The second scenario-II: thirteen bus power system with nine energy storage units.	108
Figure 7.8	The power load profiles.	111
Figure 7.9	The hourly economic schedule of power generation.	112
Figure 7.10	The hourly economic schedule for state-of-charge.	113
Figure 7.11	The hourly economic schedule for the battery units.	115
Figure 7.12	The voltage profile of the IEEE 30 bus system.	116
Figure 7.13	The flowchart of the convexification process.	117
Figure 8.1	Model of an AC transmission branch.	123
Figure 8.2	Modeling of a VSC AC/DC converter.	126
Figure 8.3	An AC power system of IEEE 5 bus.	134
Figure 8.4	A hybrid AC/DC power grid with five AC buses and three DC buses.	135
Figure 8.5	A hybrid AC/DC power grid based on the IEEE 14 bus case.	137
Figure 8.6	A hybrid AC/DC power grid based on the IEEE 30 bus case.	139

LIST OF ABBREVIATIONS

$\mathcal{N}$	The set of buses
$\mathcal{G}$	The set of generation buses.
$\mathcal{E}$	The set of transmission lines.
$n \sim j$	Buses n and j connected by a line.
H	Denotes hermitian transpose.
$\mathscr{G}$	The graph contains a set $\mathcal{N}$ of nodes and a set $\mathcal{E}$ of edges.
$\mathbb{C}$	The set of Complex numbers.
δ	Voltage phase angles.
$\|V\|$	Voltage magnitudes.
P_n	Active power at bus n.
Q_n	Reactive power at bus n.
V_n	Complex voltage at bus n.
y_{nj}	Admittance of line joining buses n and j.
S_n	The net power injection at bus n.
I_n	The current at bus n.
x	The vector of state variables.
u	The vector of control variables.
$\succeq 0$	Positive Semidefinite
SDP	Semidefinite Program.
SOCP	Second-Order Cone Program.
LP	Linear Programming.
QP	Quadratic Programming.
NLP	Nonlinear Programming.
IPM	Interior Point Method.

SLP	Sequential Linear Programming.
SM	Simplex Algorithm.
LIM	Lambda-iterative Method.
SQP	Successive Quadratic Programming.
GT	Gradient Techniques.
NT	Newton's Techniques.
CB	Circuit Breaker.
POP	Plynomial Optimization Problem.
MPPT	Maximum Power Point Tracker
OPF	Optimal Power Flow
DOPF	Dynamic Optimal Power Flow
MOPF	Multi-Objective Optimal Power Flow
AC	Alternating Current
DC	Direct Current
HVDC	High Voltage Direct Current
VSC	Voltage Source Converter
CSC	Current-Sourced Converter
GAMS	General Algebraic Modeling System
SeDuMi	Self-Dual-Minimisation Package
SpaPOP	Sparse of Polynomial Optimization Problems
CVX	Disciplined Convex Programming
IEEE	Institute of Electrical and Electronics Engineers

CHAPTER ONE

INTRODUCTION

Efficient operation of electrical power grids has been a constant preoccupation for many years. As a a major component of our modern industrial societies, electrical power grids have played an enormous role in the well-being of humanity for the last 100+ years. Indeed, a large majority of the energy used by human society nowadays is traded over electrical power grids. Consequently, even tiny improvements of the efficiency of electrical power grids have an enormous effect in terms of cost savings. This reality has been recognized for a long time and has stimulated a lot of effort to devise solutions that can contribute to a more efficient operation of electrical power grids. The optimal power flow (OPF) as a mathematical formulation of the efficient operation of an electrical power grid was originally formulated in the sixties [3] and has received enormous attention ever since.

From a numerical point of view, the OPF problem is extremely challenging. Even in its simplest formulation, it is a nonlinear, non-convex optimization problem of very high dimensions. It may therefore have local optima. It is also typically poorly conditioned. As a consequence, standard numerical optimization methods have difficulty achieving the solution. Many advanced optimization methods have been proposed over the years. In fact, the OPF problem has been often used as a benchmark problem for the validation of new optimization methods. As the numerical apparatus and the computational capacities evolved, so has the problem itself. For instance, new aspects of the grid operation were included in the formulation of the problem, such as switches that modify the topology of the grid.

If these switches are included as decision variables for the OPF problem, the problem becomes a mixed integer problem, which can only be tackled by different optimization methods. This process continues currently and will also be pursued as part of the work proposed here. The OPF problem was originally formulated from an economic point of view. However, the consequences of more efficiently working power grids are not only economical in nature. Indeed, reduced fuel consumption translates to reduced pollution levels and better use of existing resources. Both are constant preoccupations of greater importance in our times. The same preoccupations for the environment and for the continuity of energetic resources has generated important developments in the area of renewable energy sources. The development of wind and solar power has taken off and is continuing on an increasing scale. Hydroelectric energy solutions are also enjoying a great interest. Next to the traditional hydroelectric plants that have the disadvantage of being limited to particular geographical conditions and necessitating huge investments and important disruptions of natural environments, newer technologies that exploit tidal and wave energy are also being developed. As renewable energy sources receive a more important role in energy production, it becomes very important to help them operate efficiently next to the traditional plants.

This is a major challenge in the context of the OPF problem for the following reasons. Firstly, many renewable sources, such as solar power, naturally generate DC current. Incidentally, nowadays there is also a large class of consumers that need DC current. This is motivating the formulation of the OPF problem for hybrid AC-DC grids in lieu of purely DC grids, which is a subject that has only recently received attention. Secondly, most renewable sources have limited availability as they depend on natural processes that are weather dependent. Taking this into account adds a new level of complexity to the OPF problem and

necessitates the inclusion of probabilistic models for source availability. Storage levels as decision variables may also be used to add a greater degree of realism to the OPF problem and make its solution more implementable in practice.

Given the characteristics of the OPF problem as listed previously, it is clear that classical optimization methods can only provide local optima in the best scenario. This is acceptable in a situation where the optimal solution can be apriori estimated quite well. If the network topology changes only slightly in time, new solutions will likely be close to the previous solution, so classical optimization methods are readily applicable. However, if the network topology changes drastically, it is important to be able to find the new optimal solution quickly and efficiently, even if it is far from the previous solution. A particular class of optimization methods that have gained a lot of popularity in recent years are heuristic optimization methods. These methods are based on analogies from biological or physical sciences and are able to find optimal solutions for problems of high dimensionality and with many local minima beyond the capabilities of classical methods. However, their efficient application and success depends on judicious choices of design parameters and proper initialization. Also, each of these methods has specific weaknesses that must be circumvented in practice. One solution that has been actively pursued is to combine two such heuristic optimization methods into a hybrid algorithm such that the weaknesses of one method is balanced by the other method. With these approaches, the central question that will be answered in this work is to find an efficient algorithm for solving the OPF problem for a grid that includes thermal, wind energy and solar power sources, that combines a heuristic optimization method with a convex relaxation method and uses the structure of the OPF problem in order to find the best design parameters to tune the optimization algorithms. In order to clarify why this research question may contribute to the rich

body of research into numerical methods for solving the OPF problem, we present in next section an overview of the OPF problem and the current state of the art in this field. Based on this analysis, we will argue the opportunity of the proposed research.

1.1 Motivation

The increased use of direct-current micro-grids that independently include distributed generation into the electricity grid for storage and restoration of power has resulted in compliance with stringent universal cost minimization and power loss regulations. One of the several optional objectives of what is called the "optimum solution" is to minimize the power cost, generation cost, or power losses. A number of researchers have already successfully applied their results to various industrial environments to achieve this solution [4]. Despite these accomplishments, there are still limitations in using this approach [5] to obtain a what has come to be known as a globally optimal solution. The stability, reliability, development, and decision-making abilities of this intelligent power system are required to fully guarantee high performance [6] and [4]. Thus, the development of hybrid AC/DC and direct current microgrid stand-alone (DCMG) systems are the main focus in producing power to consumption, and developing a high quality of electricity while minimizing production time, generation cost, and power losses. Within this framework, both understanding alternative solution methods such as LP, QP, SDF, and SOCP, as well as executing a proper OPF technique are needed to achieve a numerically efficient solution.

The hybrid AC/DC and direct current microgrid stand-alone (DCMG) are powerful systems for the future study of intelligent micro grids, and are particularly useful due to their extreme sensitivity to tiny changes in the weather or shut-downs of the main power fuel supply. Despite these capabilities, the hybrid AC/DC and direct current microgrid stand-alone (DCMG) have not been widely used in studies

of power production under known or known power failure situations. This is not an ideal situation as it is necessary to address the applicability of new techniques to develop highly effective systems that can work under different system failure situations. The principal objective of the hybrid AC/DC and DCMGs stand-alone is to provide uninterrupted power supply to load systems, which can be located almost anywhere, such as in aircraft drones, airplanes, hospitals, rural areas, and remote isolated sites. This research will improve a technique that may be used to build effective, robust hybrid AC/DC and direct current microgrid stand-alone (DCMG) systems to generate power independently with high performance of operations, minimizing the cost generation and power losses during power operation.

1.2 Dissertation Outline

Following the introduction in Chapter 1, Chapter 2 covers the recent stage in the development of the optimization techniques in order to solve the optimal power flow (OPF) problem in general, and more precisely, for the form of the power grid systems that comprise renewable energy sources. In Chapter 3, the OPF problem is introduced. We begin by discussing the formulation and defining the general structure of an OPF problem, objective functions, state and control variables, and constraints. Thereafter, we present the difficulty of the OPF problem and the techniques to address it that are of common interest in solving a global optimization problem. The OPF problem is also formulated without considering the energy storage unit into the power systems. In chapter 4, a polynomial optimization problem (POP) relaxation based on optimization approaches is proposed to solve the non-linear of the OPF problem in DC power network. Improving the numerical stability of POP relaxation is also discussed in terms of avoiding ill-conditioned numerical operations. To ensure smooth operation and high power system reliability and quality, the recent optimization approaches for hybrid energy must be

considered. An overview of the most recent optimization techniques for hybrid energy is broadly introduced and discussed in Chapter 5. Following in Chapter 6, the optimal power flow problem with the energy storage unit is modeled and illustrated with its notations. In Chapter 7, we test and apply the semidefinite (SDP) relaxation technique on standard test networks for the problem using a strategy based on a convex semi-definite program for the OPF problem with energy storage for a large scale power systems. In Chapter 8, the proposed optimization approach is applied to the hybrid AC/DC power networks. The performance of the proposed algorithm is evaluated on different electrical power networks with various power system sizes in the order of proving the adaptability of the algorithm. Then, we conclude the dissertation and explore future work in Chapter 9. In this dissertation, all the numerical data and results are listed and summarized in Chapter 10. The flowchart below summarizes the dissertation outline.

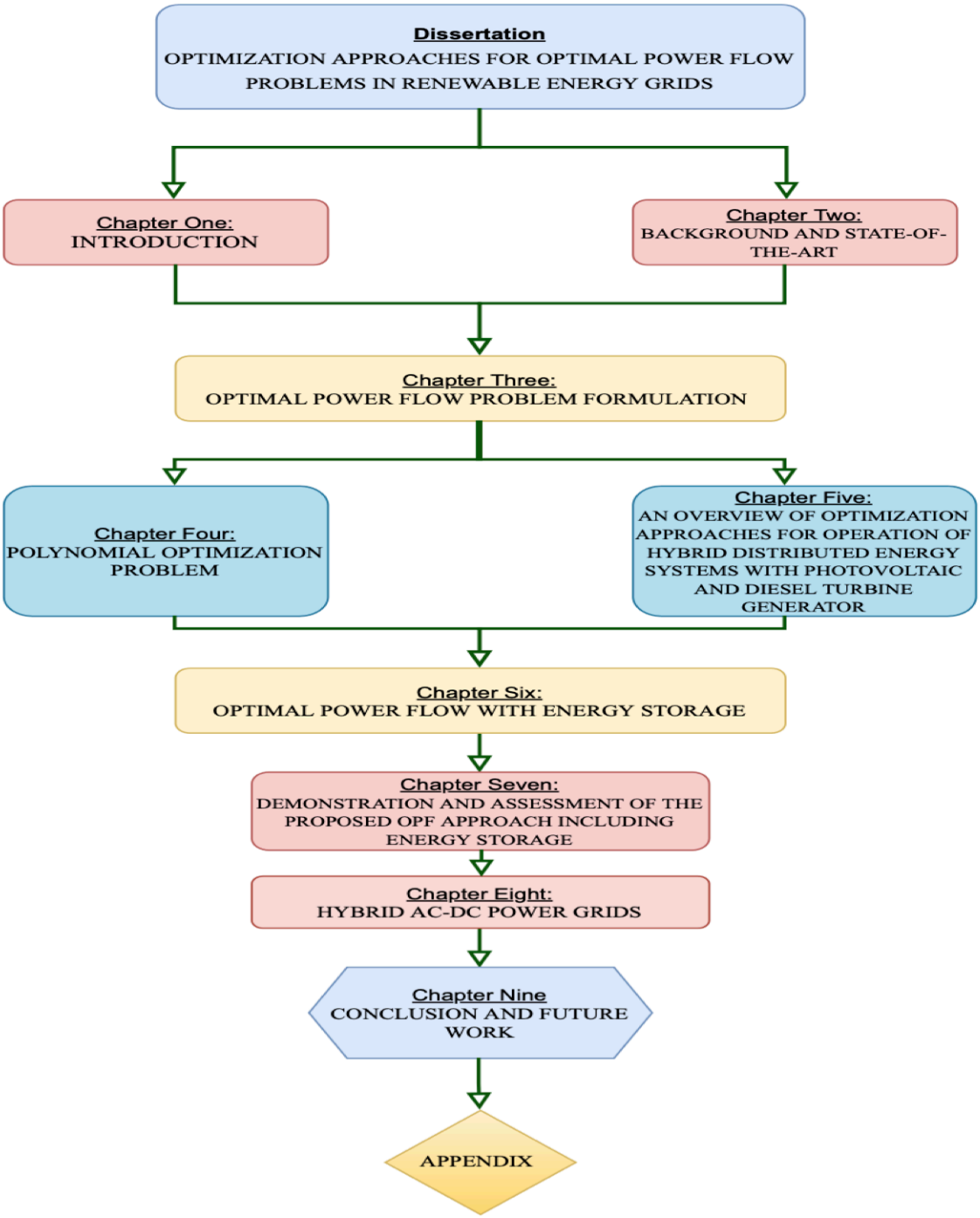


Figure 1.1: The flowchart of the dissertation outline.

CHAPTER TWO

BACKGROUND AND STATE-OF-THE-ART

In order to make explicit the purpose of the proposed work, this chapter gives a short account of the theoretical and numerical developments concerning the OPF problem in general and more specifically for the kind of power grids that include renewable energy sources.

2.1 Demand Response

Demand Response is one of the key solutions available to electrical utilities in terms of reaching higher efficiency and smoother load curve [7]. The residential portion consumes nearly 42% of the entire available energy which composes a significant element of the seasonal and daily peak load [8]. Based on the latest data released by the U.S. Energy Information Administration (EIA), U.S. electric utilities had around 94.8 million advanced (smart) metering infrastructure (AMI) installations, where nearly 89.5% of them are considered as residential smart meters. The smart metering infrastructure is an integrated system that enables two-way communication between utilities and customers [8]. It covers around 50% the 150 million consumers in the U.S. [9]. The state of Michigan stands out among the Midwest on smart metering infrastructure with a smart meter penetration rate of over 81%, according to government data [10]. Enhanced penetration of smart meters empowers higher active participation of consumers in the demand response program. The demand response is expressed as the alteration in the electric consumption from their natural consumption in response to the control signal by end-use customers. The control signal can be modeled regarding the electricity cost or reliability of the system [1]. Costumers are offered incentives by utility companies

to engage in the demand response program [11]. Since consumers are more flexible under the demand response program, the resilience of the demand is higher, as shown in **Fig.2.1**. Without considering the demand response program, the demand is expressed as a vertical line while with the demand response program, the demand curve has a negative slope compared to the original curve. Thus, a small reduction in demand leads to a large reduction in the total cost.

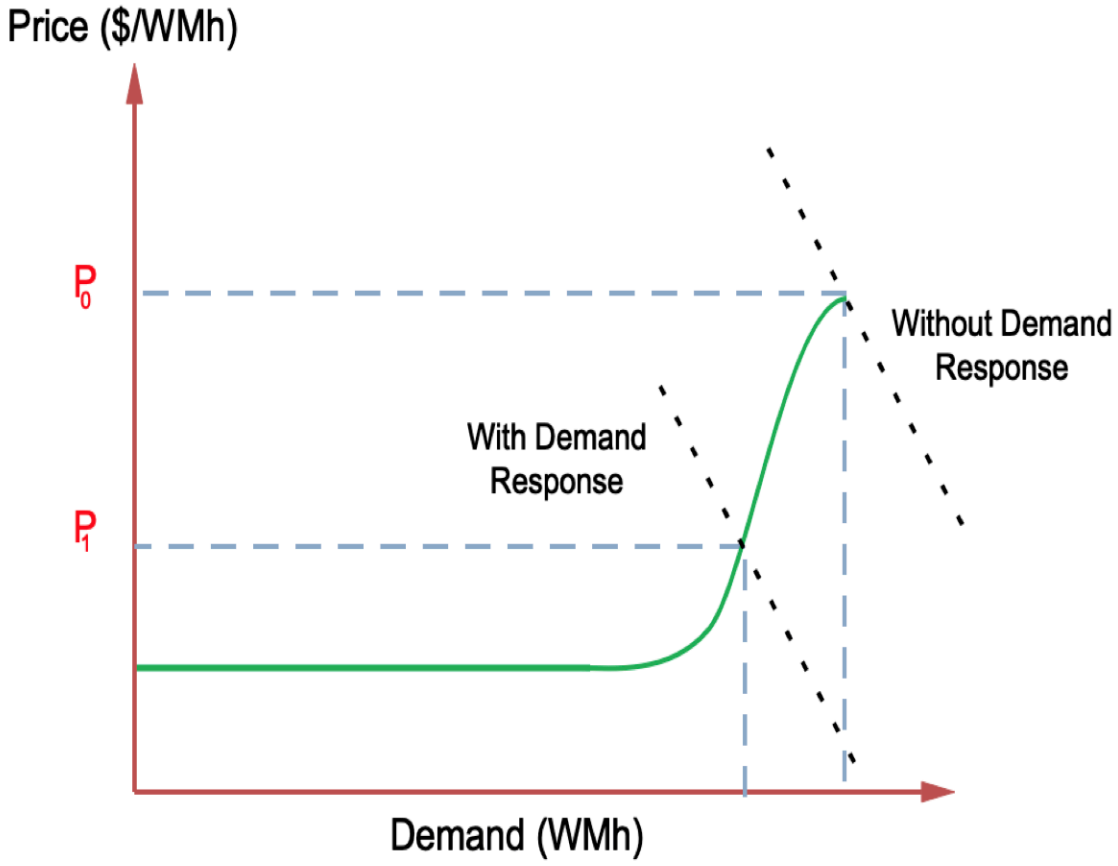


Figure 2.1: This figure depicts the effect of demand response on electricity market price [1].

The power system stability must be preserved with regard to two operating points of frequency and voltage. The traditional power secures are commonly dispatched in a load-following pattern. Large integration of demand response and uncertain renewable energy sources causes more intricate power system stability. The demand response can be utilized in a rapid and accurate way to react to the unknown and intermittent characteristics of renewable energy sources. The load frequency control and corrective voltage control have been applied for decades in terms of preserving the voltage and frequency of the power system. The effect of integrating renewable energy sources and demand response programs on load frequency control and corrective voltage control have to be accurately taken into consideration [12].

The performance and efficiency of coordinating resilient demands to minimize the overall energy cost that costumers paid has been studied in [13]. It has been introduced that proper coordination of the resilient power resources ameliorates the power system operation adequacy [14, 15, 16, 17]. The resilient electric load aggregations not only can transmit the valuable electricity service commonly provided by traditional power generators, yet also their distributed nature makes them qualified for new services [18]. Modern independent aggregators are florentine in the U.S. market due to the correct rate they bring to the market and not regulatory comparisons [19]. The two main classes of the demand response program are illustrated in **Fig.2.2** as follows:

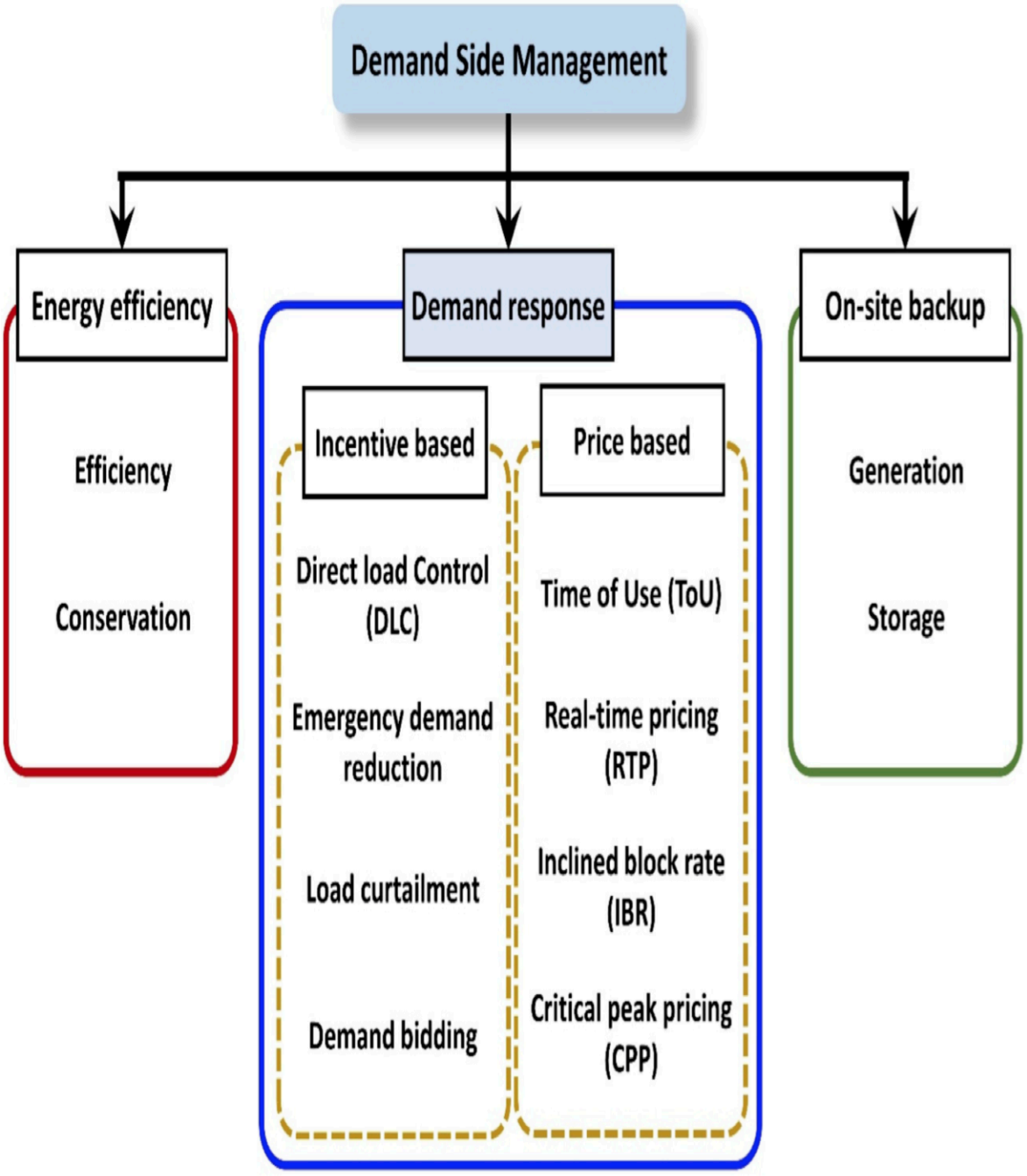


Figure 2.2: This figure depicts a schematic diagram for the demand response strategies [2].

- Price-based demand response: Customers receive their electricity consumption through communication channels and they would or would not to respond to the signals [20]. This kind of program cannot be controlled directly by the system operator and is only involved in energy market.

- Incentive-based demand response: The end-consumers are rewarded for a particular transmit or reduction of the load. This kind of program is generally predetermined and offers several stages of control to the operators. Consequently, the power system operators can be involved in the energy, power capacity, and auxiliary markets [11].

Demand response can offer diverse advantages and its advantages are not restricted to the participants only. Since the load peak is shaved using demand response, the accessible infrastructure can be applied more effectively, the required electricity from expensive generation units minimizes, and thus, the total electricity cost is lowered [21]. Furthermore, new investment in generation and transmission areas can be evaded or at minimum postponed. In a well-planed demand response program, the customers take part in minimizing the risk of outages whereas the power system operators have a broad domain of resources to preserve the system's stability. In addition, environmental advantages associated with the demand response program are accomplished by offering reserves for the power system operators and accelerates the incorporation of renewable energy into the power grid system. Some of the demand response program's advantage are summarized in **Table.2.1**

Table 2.1: This table depicts the demand response advantages.

Participant Benefits	Market wide Benefits	Reliability Benefits	Environmental Benefits
- Bill savings - Incentive payments	- Minimal wholesale market prices - Minimizing aggregate capacity system requirements - Delay the upcoming investments	- Minimal likelihood of forced outages - Various of power sources	- More renewable - Better wide usage of the land - Reducing air pollution

2.2 OPF Problem Formulations

In order to formulate an OPF problem, the electrical power grids are modelled as a set of buses that represent local networks of generators and/or electrical loads, that exchange electrical energy over larger distances through electrical transmission lines. Typically, one of the buses is chosen as a reference bus, with a fixed voltage and the (complex) voltages of the other buses are expressed relative to this bus. Using this model, a simple static mathematical model can be written consisting of power balance equations at each bus, limit constraints on power (generated or consumed), and voltages at each bus and on the currents along the transmission lines. For each bus j, the power balance equation is

$$S_n = \sum_{j:n\sim j} y_{nj}^* V_n (V_n^* - V_j^*), \tag{2.1}$$

where s_n represents the net complex power injection at bus n $(S_n = P_{gen,n} - P_{load,n})$, V_n denotes the voltage of bus n, y_{nj} is the admittance of the line from bus n to bus j, and the sum is taken over all the lines that are adjacent with bus n. Constraints are usually imposed on the magnitude of the voltages V_n, on the power injections, and on the current along the lines.

A power flow solution consists of a set of voltages and powers at each bus that satisfies all these equality and inequality constraints and, in general, there are infinitely many power flow solutions. An OPF problem formulation additionally requires a cost function to be associated with each power flow solution. The cost function can express the cost of generating real power at each generator, or the losses along the line, and can generally be expressed in terms of the bus voltages as a real valued function $C(\{V\}_n)$. The problem is to find the power flow solution(s) that minimize(s) the cost function.

Depending on the cost function, there are many OPF problem formulations. The simplest OPF problem is to minimize the transmission losses. In this case, the cost function is the algebraic sum of generated and consumed powers on the grid. Because of power conservation, this sum coincides with the power lost on the transmission lines, and minimizing this loss is an obviously desirable objective. However, technical and commercial considerations may require different cost functions and many of them have been studied in the literature. There are also more complex versions of the OPF problem. One of them is the Dynamic Optimal Power Flow (DOPF) problem (e.g. [22, 23, 24]) which attempts to optimize the power distributions over several time periods. In this formulation, constraints on the variation of operating points of some grid components can also be taken into account. Another variation of the classical OPF problem is Multi-Objective Optimal Power Flow (MO-OPF) (e.g. [25, 26, 27, 28]) which uses multiple cost functions that account for different objectives that the power solution has to satisfy. In this case, the proposed methods are attempting to find Pareto front solutions for this problem, instead of optimal solutions as in the classical OPF formulation.

The OPF problem has been addressed in the literature for a several decades. One of the first contributions in this area [29] credits the first formulation of the problem to the article [3], which indicated that the interest of the OPF problem is economic. With the gigantic amount of energy that is traded on the electric power grids around the world, it is clear that the interest for the OPF problem remains enormous and this is reflected in the research literature. Understandably, for many years, the research on the OPF problem was limited to alternating current (AC) power grids that are ubiquitous in modern economies. This is the consequence of the famous "battle of the currents" that ended with the decisive victory of AC, although the outcome was not obvious from the beginning [30].

Only recently has preoccupation for DC grids been rising, on one hand motivated by the wider use of renewable energy sources that are better compatible with DC operation, and, on the other hand, by the wider use of consumer electronics that operate on DC power. In fact, there are opinions such as [31] that we are assisting at a new battle in which DC may gain the upper hand, or, in any case, grow significantly in importance. Actually, this reference shows that DC has never completely left the market of power distribution, although it was limited to a few niche applications. Also, new technological developments have the potential to make DC a serious competition to AC. However, as we shall see further, all these new developments are not yet reflected in the literature on the OPF problem, so a meaningful literature review on this subject cannot be limited to the DC version(s) of the problem.

It is fair to say that the literature on the OPF problem is vast. As early as the nineties, we find a survey from [32]. A newer and more extensive two part survey [33, 34] lists about six hundred contributions. Both of these surveys include no reference to the version of the problem for DC grids. As DC power generators became more widely used, some research effort was directed towards hybrid AC/DC power grids and the OPF problem for this type of grids was tackled in contributions such as [35, 36, 37].

The article [38] that is analyzed here is concerned with purely DC grids. This is not the first paper that treats the OPF problem for DC grids, as its main contribution is to strengthen the results of a previous paper on the same subject [39], but these two seem to be the only papers in the literature that are devoted exclusively to DC grids. On the bright side, the OPF problem for DC grids is simpler since it does not have to deal with voltage phase and reactive power as it is the case for AC grids. Therefore, all the techniques previously employed for AC

grids could be adapted for DC grids. In fact, the techniques employed in the two cited papers [39, 38] have been previously developed for the AC grid version of the OPF problem as presented in the two part tutorial [40, 41].

No matter the type of grid for which it is formulated, the OPF problem, as an optimization problem, presents two main challenges. First of all, it is a nonlinear, non-convex problem, which means that straightforward application of numerical optimization methods is not adequate. Secondly, practical cases lead to optimization problems of very large orders. Besides, the OPF problem has to be solved again every time the configuration of the grid changes, e.g. if a load or a generator are disconnected. It is therefore very important to have efficient numerical methods to solve this problem.

2.3 Classical Optimization Methods

By examining the literature on the OPF problem using the literature surveys cited before, it can be concluded that the OPF problem was used as a benchmark for about every class of optimization methods that are currently available.

One purpose of the research was to approximate the OPF problem (at least locally) with simpler problems that can be readily solved by efficient numerical methods. Linear Programming (LP) approximations and Quadratic Programming (QP) approximations were considered. This class of methods may be very useful in practice in many situations, but they are not guaranteed to lead to a solution as they are dependent on the quality of the approximation. Further, there was a lot of work on classical iterative methods such as Gradient Methods, Newton, Quasi-Newton, etc. These methods may be very time consuming and, given the non-convexity of the original OPF problem, their convergence cannot be guaranteed.

Another class of methods is based on convex relaxation and as the two part survey [40, 41] shows, they have been extensively studied. The relaxation of an

optimization problem is another optimization problem with fewer or weaker constraints. Essentially, the feasible set of the optimization problem is enlarged so that the feasible set becomes, for example, convex. In general, the optimum of a relaxed problem is different from the optimum of the original problem, unless the solution of the relaxed problem satisfies the original set of constraints. In this case, it is said that the relaxation gap is zero, or that the relaxation is exact. The transformation of the OPF problem into a relaxed problem makes use of the intrinsic structure of the problem and its success depends essentially on this aspect. As shown in [40], the Branch Flow Model for the OPF (also used in [39, 38] for the case of DC grids) is a good candidate for performing the convex relaxation and under certain assumptions provides an exact relaxed convex equivalent optimization problem.

In principle, if the problem is reduced to a convex optimization problem, classical optimization methods are entirely able to solve the problem in a reasonable number of iterations. When convexity cannot be achieved, or if the convex relaxation is not exact, it is interesting to consider different methods such as those presented in the next section.

2.4 Heuristic Optimization Methods

In terms of increasing system dimensionality and causing non-convexity on the OPF problem, there is a need to consider more robust approaches based on heuristic optimization methods. Such methods have been proposed in numerous ways over the years with the purpose of circumventing the typical disadvantage of classical methods to converge to local minima. As the name shows, each of these optimization methods is based on some heuristic idea lent from biology or physics. Here is a short review of some popular heuristic methods and of their application to the OPF problem.

Particle Swarm Optimization (PSO): The heuristic idea of this method is to simulate the behaviour of a swarm of intelligent and communicating agents/particles that explore the space of possible solutions, changing their positions and velocities based on their own "best" visited point, and the "best" point that the group has visited. These agents represent candidate solutions and the "motion" that occurs in the (high-dimensional) space of possible solutions. The method was originally introduced in [42] and has seen important improvements and adaptations ever since. Overviews of the progress of the method and its many applications can be found in [43] and in the book [44]. Since it was noticed that the original version tended to converge very quickly to some local optimum and be "trapped" there, several improvements have been proposed over the years. Most of them were focused on the communication network between the particles. Initially, all particles communicated with each other. By limiting the communication network to, for example, m closest neighbours, premature convergence can be prevented and the performance of the algorithm is improved. A different version of the algorithm, called Aging PSO, adds to the basic uniform swarm configuration a "leader" that ages with subsequent iterations, and is replaced by another one.

The method was first applied to the Optimal Power Flow problem in [45], but there have been many other contributions such as [46, 47]. The method was also used to tackle multi-objective OPF problems in [26, 48]. There are many more contributions that try to mitigate the disadvantages of PSO by proposing hybrids with different optimization methods, as will be discussed later.

For our particular subject, the recent reference [49] deserves particular attention since it applies PSO in a power flow controller for a hybrid renewable energy grid. In this case, PSO is used to find the optimal parameters for a grid P-Q controller, which is a cascaded control system consisting of four PI regulators used

to control the voltage and current levels at the interface between the renewable power sources grid and the main grid.

Genetic Algorithm (GA): This method is based on the heuristic biological processes of evolution, mutation, and natural selection. The solution candidates at each iteration represent the individuals of the population. They are represented by a set of parameters that represent the "chromosomes" and their fitness is represented by the optimization criterion. At each iteration step, a part of the population is selected for recombination and mutation and a new generation is obtained. These "genetic operators" have a stochastic character in nature, but they need to be designed in such a way that the average fitness of the new generation is better than the old. Genetic Algorithm optimization was applied to the OPF problem in numerous contributions such as [50, 51] and it is still an active area of research as indicated by recent references such as [52, 53].

Simulated Annealing (SA): This method was developed by the technological process of annealing in metallurgy. It consists of heating a metal above recrystillization temperature and letting it cool off in a controlled manner, which tends to increase the size of the crystals in the material. The method starts with a candidate solution and takes random steps at each iteration to a neighbouring point. The new candidate is then submitted to a vetting process. It is automatically accepted if it improves the cost criterion, which makes it a better candidate than the previous one. However, in some cases it could not be the best candidate because the parameters are decreased with each iteration. If it is the worse candidate, then it may still be accepted randomly with a probability that depends on the "temperature" parameter. This parameter is decreasing with each iteration, so the method will accept worse candidates with lower probabilities as the

number of iterations increases. In this way, the method can evade local optima and approximate better global ones.

The method was first proposed in [54] as a method to solve discrete optimization problems (such as the Traveling Salesman Problem), and has been extended and improved over the years. Some relatively recent applications can be consulted in [55]. There are relatively few attempts to apply Simulated Annealing to solve the OPF problem. The first appears to be the conference paper [56] which was published later as a journal contribution [57]. Simulated Annealing is evident a second time in [58]. It turns out that the method in its original form does not provide good computational performance in the case of the OPF problem. However, there are many applications of hybrid methods that do include SA that will be discussed later.

Bacterial Foraging Algorithm (BFA): This method is inspired by the patterns exhibited by bacteria while foraging for food. It was introduced in [59] and it mimics the tendency of natural selection to eliminate bacteria with poor foraging strategies. The method was extensively used in the context of the OPF problem. For example, [60] applied to optimize the real power losses and voltage stability limits of a mesh power network. [61] developed a version of the BFA method with varying population for the OPF problem. [62, 63] presented an approach called Dynamic BFA (DBFA) to solve the OPF problem with dynamic loads, in which the variations of power loads and system topology were simulated as regular and irregular environmental changes.

Artificial Physics Optimization (APO): This method was relatively recently introduced in [64, 65] which is similar to PSO in the sense that it proceeds with a population of candidate solutions that are initially randomly distributed in the space of possible solutions. However, in contrast to PSO, the motion of the

particles is dictated by relative pseudo-gravitation forces. To determine these forces, the particles are assigned masses that depend on the value of the objective function in the current position of the particle. In this way, the method assures that "better" candidates attract "worse" candidates so that the particles tend to converge towards the optimum solution. There do not appear to be direct applications of APO to the OPF problem. However, the method was applied in hybrid forms in a few contributions that will be discussed later.

2.5 Hybrid Optimization Methods and the OPF

Although promising in theory, the practical application of heuristic methods can be challenging in practice. Firstly, there is no guarantee that the optimum outcome will be achieved. Each method has a number of tuning parameters and their choice has a strong influence on the performance of these algorithms. Unfortunately, it is not always clear how to choose these parameters in order to achieve desired performance while not affecting the convergence rate too negatively. Another important aspect is that each heuristic optimization method has specific strengths and weaknesses and therefore, there is a strong interest in devising methods that combine some of these optimization methods in order to compensate for their weaknesses.

The survey article [33, 34] lists numerous contributions to solving the OPF problem using a variety of hybrid optimization methods. These include methods that combine conventional iterative methods (SQP, Newton, Interior Point) as (meta) heuristic methods such as the ones presented before in many combinations. However, the survey does not mention any contributions to hybrid grids that include conventional energy sources and renewable energy sources.

2.6 Discussion

There is a great deal of work done on the OPF problem using heuristic optimization methods, both in pure form and in hybridized form. The work on OPF problems for grids that include renewable energy sources is relatively scarce. The references that are available at the moment use mostly hybrid heuristic optimization problems. However, these methods do not make use of the particular structure of the OPF problem that consists of a generally convex optimization criterion, with various equality and inequality constraints, few of which violate the convexity condition. Therefore, convex relaxation methods have been relatively successful in addressing the OPF problem. It is therefore recommended to make use of the structure of the OPF problem to devise better solution methods as the work proposed here will attempt to do.

CHAPTER THREE

OPTIMAL POWER FLOW PROBLEM FORMULATION

3.1 Notation

This section will present the Direct Current (DC) System notation that will be utilized throughout the dissertation. The DC power grid model is comprised of buses and lines connecting all buses with each other. As shown in **Fig.3.1**, these lines can be linked in tree, mesh, or radial topology.

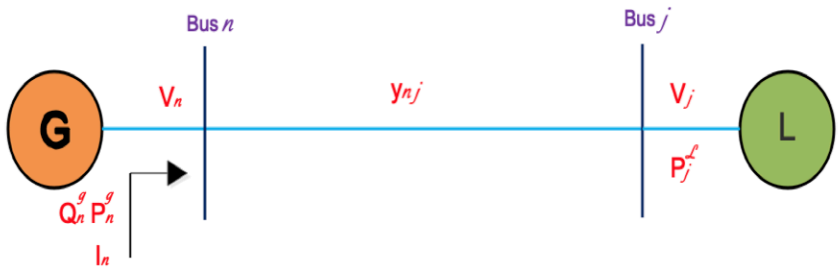


Figure 3.1: Summary of the power system notation.

A Graph $\mathcal{G}:=\{\mathcal{N},\mathcal{E}\}$ contains a set $\mathcal{N}$ of nodes and a set $\mathcal{E}$ of edges. Each line connects an ordered pair (n,j) of buses. If two microgrids n and j are connected by a tie line directly, we denote $(n,j)\in\mathcal{E}$ by $n\sim j$. For each bus $n\in\mathcal{N}$, V_n represents the voltages, I_n represents the current injections, and P_n represents the power injections. At each line let y_{nj} represent the admittance, and I_{nj} represents the current flow between buses $n\sim j$ from n to j, also marking out the $Z_{nj}:=\frac{1}{y_{nj}}$. For each microgrid $n\in\mathcal{E}$, let $P_n^g(t)$ denotes the generation at time t

and $P_n^d(t)$ denotes its constant load demand. Notice that all the above parameters are real numbers since we are working in DC network.

3.2 Mathematical Model and Problem Formulation

3.2.1 The Optimal Power Flow in the Absence of Energy Storage

The derivation of the optimal power flow equation will be introduced in this section, see [66] and [5] for more details. This formulation will include energy storage elements. To illustrate this, see a fully connected **3** bus system in **Fig.3.2**. The Power flows in network are controlled by the below physical rules:

$$I_{nj} = (V_n - V_j) y_{nj} \ , \forall \{n, j\} \in \mathcal{E} \quad \text{(Ohm's Law)}$$

$$I_n = \sum_{j:n \sim j} (I_{nj}) \ , \forall \{n, j\} \in \mathcal{N} \quad \text{(Current balance)}$$

$$P_n = V_n I_n \ , \forall \{n, j\} \in \mathcal{N} \quad \text{(Power Balance)}$$

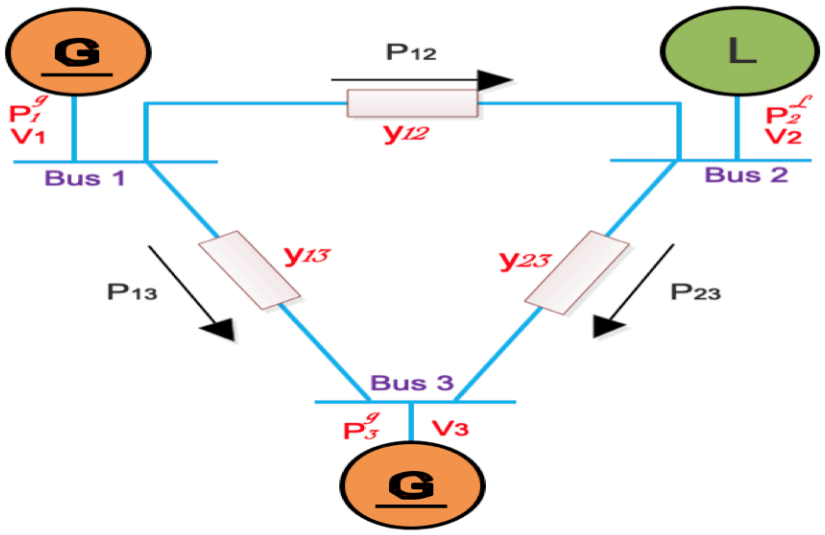


Figure 3.2: This figure depicts a diagram of a three bus power system.

In the next model we show the power flow in the DC network by removing the current variable, as follows:

$$P_n = V_n \sum_{j:n\sim j} (V_n - V_j) y_{nj} \ , \quad \forall \{n, j\} \in \mathcal{N} \tag{3.1}$$

Subsequently, the OPF equation of this particular example is:

$$\min_{V_n, P_n} \sum_{n=1}^{3} f_n(P_n^g). \tag{3.2}$$

Subject to,

$$P_n = V_n \sum_{j:n\sim j}^{3} (V_n - V_j) y_{nj} \qquad n = 1, .., 3 \tag{3.3}$$

$$P_n{}^- \leq P_n \leq P_n{}^+ \qquad n = 1, .., 3 \tag{3.4}$$

$$V_n{}^- \leq V_n \leq V_n{}^+ \qquad n = 1, .., 3 \tag{3.5}$$

Where $V = V_n \in \mathcal{N}$, and n is represented at each bus. The cost (3.2) is a function of generation in each node, which should satisfy that $f_n(P_n^g)$ is strictly increasing $\forall n \in \mathcal{N}$. The equality constraint (3.3), non-linear in V_n, can be replaced by a linear constraint on VV with a new matrix variable U. However, in the term to make the map from V to U invertible, U must be constrained to be both Positive Semidefinite (SDP) with rank equals to one, then eliminate the rank to be convex, since the rank makes it non-convex. One way that we can make the OPF convex problem is by relaxing the rank constraints to (3.10); that in turn leads to a second-order cone programming (SOCP) relaxation.

Now, The OPF can be reformulated as follows:

$$\min_{P_n, V_n, M_{nj}} \sum_{n=1}^{3} f_n(P_n^g) \tag{3.6}$$

Subject to,

$$P_n = \sum_{j:n\sim j}^{3} (v_n - U_{nj}) y_{nj} \tag{3.7}$$

$$P_n{}^{-} \leq P_n \leq P_n{}^{+} \tag{3.8}$$

$$(V_n)^{2^{-}} \leq v_n \leq (V_n)^{2^{+}} \tag{3.9}$$

$$M_{nj} = \begin{bmatrix} v_n & U_{nj} \\ U_{jn} & v_j \end{bmatrix} \succeq 0 \quad \forall n \sim j \tag{3.10}$$

Notice: If Positive Semidefinite relaxation obtains a solution subject to optimal U and it has rank one, the actual problem is solved. Eliminating the rank one constraint results in a convex problem of Positive Semidefinite relaxation.

This provides a better understanding of the formulations that have been presented above in two steps, which are transformation and relaxation, see (3.10) and (3.12). The slack variable has been shown in a transformation stage as follows:

$$\widehat{M} := \begin{bmatrix} V_1 \\ V_2 \\ \vdots \\ V_n \end{bmatrix} \begin{bmatrix} V_1 & V_2 & \cdots & V_n \end{bmatrix} \tag{3.11}$$

In the transformation step, inserting the slack variable is shown in the following by using:

$$v_n = V_n^2 \ , n \in \mathcal{N} \tag{3.12}$$

$$U_{nj} = V_n V_j \ , n \sim j \tag{3.13}$$

After that, (3.3) is converted to a linear equality constraint, as shown in (3.7) in (P, v, U). For each line $n \sim j$ where $n < j$, let it be assumed that $R^{2\times 2}$ then we will use (3.10) and (3.11) to derive the following equation:

$$M_{nj} = \begin{bmatrix} v_n & U_{nj} \\ U_{jn} & v_j \end{bmatrix} = \begin{bmatrix} V_n \\ V_j \end{bmatrix} \begin{bmatrix} V_n & V_j \end{bmatrix} \tag{3.14}$$

Then, the non-convexity in (3.3) is converted to another non-convexity in

$$Rank(M_{nj}) := 1 \tag{3.15}$$

assuming that $V_n \neq 0$ and SDP.

In terms of relaxation, during the second stages, the rank constraint (3.15) is eliminated; however, the positive semidefinite constraint (3.10) is necessarily kept. We hereafter called this relaxation SDP.

3.2.2 The Optimal Power Flow with Energy Storage

An OPF problem optimizes both variables V and P over the solution collections of the bus injection model in (3.3). Additionally, all voltage magnitudes must satisfy (3.9), where the lower and upper bounds are represented by $(V_n)^-$ and $(V_n)^+$, by assuming that the lower bound of voltage magnitude is greater than zero,$(V_n)^- \geq 0$, due to avoiding the triviality in the system. The power injection is also bounded as shown in (3.8) as it is in the voltages magnitude, where ${P_n}^-$ and $\overline{P_n}$ are given bounds on the injections at bus n.

We now formulate an optimal power flow with energy storage and time-varying generation costs and demands. In this formulation of DC systems, the reactive power is ignored and only the active power is kept. $r_n(t)$, represents the value of the power at time (t) where it charges or discharges.

It charges when $r_n(t)$ has a negative value:

$$r_n(t)^- < 0 \tag{3.16}$$

It discharges when $r_n(t)$ has a positive value:

$$r_n(t)^+ \geq 0 \tag{3.17}$$

$b_n(t)$, represents the value of the energy storage at time (t). The amount of the energy storage is modeled to follow the first order differential equations.

$$b_n(t+1) = b_n(t) + r_n(t)\beta \tag{3.18}$$

where β is denoted the time interval $[t, (t+1)]$ given that the initial value of the energy level is $b_n(0) \geq 0$ at each bus $n \in \mathcal{N}$, are modeled as follows:

$$0 \leq b_n(t) \leq {B_n}^+ \tag{3.19}$$

${B_n}^+$ is the maximum value of the energy storage.

Moreover, the charge and discharge battery are bounded as follows

$${R_n}^- \leq r_n(t) \leq {R_n}^+ \tag{3.20}$$

where t = 1,...,$(T+1)$

The network constraint at each bus $n \in N$ and time $t \in T$ are

$$\sum_{j:n\sim j}^{3} (v_n - U_{nj}) y_{nj} = P_n^g(t) - P_n^d(t) - r_n(t) \tag{3.21}$$

where, $P_n^g(t)$ represents the generation at time (t) and $P_n^d(t)$ represents its constant load demand.

Thus, the final formulation of adding energy storage for the DC microgrid system stands alone as follows:

$$\min_{P^g(t),V,b(t)} \sum_{n\in\mathcal{N}} \left\{ \sum_{t=1}^{T} f_n(P_n^g) + h_n^t(b_n(T)) \right\} \tag{3.22}$$

Subject to,

$$V_n{}^- \leq V_n \leq V_n{}^+ \tag{3.23}$$

$$P_n^g(t)^- \leq P_n^g(t) \leq P_n^g(t)^+ \tag{3.24}$$

$$0 \leq b_n(t) \leq B_n{}^+ \tag{3.25}$$

$$b_n(t+1) = b_n(t) - r_n(t)\beta \tag{3.26}$$

$$R_n{}^- \leq r_n(t) \leq R_n{}^+ \tag{3.27}$$

$$\sum_{j:n\sim j}^{3} (v_n - U_{nj}) y_{nj} = P_n^g(t) - P_n^d(t) - r_n(t) \tag{3.28}$$

Where

- $f_n(P_n^g)$ is the quadratic problem, which represents generation cost and battery costs.

- $h_n^t(b_n(T))$ represents the terminal costs.

CHAPTER FOUR

POLYNOMIAL OPTIMIZATION PROBLEM

4.1 Introduction

Polynomial Optimization is an active field of research and remains the focus of researchers from different areas as semidefinite programming, real algebraic geometric, and operator theory. The basic idea to employ a convex optimization method to minimize unconstrained multi-variable polynomial was presented by [67]. Moreover, the first discussion of taking advantage of the duality of moment cones and cones of non-negative polynomials in a convex optimization scope was developed by [68]. Nesterov's works show that the characterization of a moment cone by linear matrix inequalities, i.e., semidefinite constraints, in case the elements of the corresponding cone of non-negative polynomials can be written as sum of squares. The next significant achievement in reducing the multivariate polynomials was explored by Lasserre [69], who realized that to employ the recent real algebraic solution that was given by Putinar [70] there must be a sequence of semidefinite program relaxations whose optima converge to the optimum of a polynomial optimization problem (POP). The modern improvements in polynomial optimization are, for example, the utilization of sparsity in order to accomplish the best numerical developments by suggesting a sequence of sparse SDP relaxations by Waki, Kim, Kojima and Muramatsu [71], and other approaches to characterize the POP by semidefinite programs via finite varieties by Laurent [72].

4.2 Application

Polynomial Optimization problems (POPs) arise from different applications in science and engineering, for instance, control theory signal processing, speech

recognition, numerical linear algebra, graph theory, and investment science. It is essentially hard to list, even very partially, the accomplishments of using POPs, intelligibly due to its massiveness in the literature. To prompt our research, we will nevertheless discuss some sample applications to explicate the benefits of utilizing POPs.

POPs have an existing application in investment science, for example, the celebrated mean-variance model presented by Markowitz [73] early in 1952, where the portfolio selection problem is modeled by reducing the variance of the investments subject to its objective recurrence. In control theory, the polynomial optimization of stochastic feedback control for stable plants was established by Roberts and Newmann [74]. In diffusion magnetic resonance imaging, a situation for the fourth order tensor approximation was proposed by [75]. In fact, there is a huge class of (POP) appearing from tensor approximations and decompositions, which are invented from applications in psychometrics and chemometrics (for more detail, see the survey written by Kolda and Bader [76]). In addition, POPs have applications in signal processing. A quartic polynomial model for blind channel equalization in digital communication was explored by Maricic [77], and conducted global optimization for high degree polynomial minimization models arising from signal processing by Qi and Teo [78].

The aim of this chapter is to propose the modern practical SDP relaxation for a sparse POP and present its performance for solving the OPF problem of the power system model via the polynomial optimization technique. By using the previous model of the six-bus example, we will illustrate the algorithm procedure via polynomial optimization technique for demonstration.

4.3 The Polynomial Optimization Problem (POP)

$$\min_{X} f = [5P_{g1} + 7P_{g2}] \tag{4.1}$$

$$X^T := \begin{bmatrix} P_{g1} & P_{g2} & V_1 & V_2 & V_3 & V_4 & V_5 & V_6 \end{bmatrix} \tag{4.2}$$

Subject to,

$$P_1 = P_{g1} - P_{L1} + (V_1V_5)(y_{15}) - (V_1)^2(y_{15}) \tag{4.3}$$

$$P_2 = P_{g2} - P_{L2} + (V_2V_6)(y_{26}) - (V_2)^2(y_{26}) \tag{4.4}$$

$$P_3 = P_{g3} - P_{L3} + (V_3V_4)(y_{34}) + (V_3V_5)(y_{35}) - (V_3)^2\ [y_{34} - y_{35}] \tag{4.5}$$

$$P_4 = P_{g4} - P_{L4} + (V_4V_3)(y_{43}) + (V_4V_6)(y_{46}) - (V_4)^2\ [y_{43} - y_{46}] \tag{4.6}$$

$$P_5 = P_{g5} - P_{L5} + (V_5V_1)(y_{51}) + (V_5V_3)(y_{53}) + (V_5V_6)(y_{56}) - (V_5)^2\ [y_{51} - y_{53} - y_{56}] \tag{4.7}$$

$$P_6 = P_{g6} - P_{L6} + (V_6V_2)(y_{62}) + (V_6V_4)(y_{64}) + (V_6V_5)(y_{65}) - (V_6)^2\ [y_{62} - y_{64} - y_{65}] \tag{4.8}$$

$$[P_{gn},\ P_{L_n},\ V_n] = \begin{cases} 0 \le P_{g1} \le 10K \\ 0 \le P_{g2} \le 10K \\ 350 \le V_{[1,..,6]} \le 450 \\ V_1^{ref} = 380 \\ P_{L3} = 10K \\ P_{L4} = 6K \end{cases}$$

Where $V_{[1,..,6]}$ is represented the voltages at each bus.

4.3.1 Solution Report and Analysis

I - Approximate Optimal Solution Information

Table 4.1: This table depicts the results of the IEEE 6 bus power system.

No.	P_g	V
1	9999.9992	380
2	6,5164	375.47
3	0	366.35
4	0	366.41
5	0	366.84
6	0	366.80

II - Approximate Optimal Value Information

The SDP solver, called SeDuMi, takes 2.58 second to reach the minimum cost of the system with 3.07 second of total CPU time, 0.37 second per iteration.

Table 4.2: The objective values obtained from the Matlab-SparsePOP programming solver.

No.	Type of Approaches	Value
1	The SDP Objective Value	9,5615.01
2	The POP Objective Value	9,5614.96
3	Relative Objective Error	+5.703e-07
4	The POP absolute Error	-2.565e-03
5	The POP scaled Error	-1.869e-10

4.3.2 Result Summary

This chapter presents the OPF solution of a six-bus system. The system is modeled via the polynomial optimization model. SparsePOP applies the procedure of constructing an SDP relaxation problem with given parameters, solving it using SeDuMi, and reports a global optimal solution. The result shows that the proposed OPF algorithm is effective and more accurate by using SparsePOP solver for a large size system. In fact, the computational efficiency of solving SparsePOP thus depends on how the SDP relaxation problem is constructed and solved. In conclusion, the minimum solution is satisfied constraints and the final cost using the Matlab SparsePOP solver is $9,5615\$/h$, which is very close to the final cost using the CVX Solver.

4.4 The Proposed Research Problem

This section describes the problem statement of this research study to give an explicit understanding of what the major issue is and what type of approach is considered to tackle the OPF problem in terms of widely enhancing the use of standalone DC microgrid systems. In this publication, we define the approach steps for simply solving the OPF problem in the last section to provide a better understanding of how we are going to deal with the OPF problem associated with

the use of standalone DC microgrid systems. This research study offers two main contributions. One contribution is to prove sufficient conditions for the relaxation to be numerically exact and introduce stronger convexifications for the OPF problem than those currently presented in the literature. As a secondary contribution, the paper beholds improving the numerical conditioning of the OPF problem by an equivalent transformation based on convex optimization methods. Then, a larger instance than those published in the current literature are solved to global optimality by exploiting structured sparsity of the OPF problem. Finally, we provide proof of convergence of the sparse hierarchy of SDP relaxations for OPF. Notably, both of the presented techniques improve upon the Lavaei-Low SDP relaxation, whenever the Lavaei-Low SDP relaxation does not provide the global optimum. The central contribution of this research considers solving the formulated OPF problem as a polynomial optimization problem that has been divided into three phases. The first two phases are to transform the OPF problem into a second-order conic programming problem. The first phase is used to improve the numerical conditioning of the OPF problem. The second phase is an equivalent transformation of the original OPF problem. The non-convex optimization of the OPF problem is transformed into a second-order conic optimization problem with a supplemental non-convex constraint that a number of second-order matrices have an inequality constrained with a rank one. The third phase is a relaxation stage, which consists simply of removing the rank constraint. The fact that this relaxation is exact, under some mild conditions, is the main theoretical result of the publication [79].

4.5 Model Description and Problem Formulation

In the following subsection, a description of the system model for the DC network is provided along with a mathematical approach of the optimal power flow equation.

A - The Model Description

In this subsection, the proposed method of this study is validated in the IEEE **30** bus test system to empirically evaluate the suggested approach while the microgrid system is operated in two different modes of operations and network topologies. The proposed power system has a three feeder system, as shown in **Fig.4.1**. The line-data and the bus-data can be found in [80] and [81]. The cited reference assumed the network on AC power and studied the effect of re-configuring the network in relation to the feeders in order to minimize power loss. However, in this study a modification has been made by considering it as a DC power network and by then adding power generators in certain busses' networks.

As can be seen by **Fig.4.1**, the proposed microgrid system consists of **six** distributed generators with a capacity of **10MW**. The proposed system is composed of three feeders, twenty-nine sectionalizing (usually closed) breakers, and nine tie (usually open) breakers. The solid line in **Fig.4.1** depicts the sectionalizing breakers and a dotted line depicts the tie breakers.

In this systems, all the tie and sectionalizing breakers are considered as candidate circuit breakers for network topologies. In this proposed work, two different types of operations are considered to support the loads, namely, a grid-connected of three feeders and standalone where the main power grid is switched off. These two different types of operations are assumed to be evaluated under different types of network configurations, namely tree and mesh

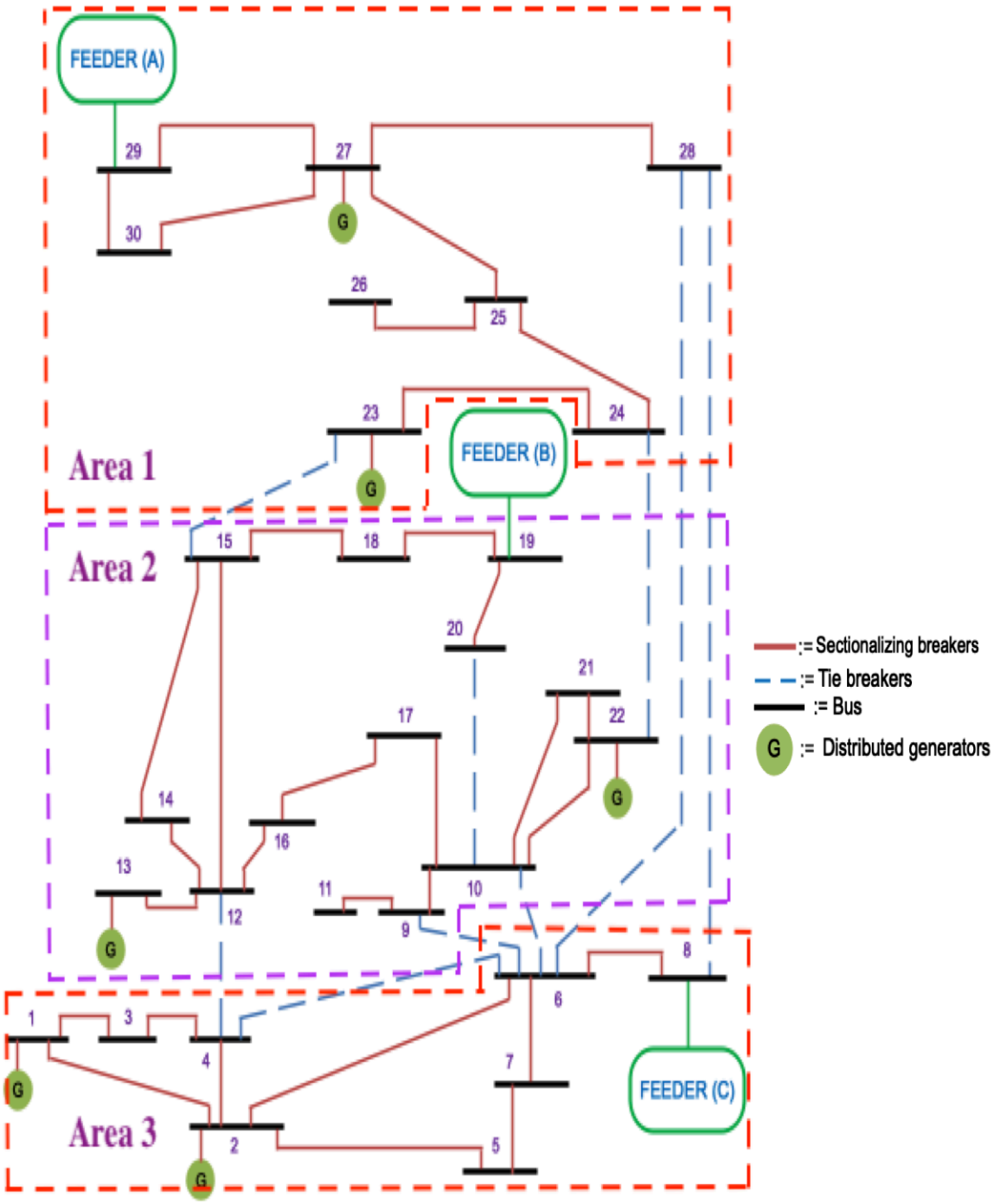


Figure 4.1: This figure depicts a schematic diagram for a 30 bus MG system.

configurations. In the tree configuration, all the circuit breakers are assumed to be disconnected and this assumption is tested for both grid-connected (G-tree) and standalone (S-tree) configurations. However, in the mesh configuration, circuit breakers are assumed to be connected and this assumption is tested for both different types of operations as (G-mesh) and (S-mesh). The main idea of considering different types of operations at two different network configurations is to prove whether the relaxation of OPF problem for the DC network does depend on the configuration and/or operating mode, as stated for the AC network by [82]. As aforementioned, the main objective for this work is to reduce both the total cost and loss of power system by using the convex relaxation approach based on a polynomial optimization problem.

B - Problem Formulation

The problem formulation considered in this study is based on a simple model of a DC microgrid system. It is regarded as a graph with vertices $n \in \mathcal{N} := \{1, 2, \cdots, m\}$ denoting buses and the $\mathcal{E}$ denoting the sets of all lines. The line connecting bus n with bus j is denoted $n \sim j$. Each bus is described by its voltage V_n and the power injection p_n. In general, these variables are constrained by given boundaries as follows:

$$\begin{aligned} V_n^- \leq V_n \leq V_n^+ \qquad & \forall n \in \mathcal{N} \\ p_n^- \leq p_n \leq p_n^+ \qquad & \forall n \in \mathcal{N} \end{aligned} \tag{4.9}$$

and it can be assumed with no loss of generality that $V_n^- > 0, \forall n \in \mathcal{N}$. The current flow through $n \sim j$ is characterized by equation (4.10), where y_{nj} is described the conductance on the lines and it has to be $y_{nj} > 0$

$$I_{nj} = (V_n - V_j) y_{nj} \qquad \forall \{n, j\} \in \mathcal{N} \tag{4.10}$$

For each bus, the power balance equation (4.11) expresses the fact that the power injection has to be equal to the transmitted power over the lines close to each bus.

$$p_n = \sum_{n \sim j} V_n (V_n - V_j) y_{nj} \qquad \forall \{n, j\} \in \mathcal{N} \tag{4.11}$$

By involving a cost function f_n for the power generation at each bus, it is possible to define a total operation cost for the power system

$$h(p) = \sum_{n \in \mathcal{N}} f_n(p_n) \tag{4.12}$$

The fundamental version of the OPF problem comprises of finding the minimum of (4.12) under the equality constraints (4.11) and inequality constraints. The decision variables for this problem are both the voltages V_n and the power injections p_n at each bus. Because of the equality constraints, this is a nonlinear, nonconvex problem. The generation cost functions f_n may be linear or affine. In the simplest case, they all coincide with the identity function $f_n(p_n) = p_n$, in which case the OPF problem is simply to minimize network losses. A more realistic version of the OPF problem imposes additional constraints on the currents through as follows:

$$I_{nj}^{2\,-} \leq I_{nj} \leq I_{nj}^{2\,+} \qquad \forall \{n, j\} \in \mathcal{N} \tag{4.13}$$

Although these constraints are convex, their addition complicates the problem as it turns out that the relaxation procedure applied to solve the original problem is not generally exact if such constraints are included. Contrary to this formulation, [6] assumes the existence of a particular bus with a fixed voltage and an unbounded power injection. Such a bus, called a substation, can be a model of a large power system to which the DC microgrid is considered. It is not a realistic assumption for a standalone microgrid. On the other hand, [6] allows for discrete value sets for the voltages and power injections, that correspond to the case that

some power buses can be turned off ($p_n = 0$) or turned on ($p_n = P_n$). The results in [38] do not allow for such cases. Indeed, the proof of the results depend heavily on the fact that the decision variables take continuous values. The results of the paper follow the same approach as those of [6] except that different assumptions are made. First of all, the OPF problem is converted into an equivalent problem by introducing additional variables as follows:

$$\begin{aligned} v_n &:= V_n^2 \quad \forall n \in \mathcal{N} \\ U_{nj} &:= V_n V_j \quad \forall n \sim j \end{aligned} \tag{4.14}$$

Therefore, the power balance equation (4.11) becomes a linear equality constraint as follows:

$$p_n = \sum_{n \sim j} (v_n - U_{nj}) y_{nj} \qquad \forall \{n, j\} \in \mathcal{N} \tag{4.15}$$

and the voltage constraint converts into the following equation

$$V_n^{2^-} \leq v_n \leq V_n^{2^+} \quad \forall n \in \mathcal{N}$$

the slack variables U_{nj} satisfy the inequality constraint $U_{nj} \succeq 0$ and the equality constraint $U_{nj} = U_{jn}$ for $n \sim j$. The relationship between the v_n and U_{nj}, namely $v_n v_j = U_{nj}^2$ is expressed in an positive definiteness constraint as follows:

$$M_{nj} = \begin{bmatrix} v_n & U_{nj} \\ U_{jn} & v_j \end{bmatrix} \succeq 0 \quad \forall n \sim j$$

with the rank condition

$$\mathbf{Rank}(M_{nj}) := 1 \quad \forall n \sim j \tag{4.16}$$

The first main result of this research states that the change of variables leads to an equivalent optimization problem in the decision variables v_n, U_{nj} and p_n.

Although the new problem is nonlinear and non-convex as well, and in addition involves more decision variables than the original OPF problem, it has significant merit. The only non-convex constraint is the rank condition (4.16), and all the other constraints are convex. The elimination of this condition leads to a relaxed problem that belongs to a subclass of convex optimization problems known as **POP**, for which very efficient algorithms have been devised. Of course, this is only useful if the solution of the relaxed problem satisfies the additional constraints (4.16). This is proved in [6] and [4] under two relatively mild assumptions that hold for practical standalone DC microgrids: all the upper values of the voltages V_n^+ are equal, and the sum of all power injections is positive. Since there is no transmission line that is perfectly lossless, the last assumption is automatically satisfied. Finally, the relaxed problem is converted into another equivalent optimization problem using the Branch Flow Model (BFM) map. This conversion is based on a technique previously developed for AC networks. An extensive presentation of the BFM and its application to the OPF problem for AC grids can be found in [83] and [84], however, it originated earlier in contributions such as [85]. In order to write the BFM, the graph that describes the power network is converted into an oriented graph by assigning an arbitrary orientation to each edge (i. e., transmission line). In this research, the orientation of the edge $n \sim j$ is from n to j if $n < j$, and in this case the edge is denoted $n \to j$. For each oriented edge $n \to j$, a new decision variable is introduced

$$l_{nj} = (v_n - U_{nj} - U_{jn} + v_j)y_{nj}^2 \qquad \forall n \sim j$$

By the definition of v_n and U_{nj}, $l_{nj} = (V_n - V_j)^2 y_{nj}^2$ is the square of the current through the line. Also, for each edge $n \sim j$,

$$P_{nj} = (v_n - U_{nj}) y_{nj} \quad \forall n \sim j$$

is the power flow through the line. With these new decision variables, the variables U_{nj} are eliminated and a new optimization problem can be written in terms of v_n, p_n, P_{nj}, l_{nj}. The power balance equation becomes

$$p_n = \sum_{n \sim j} P_{nj} \quad \forall n \in \mathcal{N}$$

the limit constraints on p_n and v_n are unchanged. In addition, three equality constraints have to be added for each oriented edge $n \to j$

$$\begin{aligned} P_{nj} + P_{jn} &= z_{nj} l_{nj} \quad \forall n \to j \\ v_n - v_j &= z_{nj}(P_{nj} - P_{jn}) \quad \forall n \to j \\ l_{nj} &= P_{nj}^2 / v_n \quad \forall n \sim j \end{aligned}$$

where $z_{nj} = 1/y_{nj}$ is the impedance of the transmission line. A new optimization problem is obtained that is equivalent with the original OPF problem. Its convex relaxation is obtained by substituting the last equality constraint with an inequality constraint

$$l_{nj} \geq P_{nj}^2 / v_n \quad \forall n \sim j$$

The problem that is obtained in this way is a **POP** that is better conditioned than the previous relaxed problem. The fact that the two relaxed problems are equivalent is proven in the paper as Theorem 3. Considering current line constraints is equivalent to add to the set of the inequality constraints

$$l_{nj} \leq \bar{I}_{nj}^2, \quad \forall n \sim j$$

It is argued that including additional constraints may render the relaxed problem inexact, though we provide sufficient cases for exactness formulated in [6] and [4]. However, these cases enforce serious limitations on the networks. Essentially, in both cases, the line current constraints are traded for the constraints on the power injections. Intuitively, if there is a possibility to reduce the generated or the demanded power levels, or to skip the power constraints altogether, the bounds on the line currents can be circumvented without affecting the exactness of the relaxation.

4.6 Numerical Experiments and Discussions

In this section, we have empirically examined the research approach to evaluate that both the POP exactness and its computational time for all four different configurations, whether they are reliable and sufficient or not, to solve a large power system. The simulations were carried out on a desk-computer with 16GB RAM and 3.50 GHz CPU, the proposed problem was tested for the IEEE 30-bus test system (all values are assumed to be in per-unit), running a 64-bit Windows 10 professional operating system. In this system, the lower and upper limits of the voltage are set to be in per unit of 0.95 and 1.05, respectively. In this study, the main objective is to reduce the total network loss and the problem is solved via **GloptiPoly** [86], and the test network is modified from the Matlab environment using **Yalmip** [87] as an interface to the semi-definite programming by disregarding both the reactance in transmission lines and reactive power flows. The results are summarized and compared to each configuration in the following figures **4.2** and **4.4**.

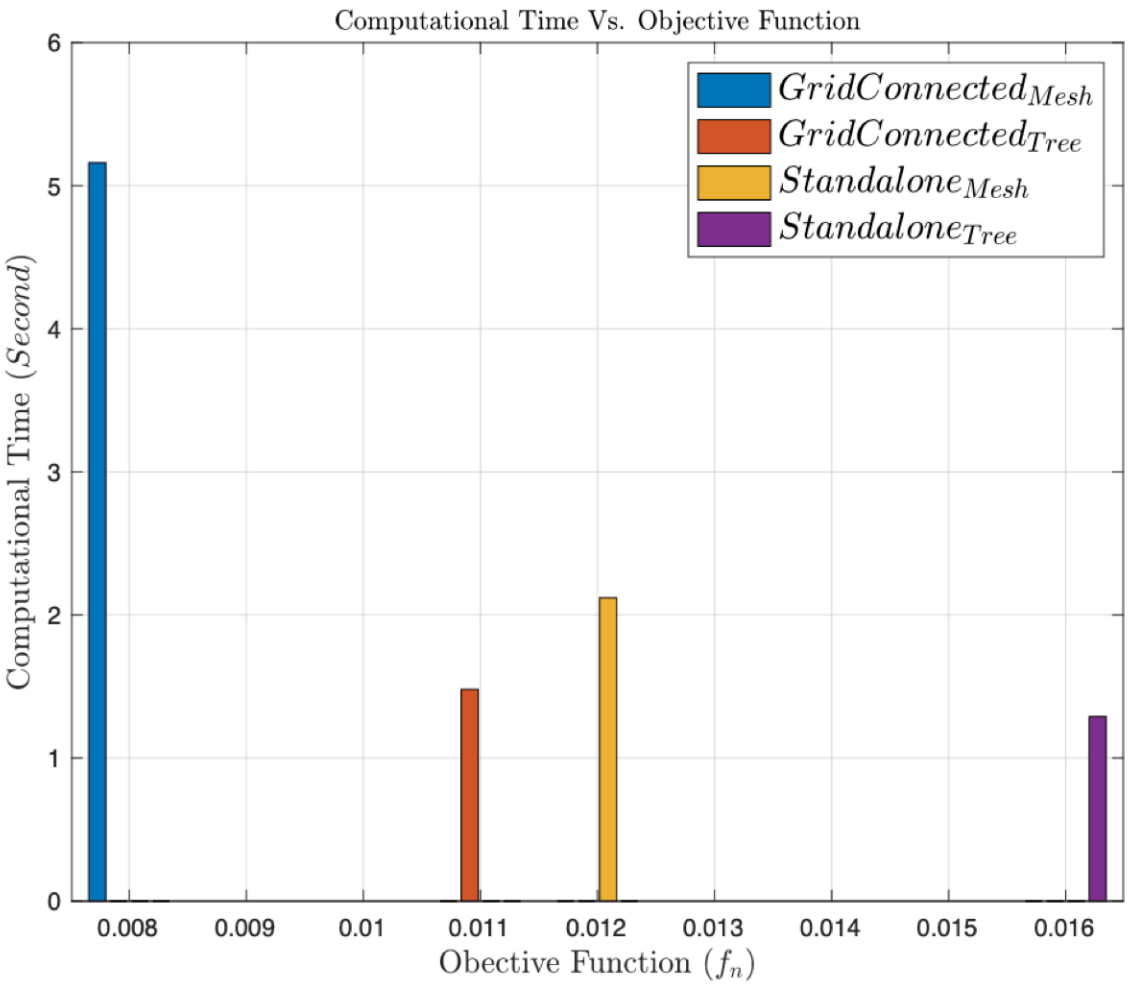


Figure 4.2: This figure depicts the results of the IEEE 30 bus test system.

From this figure **4.2**, it can observe that the proposed relaxation method does not rely on power network topology and/or operating modes. The the object function which indicates that the mesh network topology can minimize the total network losses in both operating modes with the capability of handling high nodal voltage values. Also, the computational time indicates that the solver takes less time compared to other approaches where the minimum total network losses of the system reached in all cases is due to having a better memory and machine. It can

be also noticed that the grid-connected mode, in both network topologies, faces slightly fewer network losses compared to standalone mode, since more power is received from power sources in terms of high nodal voltage values. **Fig.4.3** shows that the outcomes of received power profiles at each bus.

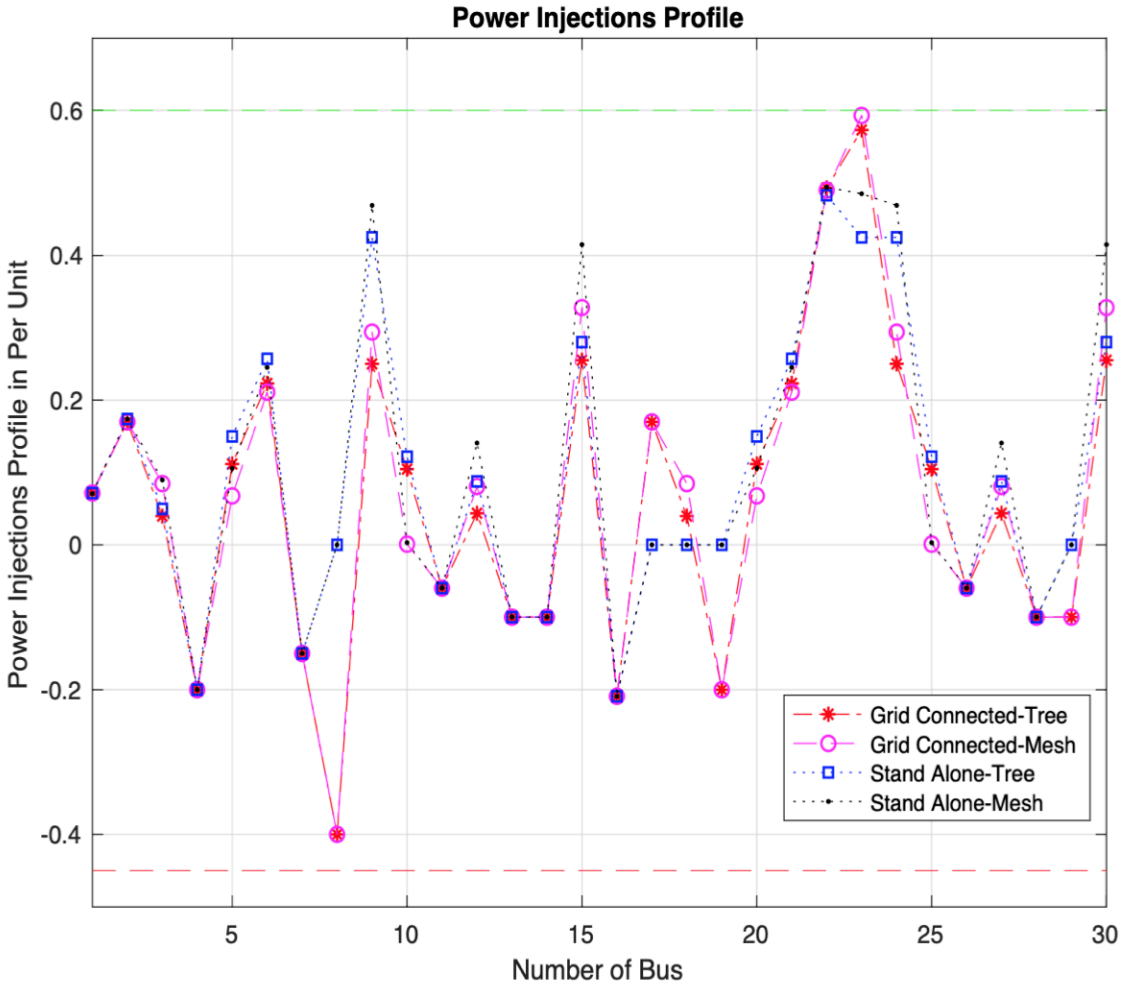


Figure 4.3: This figure depicts the power injection profiles.

Based on the results, it is illustrated that our experiments offer better results in each case and shorter conversions for the relaxed problem. Therefore, we can indicate that the suggested approach can handle the non-convexity of the power system and can satisfy the network constraints, even if some constraints are added. The figure **4.2** shows the results where the line constraints are included and indicates that no case was found in which the relaxation is not exact.

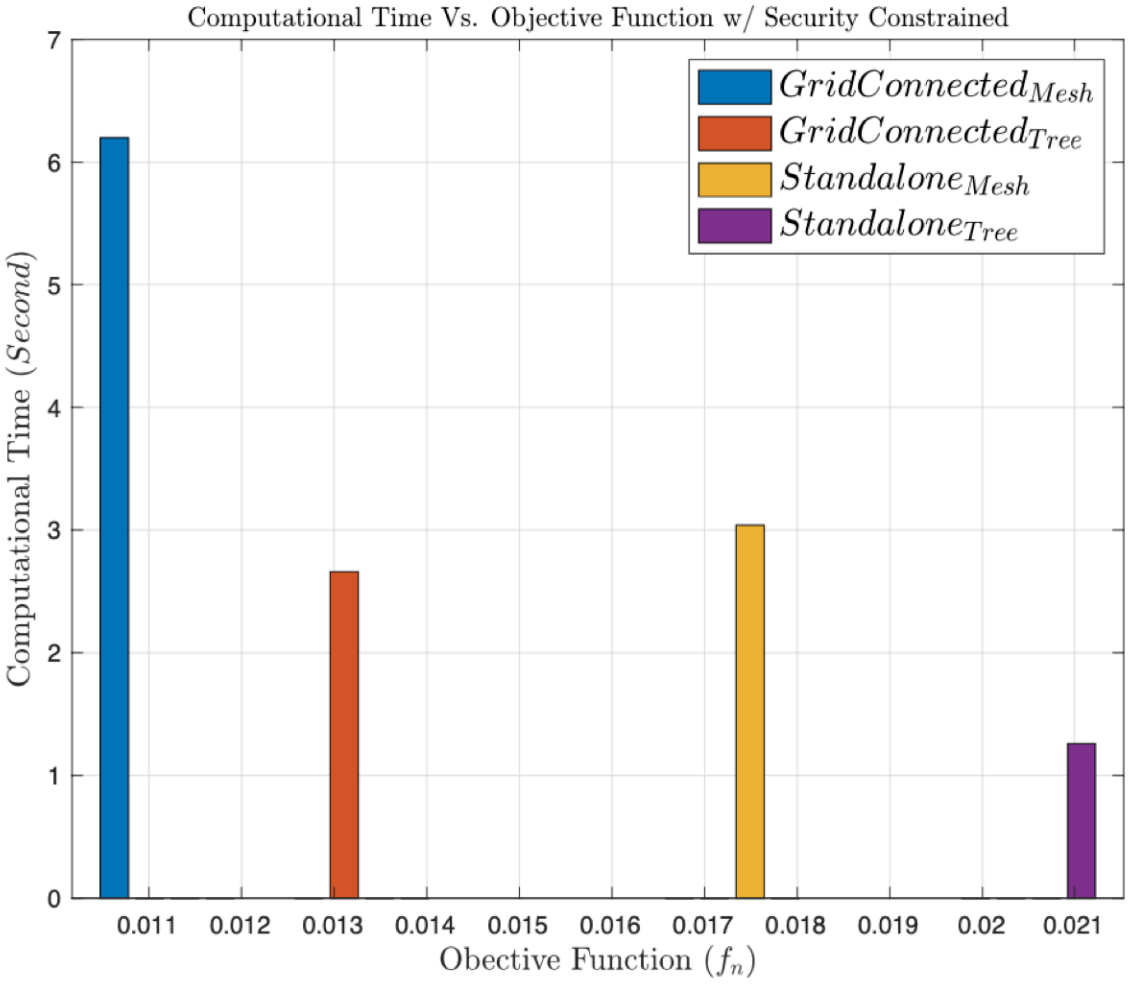


Figure 4.4: This figure depicts the results of the IEEE 30 bus test system

The following **Fig.4.5** shows the average voltage profiles for each different configuration on each bus. There are two dotted lines which show the maximum and minimum limit of voltages (i.e., 0.95-1.05p.u), respectively. Upon close examination, it can be noticed that the average voltage profiles in all configurations are within the system limits.

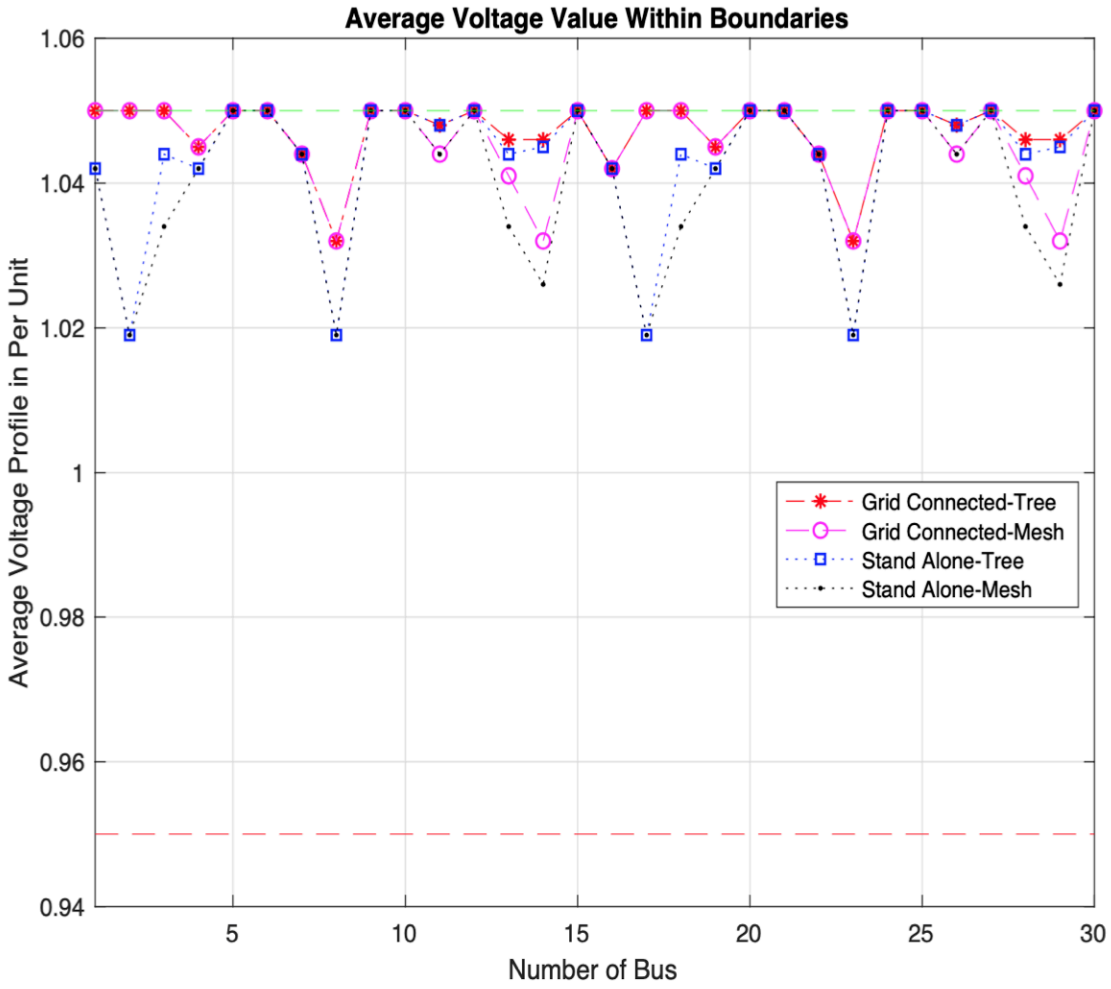


Figure 4.5: This figure depicts the nodal voltage profiles.

4.7 Conclusion

This research paper aimed at improving the use of the standalone DC-microgrid system to the world by minimizing common issues, e.g., global warming emissions and the increasing cost of power systems. This study focused on one of the major issues in power network operation, which is the OPF problem in the DC system, to economically schedule the demand and provide enough energy so as to minimize the power network costs and losses during the entire time horizon. Indeed, the OPF problem is hard to solve since power flow is governed by nonlinear physical laws. Therefore, this paper proposed a polynomial optimization problem (POP) relaxation based on optimization approaches to solve the non-linear aspect of the OPF problem in a DC power network. The paper discussed how to improve the numerical stability of POP relaxation by considering different variables to avoid ill-conditioned numerical operations. Moreover, in this research study, an assumption has been made by considering line constraints on the DC network to theoretically improve that POP relaxation can effectively satisfy the original power flow equations.

Based on the numerical results, it can be indicated that the proposed approach does not depend on the operating mode of grid and network topology. We believe evaluations such as this achievement will strengthen the use of this convexification approach to be applied in large scale systems to reduce energy expenses and network system losses.

4.8 Future Work

In this chapter, several future trends can be addressed to model a power system that can be efficiently utilized to enhance the performance of a multi-power systems' sources. These future research studies can be exposed and split into two

subcategories and then one or two of these subcategories shall be emphasized in detail as a tendency driving the future of this research paper.

- It is important that the microgrid protection controllers are developed to guarantee that the power network systems are more efficient and reliable to meet the required loads without any intermittency issues. This development of microgrid protection controllers offers smooth electricity operations under any expected or unexpected events, including a blackout.

The protection controller system ought to immediately respond to the network failures and seek another path to continue covering the required loads while ensuring there is no partially or full delays or power outages on the system. For instance, if the power network failures happen in a particular location in the network, the desired response ought to immediately take action and make the decisions to isolate all the components and device units at that specific line or bus, as illustrated in **Fig.4.6**.

Thus, the protection controller should be designed to be more durable, reliable, and adequately rapid to protect the equipment on the network and decrease the disruption that is raised by the fault on the network. Furthermore, the evaluation performance of the protection controller shall be tested based on the number of separate protection zones and the rapidity of discovering the exact place of the fault on the network. Subsequently, quicker procedure communications are highly necessary for ensuring comprehensive network protection through the operational time. For guaranteeing the high efficiency and reliability of the network protection, controller system needs to be designed to dislink all power generators and equipment on the existence of the fault.

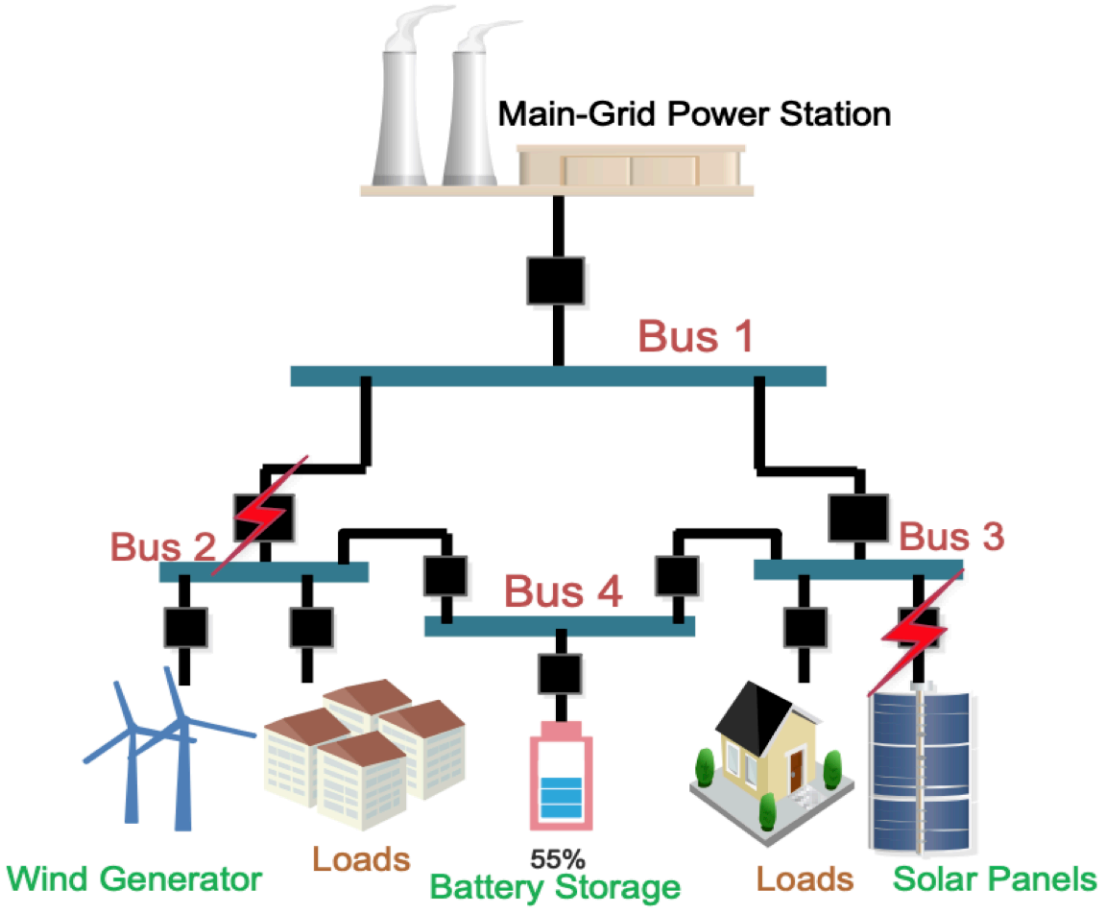


Figure 4.6: This figure depicts a partial power network failure.

In addition, advanced protection schemes are needed to detect and locate the network failure in different modes of operation, e.g., grid-connected and islanded modes. Consequently, the major philosophy of both modes of operation is fairly identical. However, there are some requirements that have to be considered based on, in some cases, how the relay switches are designed and the current value on the circuit that it is allowed to pass through the switches for these two modes. The designations for these relays, i.e, upon circuit breaker (CB) switches, shall be considered in a future study. To achieve perfect outcomes for this future study, a

knowledgeable developer with a very solid background in both programming and the electrical power system transmission and distribution are required to carefully handle this case study.

- The energy storage system, on the other hand, has seen many exciting upheavals and successes. The main function of an energy storage system is to coordinate with the main utility power system to ensure the microgrid generation sufficiency and also to minimize the energy expenses.

The energy storage systems will be valuable to assist in managing the power system and significantly essential for various stimuli. A number of these major aspects will be based on the measuring of the energy storage, an optimum lifespan for the battery, and optimal energy storage charging/discharging techniques. For instance, hydro pumps are considered as the earliest type of energy storage, where the fundamental approach is based on that idea that the power is stored in the form of water in an impoundment, whereas batteries store electrical energy in their chemistry. Moreover, energy storage systems can be considerable microgrid constituents which promotes the prime grid system in various paths, such as keeping the flow of the electricity to support the demand loads and reduce the cost of both transportation and fuel, etc. Therefore, this energy storage will be designed to give the storage unit the capability to interact expeditiously to any unexpected transitory power alterations in grid-connected operations and to maintain a full charge. This approach will provide numerous advantages which can be applied in the microgrid with an incorporation of renewable energy resource systems to minimize cost and to be considered as a standby system for rural regions, as shown above in **Fig.4.6**.

CHAPTER FIVE

AN OVERVIEW OF OPTIMIZATION APPROACHES FOR OPERATION OF HYBRID DISTRIBUTED ENERGY SYSTEMS WITH PHOTOVOLTAIC AND DIESEL TURBINE GENERATOR

Humanity is presently confronting a global energy crisis due to an insufficiency in traditional energy sources while the worldwide energy demands continue to increase. In response to this crisis, improving energy efficiency and sustainability and are becoming critical. Therefore, distributed energy systems are extremely important in terms of having multiple energy sources to meet time-varying consumer demands. Recently, hybrid distributed energy system has become widely applied to raise system reliability and improve power quality instead of depending on one type of conventional energy sources such as diesel generators. Yet, it faces some challenges in its widespread deployment, such as unpredictable nature and intermittently varying renewable energy sources like solar radiation. This issue can be overcome by integrating energy storage that manages the time mismatch between energy production and load requirements. Hence, it is important to review the recent promising approaches for the optimization of hybrid systems to reduce the operation cost and total network losses. This work encompasses a review of the recent optimization approaches for hybrid energy systems with PV, diesel turbine generators, and energy storage systems to give the basis for solving difficult and intricate real-world problems related to distributed energy system operation.

5.1 Introduction

The traditional energy resources, such as fossil fuel, have become rarer as a result of the increase in the electrical load for the community such as commercial area, industrial area, residential area, etc. Considering alternative energy resources

(such as wind energy, solar panel, hydroelectricity, and geothermal energy) is most common in the last decade to improve the power system reliability and efficiency. Renewable energy is being used beside non-renewable energies to cover the required loads and to maximize power efficiency. Therefore, hybrid energy is the most popular option that has been applied to give a better choice than relying on one type of power source in terms of minimizing the cost and improving the power efficiency of the system. The hybrid energy is commonly composed of two or more power sources utilized altogether to offer a greater balance in energy supply. Several types of hybrid energy combinations are convenient to be used but they depend on the power system location and which kind of power sources are available and suitable to be proposed to cover the required demand loads at lowest cost. Therefore, increases in the use of distributed energy systems have risen parallel with price reductions in solar, wind and inverter technologies. Depending on the connection of power systems to the main grid, the power systems can be broadly classified into grid-connected systems and standalone power systems [88]. A standalone power system does not have a connection to the main electricity grid. A grid-connected system is connected to a larger independent grid, typically the public electricity grid, and feeds energy directly into the grid.

By taking the maximum benefits of the hybrid energy system, the microgrid system is one of the key elements in giving the significant momentum to distribute the power generations. The microgrid system is significantly important to ensure smooth operation and high power system reliability. Microgrids consist of a collection of distributed generation systems coordinated with each other in a way that increases the capacity of the system and improves the power quality [89, 90, 91, 92], and [93]. There are some advantages associated with this hybrid energy combination, which can be classified as: technical, economical, and

environmental. From a technical perspective, hybrid energy distributed generation systems can effectively support the energy of remote places and provide very high efficiency while lacking the fixed source vulnerability of large-scale networks, which is a factor in the failure of power systems [94] and [93]. From the economic point of view and according to market research studies, distributed generation minimizes line losses and interruption costs for consumers while reducing fuel cost [95]. The environmental advantages of hybrid energy combination systems are investigated in [96] and include reducing the emissions of pollutants and greenhouse gases and easier integration of clean energy sources. In most recent research, considering the significance of new technology integration and renewable energy insertion to power systems it has been discovered that the reliability aspect is one fundamental issue of progress in sustainable energy.

The reliability of the power system is required due to the adoption of a hybrid energy combination system that allows multiple power sources. One common type of hybrid system is the PV-diesel turbine generator. The system components are PV arrays, diesel turbine, inverter, converter, controller, and energy storage (ES). The schematic is shown in **(Fig.5.1)**. The energy storage will be charged by the solar and diesel turbine and discharged by the loads during the operational time. To be more specific, the power generated from the solar and diesel turbine charges the battery after meeting demand loads but if generated power is lower than demand loads, then the battery will support the loads as per storage capacity. The other fundamental issue of progress in sustainable energy refers to mathematical optimization for the operating and planning of hybrid distributed energy systems.

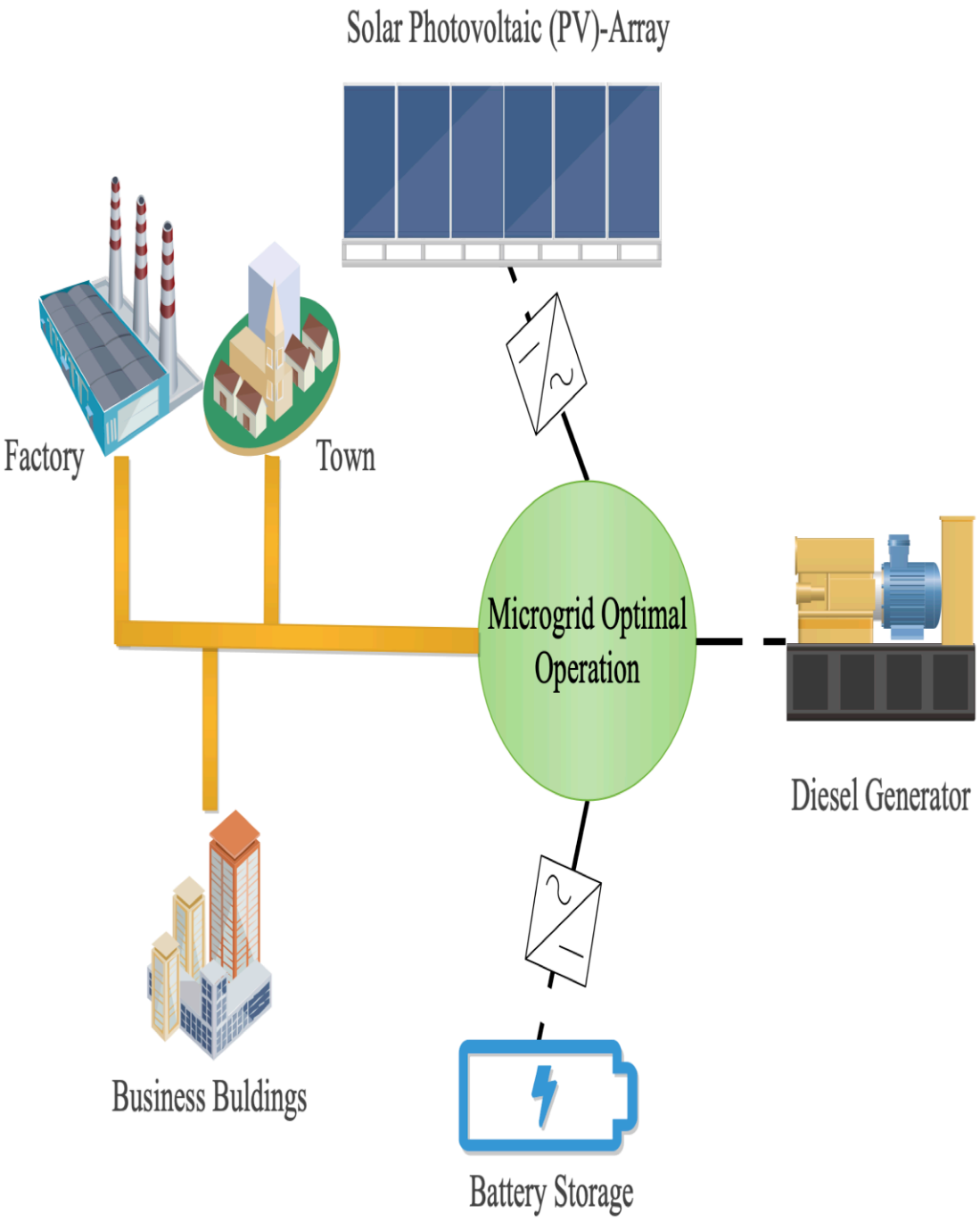


Figure 5.1: Schematic of PV-Battery-Diesel Microgrid systems.

Mathematical optimization has been applied over recent years for many power systems' planning, operation, and control problems. Mathematical formulations of real-world issues are obtained under certain hypotheses, and even with these hypotheses, the results of distributed energy systems are not simple. There are many uncertainties in power system problems because power systems are complex and geographically broadly distributed. More recently, the fluctuation of power sources has inserted new issues into the existing problems. It is highly required for the solution of power system problems to be optimum or nearly optimum, which is the best-known solution among all possible solutions, but the solution searched by mathematical optimization is usually optimum locally. These facts make it hard to deal effectively with numerous hybrid distributed energy system problems through strict mathematical formulation alone.

This review paper considers one type of these hybrid energy combinations which is the solar photovoltaic, diesel turbine generator system, and energy storage. Solar photovoltaic and energy storage are the most popular type of renewable energy source that can be integrated into modern power systems and microgrids (MGs) [97] and [98].

This review paper sheds light on the diverse existing optimization methods applied to the operation of various power sources. The focus is on finding a way of solving the problem of integrating and operating a variety of power units. A synopsis grouping all the discussed optimization methods provided at the end will help to choose the most effective technique to model a similar problem and solve it.

5.2 Optimization Formulation Framework for Hybrid Power Systems

In this section, a brief formulation framework of optimization for hybrid power systems with their objectives, variables, and constraints are discussed. The hybrid power systems are generally designed for the generation of electrical power using a number of power generation devices such as wind turbine, PV, micro hydro and/or other conventional generators using fossil fuels. Such systems can range from small systems capable for providing power for a single home to large systems which can power a village or an island. Hybrid power systems are thought to provide power to many remote communities especially in the developing world where the national grid is economically and technically not viable, as shown in **(Fig.5.1)**.

5.2.1 The Standard Formulation for the Optimization

The Optimal Power Flow (OPF) problem includes minimizing the overall cost of generation while assuring that the Power flow equations are met at each bus of the power system. In addition, voltage, generation, and other constraints are enforced. A detailed outline of the optimal power flow problem algorithms will be explored and described to apply them for solving the OPF problem.

5.2.1.1 Objective Function

The objective function is used to reduce the overall cost of the produced power, occasionally taking into consideration the active transmission losses in the whole or portion of the power network as well. For the convergence, the generation cost functions are considerably approximated by either linear or quadratic functions [99]. In some conditions, the cost is a function of both the generation active and reactive power in the network. Other types of costs which can be comprised in the objective function are power transfer capability, investment cost, load shedding, environmental influence, etc [100]. Throughout the years, some researchers have

defined several optimization objective functions whilst structuring the renewable energy system. A number of the most extensively utilized objective functions, such as cost and reliability, are concisely described in the proceeding section.

A - The Cost Analysis of the Power System

The main objective of operating the renewable energy system is to determine the authentic size of every single component in the system that will meet the minimum cost of load demand with respect to some constraints on the system. In order to assess the cost objective function, the following costs are generally taken into account.

- Cost of maintaining the components.
- Cost of the hybrid system components such as the fuel cell, electrolyzer, and photovoltaic (PV) module etc.
- Cost of replacing faulty system components.
- Cost of fuel throughout the entire lifespan of the system.

Various approaches were applied in assessing the cost of the power system including the net present cost, annualized system cost, levelized energy cost, and lastly life-cycle system cost. The characterization of the cost functions including their formulation will be demonstrated in **Table.5.1**.

Table 5.1: A synopsis of the cost objective functions and their equivalent formulation.

Cost Indices	Definition	Formulation
$\frac{\text{Net present cost}}{\text{Total system cost}}$, Ref. [101]	During the useful lifetime of the system, as a sum of the capital cost, the installation costs, replacement costs, fuel costs, operation, and maintenance cost.	$F(\$) = \sum_{i=1}^{n} N_i \times \left[(CP_i + RC_i) + \sum_{i=1}^{R} OMC_i \times \left(\frac{(1+i_{inflaction})}{(1+i_{rate})}\right)^{l}\right] + C_{inst}$ where, CP_i represents procurement cost, RC_i refers to replacement cost, OMC_i describes operation and maintenance cost, $i_{inflaction}$ refers to annual expected inflation, i_{rate} represents annual interest rate, and C_{inst} is installation cost.
$\frac{\text{Annualized cost of the sys.}}{\text{Total annual cost}}$, Ref. [102]	Describing the summation of the annual capital cost of the system ($A_{cap_{cost}}$), the annual maintenance cost ($A_{main_{cost}}$), and annually replacement cost ($A_{rep_{cost}}$) of all component that form part of the system.	$F(\$/Yer) = A_{cap_{cost}} + A_{main_{cost}} + A_{rep_{cost}}$
Levelized cost of energy, Ref.[103]	The ratio of the annualized cost of the system to the overall electricity generated by the system.	$F(\$/kwh) = \frac{\text{Annualized cost of the system}}{\text{Total annual electricity generated}}$
Life-cycle cost, Ref. [101]	The summation of all one-time (non-recurring) and recurring costs during the useful lifespan of the system. This includes the operating cost, installation cost, initial purchase price of system components, upgrading costs, maintenance, and salvage value.	$F(\$) = \sum_{i=1}^{n}(CC_i + RC_i + OMC_i)$ where, CC_i is representing the capital cost.

B - The Power System Reliability

Reliability indices have been utilized to rate the performance of the power system in several domains of engineering. The main conception of reliability, thus, may not be entirely captured by a particular definition [104]. Power system reliability is realized as the ability of the power system to convey enough electricity to customers in a secure manner. Several of the most broadly and latterly utilized reliability indices are considered while evaluating the renewable energy system performance, including probability of power generator loss, loss of energy expected, loss of load expected, and equivalent loss factor. The description of the reliability indices and their respective formulation is given in **Table.5.2**.

5.2.1.2 Variables

Analysis of the OPF equations exposes two kinds of variables: dependent and decision variables, also known as state and control variables, respectively. In general, the vector state x in the OPF problem represents the electrical state of the network. These can be described as voltage phase angles, voltage magnitudes, active power output of the slack bus only, and reactive power of all generations at every bus, comprising the power loads and line flows. These state variables can be represented as continuous in nature. On the other hand, the control variables u in the OPF problems commonly contain a subset of the state variables and also variables describing control appliance adjustments, such as the active power at the generator buses, tap changes in transformer, position of the phase shifting taps, and the status of the switched capacitors and reactors (switchable VAR sources). The selections of the state variables x are imposed by the structure of Power Flow (PF) equations utilized, whereas control variables vary among OPF formulations depending on the nature of the particular problem [45] and [109].

Table 5.2: A synopsis of the reliability objective functions and their equivalent formulation.

Reliability Indices	Definition	Formulation
Probability of power generator loss, Ref.[105] and [106]	Represents the ratio of the deficit in energy generation to the load demand for an interval of time.	$F = \frac{\sum_{i=1}^{N} \text{Power supply losses}^{(\kappa)}}{\sum_{i=1}^{N} \text{Load}^{(\kappa)}}$
Expected energy not supplied	Represents the energy which is not generated in response to the load demand. It happens as an outcome of an unexpected rise in the load demand that overrides the present generation capacity.	$F = \sum_{S=1}^{8760} \left[\text{Average annual load}^{(\kappa)} \times \text{Duration in which the load is not met}^{(\kappa)} \right]$
Loss of load expected Ref.[102] and [107]	A reliability index that expresses the percentage of load served during the operational period of the system. It is expressed as one minus the ratio of total number of hours in which the system can not serve the load to the operational time of the system	$F = 1 - \frac{\text{Total time load not delivered}}{\text{Total operational hour}}$
Level of autonomy, Ref.[102]		
Equivalent loss factor, Ref.[108]	The ratio of effective forced outage period to the total time of the system operation, in hours. For a standalone system, the acceptable value of the equivalent loss factor is less than 0.1	$F = \frac{1}{T} \sum_{\kappa=1}^{m} \frac{\text{Amount of load not satisfied}^{(\kappa)}}{\text{Load}^{(\kappa)}}$

5.2.1.3 Constraints

Constraints are commonly considered an integral portion of a particular optimization problem playing a critical role in its categorization, for instance, convex vs non-convex. In the OPF problem, the network variables have to be within admissible bounds or else the electrical power network devices can be damaged or cause a malfunction. Typically, the constraints are classified as equality and inequality constraints [45] and [109].

In OPF problems, equality constraints are the power flow system equations [110]. Inequality constraints designate upper and lower bounds on the control and state variables of the devices of the electrical power network and also the bounds required to guarantee network security and stability [111]. The inequality constraints on the state and control variables can be partitioned as follows: the state variables bounds are been on the magnitude angle of voltage, and the power lines. The control variables bounds are on the active and reactive power generation, voltage generation, and transformer tap position. Furthermore, the inequality constraints can also locate forbidden areas of branch flow boundaries, interface boundaries, active/reactive power reserve boundaries, power of the PV power source constraints [112], power of the diesel turbine source constraints, spinning reserve requirements, transient security, transient stability, transient contingencies, environment constraints, rotor angle stability, etc. [113].

I - Photovoltaic (PV) System

In this subsection, the photovoltaic system is discussed and its constraints are introduced. The photovoltaic power generation system consists of one or a set of solar panels incorporated with an inverter device, controller and other electrical components. This kind of renewable energy is used to generate electricity through

solar energy. The photovoltaic power generations are currently implemented on a wide range, with several energy investing companies promoting it. However, it requires a high level of expertise for enforcement, modeling, and improvements. Today, several countries are interested in harnessing their geographical position to install the solar energy to help them reduce cost and support their needs for the electricities. The photovoltaic power generation system is comprised of a photovoltaic array which transmutes the sunlight (photons) falling on it to electrons. This produces a direct current (DC) which can be enhanced with DC-DC converters and then reversed to give an AC power to the loads. Consequently, the most important device in terms of linking the PV to the grid is the power electronic device. Moreover, a particular maximum power point tracking system (MPPT) is needed to vest photovoltaic system to reduce maximum energy from the sun by changing the slanting angle of its beams all throughout the day-time. Lastly, the low-pass filter systems are required to be considered in terms of ignoring unwanted harmonics before it enters the grid.

Most of photovoltaic power generation system are made of semiconductor crystalline materials. Since there are several types of materials that are used to design the PV system, a new material in designing the PV system was discovered to improve the power efficiency of the system, which is known as titanium-oxide coated PV cells. Thus, the PV cells are placed in a group to shape modules which can either be electrically correlated in parallel and/or in series shaping large system with scaled voltages and improved power outputs. The MPPT systems are significantly substantial for optimal absorption of solar energy to maximize the efficiency and reliability of the transformation system. Although the solar insolation may differ naturally during the day-time,the MPPT system regulates the PV array output to produce the highest real power at a fixed voltage. Reactive power control

is done utilizing an inverter controller operating in fixed power factor mode. A silicon PV module output relies on numerous variables comprising the sort of material, temperature, and solar irradiation incident on the surface of the module [114]. Its output can be formulated as following

$$P_{out} = P_{rat} \times \frac{G_c \times [1 + \kappa(T_c - T_{rat})]}{G_{rat}} \tag{5.1}$$

where P_{out} represents the power output of the PV system in W; G_{rat} represents the solar insolation in Wm^{-2}; G_c represents the insolation of the operating point; κ represents the temperature coefficient of the power; P_{rat} represents the rated output generated by the module under standard test conditions in watts [115]. The T_c represents the temperature and it can be obtained as following

$$T_c = T_a + \frac{(N_T - 20)}{0.8} \times S_g \tag{5.2}$$

where T_a represents ambient temperature, S_g represents the global solar insolation incident on a horizontal plane united as kWm^{-2}, and N_T represents the normal operating cell temperature, which is around $48C$. The Assumption that the PV system can be correlated in series and/ or parallel was illustrated previously to improve the output of both the voltages and currents. A matrix of $\mathcal{N} \in (n_s \times n_p)$ represents that the number of models are connected in series (n_s) or parallel (n_p), respectively. The voltage outputs of the PV array V_{pva}, and power of the PV systems P_{pv}, are expressed as following

$$V_{pva} = N_{pvs} V_{Pv} \tag{5.3}$$

$$P_{pv} = n_s \times n_p \times P_{sys} \times \eta_{MPPT} \times \eta_{loss} \tag{5.4}$$

where N_{pvs} represents the serial connection number of the PV modules, η_{MPPT} is the efficiency of the MPPT system, P_{sys} indicates the maximum power output

delivered by the PV system, and η_{loss} is the factor which represents cable resistance and other losses [15]. The local observatories usually provide data on solar irradiance as incident on a horizontal plane. Hence Hongxing et al. [116] employed the Perez model which helps to find the solar irradiance data for slanting planes with the aim to exploit maximum η at any time.

II - Diesel Turbine Generator

In this subsection, the diesel turbine system is discussed with its constraints introduced. Enhancing clean energy, diesel turbine generators are now mainly utilized as standby resources in a hybrid power system. In the situation of failures on the renewable sources and battery systems to provide power to meet the required loads, the diesel turbine generator is brought into action. There are several crucial factors for operating of diesel turbine generator including demand loads, and also the costs of both transportation and fuel, etc. have to be taken into consideration [117] and [114]. An example was considered by Deshmukh and Deshmukh, where they operated engine generator under two situations a one when the diesel turbine generator is directly connected to the demand load and another when it is employed as a battery charger [118]. Overall, the diesel turbine generator efficiency can be expressed as

$$\eta_{\textbf{total}} = \eta_{\textbf{brake thermal}} \times \eta_{\textbf{generator}} \tag{5.5}$$

where $\eta_{\textbf{brake thermal}}$ represents the brake power of a heat engine as a function of the thermal input from the fuel in the diesel engine and $\eta_{\textbf{generator}}$ is the power efficiency of the diesel engine. Indeed, the generator operation at $70 - 90\%$ of full load is discovered to be economical. Hence, diesel turbine generator is beneficial in promoting power during peak demand hours and later for energizing the energy storage units as and when desired. The power constraints for diesel turbine

generators can be written as

$$k_{gen}P_{D_{gen}}^{-} \leq P_{D_{gen}} \leq P_{D_{gen}}^{+} \tag{5.6}$$

the value of k_{gen} sets to be 0.3 based on the manufacturer' suggestion [115]. The minimum and maximum power constraints for the diesel turbine can be represented by $P_{D_{gen}}^{-}$ and $P_{D_{gen}}^{+}$, respectively.

III - Energy Storage System (ESS)

This subsection discusses the energy storage system and introduces its constraints. Exploring energy storage systems from a power management standpoint is going to be considerably momentous for numerous motivations. Some of these major aspects are measuring of the energy storage and optimal charging/discharging procedures. One of the initial sorts of energy storage is hydro pumps, where the power is stored in the form of water in an impoundment, whilst batteries store electrical energy in their chemistry. Furthermore, energy storage is a considerable microgrid constituent which assists the main grid in numerous ways such as ancillary services comprising load following, operational reserve, renewable integration and relieving congestion and constraints. Indeed, energy storage units must have the adequacy to react sufficiently rapid to transient power changes in grid-connected mode and to retain themselves entirely charged. In addition, there are several other applications that can apply energy storage devices in microgrids, comprising consumers energy management (minimize cost) and incorporation of renewable energy sources [119].

- **Model of Battery Source: An example of modelling of a lead–acid**

The battery storage units are described here. At any given time, there are some limitations for the State of Charge (SoC) of the lead-acid battery units which

can be defined as

$$SoC_n^- \leq SoC_n(\kappa) \leq SoC_n^+, \quad \forall n \in \mathcal{N}, \quad \kappa \in \tau \tag{5.7}$$

where SoC_n^+ is the upper limit, and SoC_n^- is the lower limit SoC_n for the battery. Similarly, limits for the output power of the lead-acid battery can be defined as

$$r_n^- \leq r_n(\kappa) \leq r_n^+, \quad \forall n \in \mathcal{N}, \quad \kappa \in \tau \tag{5.8}$$

where r_n^- and r_n^+ are the minimum and maximum allowed charging and discharging power for the battery, r_n is positive when discharging, and negative for charging. The SoC_n value at time $(\kappa + 1)$ is related to SoC_n value at time κ by the following equation:

$$SoC_n(\kappa + 1) = SoC_n(\kappa) + \alpha_n r_n(\kappa), \quad \forall n \in \mathcal{N}, \quad \kappa \in \tau \tag{5.9}$$

where α_n denotes the time interval $[\kappa, \kappa + 1]$. Assuming the initial energy stored is $SoC_n(0) \geq 0$ at each bus $n \in \mathcal{N}$. In Equation (5.9), the battery SoC at the end of current time interval is equals to the SoC at the end of last time interval plus the energy charged minus the energy discharged during current interval. The energy storage outputs are subject to power factor limits in both charging and discharging states as in Equations (5.8). The charging and discharging rates are both assumed to be 90%, according to the practical situation of the Dongfushan Island system [120]. Today we are able to generate only less than 20% of the volumetric capacity from batteries [120, 121, 122]. Battery storage units technology is a fast growing area where there is vast opportunity to harness the power extracted from renewable sources. In spite of its poor efficiency, hydrogen storage systems will become competitive in the near future due to increasing fossil fuel prices and reduced lifetime of battery storage units. Similarly, all other energy storage are also seeing

rapid increase in research and development to improve overall efficiency of stored energy both economically and in an Eco-friendly manner.

IV - Network Constraints

In this subsection, we present two mathematical models of the power system networks and show their equivalence. Let the set of buses be $\mathcal{N}$:=$\{1, 2, 3, .., n\}$, the set of transmission lines $\mathcal{E} \subseteq \{\mathcal{N} \times \mathcal{N}\}$ of edges. Then $n \sim j$ denotes a line between the buses n and j. The general bus injection model is defined by the following power flow equations that represent Kirchhoff's laws at each bus

$$S_n = \sum_{j:n\sim j} V_n(V_n^H - V_j^H)y_{nj}^H, \forall n \in \mathcal{N} \tag{5.10}$$

the superscript H denotes hermitian transpose. Let the set of solutions of the power flow V for each S to be:

$$\mathcal{V} := \{V \in C^{(n+1)} |\ V \text{ satisfies } (5.10)\} \tag{5.11}$$

The buses in the power networks can be divided into three classes: slack, generation, and load buses. The next quantities are generally identified at each bus: voltage phase angles δ, voltage magnitudes $|V|$, active power output of the slack bus only P_s, and reactive power of all generations Q_n. Usually the voltage magnitudes and the angles are described by one complex variable V rather than real and imaginary variables. Let us now consider the general power network modeled by the subset of buses $\mathcal{N}$:=$\{1, 2, 3, .., n\}$, the set of transmission lines $\mathcal{E} \subseteq \{\mathcal{N} \times \mathcal{N}\}$ of edges, and the set of generation buses $\mathcal{G} \subset \mathcal{N}$.

- $P_n^d + iQ_n^d$: Complex power of the load connected to bus $n, \forall n \in \mathcal{N}$.
- $P_n^g + iQ_n^g$: Complex power output of the generator connected to bus $n, \forall n \in \mathcal{N}$

- V_n: Complex voltage at bus $n, \forall n \in \mathcal{N}$.

- y_{nj}: Admittance of the transmission line $(n, j) \in \mathcal{E}$, $y_{nj} = g_{nj} + ib_{nj}$.

Define V, P^g, Q^g, P^d and Q^d as the vectors formed stacking, in lexicographical order the values at all the buses of the corresponding variables V_n, P_n^g, Q_n^g, P_n^d, and Q_n^d $\forall n \in \mathcal{N}$, respectively. Assume $f_n(\cdot)$ is a convex function representing the cost associated with bus $n \in \mathcal{N}$. The objective is to minimize the total cost of the system. This problem can then be formulated as follows:

$$\min_{P_n^g, V_n} \quad f = \sum_{n \in \mathcal{N}} f_n(P_n^g) \tag{5.12}$$

subj. to (5.13)

$$|V_n^-| \leq V_n(\kappa) \leq |V_n^+|, , \quad \forall n \in \mathcal{N}, \quad \kappa \in \tau \tag{5.14}$$

$$P_n^{g-} \leq P_n^g(\kappa) \leq P_n^{g+}, \quad \forall n \in \mathcal{N}, \quad \kappa \in \tau \tag{5.15}$$

$$Q_n^- \leq Q_n(\kappa) \leq Q_n^+, \quad \forall n \in \mathcal{N}, \quad \kappa \in \tau \tag{5.16}$$

$$V_{pvn(\kappa)} = N_{pvs} V_{pvn(\kappa)}, \quad \forall n \in \mathcal{N}, \quad \kappa \in \tau \tag{5.17}$$

$$k_{gen} P_{Dgen_n}^- \leq P_{Dgen_n}(\kappa) \leq P_{Dgen_n}^+, \quad \forall n \in \mathcal{N}, \quad \kappa \in \tau \tag{5.18}$$

$$P_{pv_n}(\kappa) = n_s \times n_p \times P_{sys_n}(\kappa) \times \eta_{MPPT}(\kappa) \times \eta_{loss}(\kappa), \quad \forall n \in \mathcal{N}, \quad \kappa \in \tau \tag{5.19}$$

$$P_{pv_n}^- \leq P_{pv_n}(\kappa) \leq P_{pv_n}^+, \quad \forall n \in \mathcal{N}, \quad \kappa \in \tau \tag{5.20}$$

$$SoC_n^- \leq SoC_n(\kappa) \leq SoC_n^+, \quad \forall n \in \mathcal{N}, \quad \kappa \in \tau \tag{5.21}$$

$$r_n^- \leq r_n(\kappa) \leq r_n^+, \quad \forall n \in \mathcal{N}, \quad \kappa \in \tau \tag{5.22}$$

$$SoC_n(\kappa + 1) = SoC_n(\kappa) + \alpha_n r_n(\kappa), \quad \forall n \in \mathcal{N}, \quad \kappa \in \tau \tag{5.23}$$

$$|V_n(\kappa) - V_j(\kappa)| \leq \Delta V_{nj}^+(\kappa), \quad \forall (n, j) \in \mathcal{E} \tag{5.24}$$

$$P_n^g(\kappa) + Q_n^g(\kappa) = P_n^d(\kappa) + Q_n^d(\kappa) + r_n(\kappa) + P_{pv_n}(\kappa) +$$
$$P_{Dgen_n}(\kappa) + V_n(\kappa) \sum_{j:n\sim j}^{n\in\mathcal{N}} \Big\{ V_n(\kappa) - V_j^H(\kappa) \Big\} y_{nj}, \quad \forall n \in \mathcal{N},\, \kappa \in \tau \tag{5.25}$$

In this formulation P_n^g and Q_n^g are controllable variables, and P_n^d and Q_n^d are given external disturbances. The solution will give values of P_n^g and Q_n^g, at every bus, that minimize the cost and satisfy the physical and operational constraints of the network. In the remainder of if we specialize to only DC power systems the Q_n^g $= Q_n^d = 0$ and the constraints are P_n^-, P_n^+, P_n^d, V_n^-.

5.3 Types and Approaches of Optimization in Power System Operations

This section offers an overview of optimization approaches for power system operation and energy management in two aspects, namely, different operation characterization of aspect and the preferable of the optimization approaches based on the power operation problem. It also explains the advantage of optimization methods in terms of simplifying the power system operation problem from three different aspects, namely generation, control, and demand. Then, the deterministic, stochastic, and hybrid approaches are reviewed, and a comparison between the advantages and disadvantages of is summarized.

5.3.1 Types of Optimization

In this subsection, we define the optimization problem as it is used to obtain the best solution from a cluster of feasible solutions from three different aspects, namely generation, control, and demand. Power system optimization problems are very hard to solve because power systems are very large, complex, geographically widely distributed and influenced by many unexpected events, in terms of both

quality and reliability. It is, therefore, necessary to employ efficient optimization methods to solve the power system operation problem. Any stage in the microgrid system operation such as controlling, operating, maintaining, and scheduling calls for the application of optimization in multiple domains.

I - Generation Aspect

In order to operate a hybrid power system, a full study on determining a way to integrate a different power source and operate a multi-power generation system is crucial. In this case, the optimization tools and techniques have been widely considered and applied to improve the capability and efficiency of the hybrid power systems via reducing the annualized cost and the probability of power supply loss [123, 124, 125, 126, 127, 128]. There have been several research studies in terms of integrating a multi-power generation system and most of them have been done utilizing diverse optimization approaches [129, 130, 131].

II - Control or Operation Management Aspect

The control or operation management of a microgrid offers enormous intricate decision-making domains where optimization techniques can be suitable to consider in terms of conveying reliable, secure, and high-quality power to the customers at all operational times. Optimization techniques are used to manage the energy between power generation, load, and energy storage, providing a stable and efficient renewable power system. A dynamic method based on a numerical model for a real-time optimal solution for control management of a hybrid system integrating hydro-power, wind power, and fuel cells was proposed in [132]. The most substantial decision is to determine the best operating modes of the microgrid system i.e., whether to remain connected to the main grid or to produce energy in

island mode at any given point of time. Another important decision is about the power required to be controlled midst the alteration of operating modes. In the microgrid system, there are mainly three phases of control technique which have to be considered, namely, primary, secondary and tertiary control phases. Several research works have discussed and studied the system behavior during the exchange between connected and island modes taking into account the three phases of control techniques in detail [133, 134, 135]. In this work [136], for instance, a hardware communication-less control technicality is discussed in terms of exchanging operating modes of the microgrid system. Moreover, an analysis of the operation of the microgrid has been investigated by [127]. The analyzing in this study was done by optimizing controller parameters, power-sharing coefficient, and damping resistance during two different modes of operation, while connecting or disconnecting to the main grid and also considering load variations. An optimal power control scheme based on a real-time self-tuning approach is investigated by [137]. The parameters considered for the performance assessment are both the voltage and frequency regulation and power- sharing. The system performances are rated while considering alteration operation mode of microgrid especially when there are unexpected load variations. More analysis is done by [138], in which a real-time self-tuning of power controller parameters for voltage source inverter-based distributed generators were also evaluated to guarantee minimal integral time absolute error whilst exchanging power evenly with the main grid power system.

III - Demand Aspect

From the demand aspect, the principal missions of scheduling demand tracking and optimal energy management offer a considerable scope of research. A probabilistic framework based on $2m$ point estimate approach, to examine the

uncertainties in the optimal energy management of the microgrids comprising diverse renewable power sources, is proposed by [139]. Scheduling and dispatching of the generated power whilst reducing the emission costs are studied in [140, 141, 142]. While the former work utilized a niching genetic technique to minify both the cost of emissions and operations, the latter applied the differential evolutionary technique for heat balancing in a combined heat power in accordance with microgrid systems. More details can be found in [143] and [144], for evolving a novel economic dispatch utilizing a hybrid genetic technique.

5.3.2 Optimization Approaches

This subsection includes some recent optimization approaches that should enable us to solve power system operation problems. For this, it is necessary to optimize the operation of a power system, minimizing or maximizing one of its multi objectives such as the total power cost, power loses, power system stability, etc.. This kind of operation problem can be solved based on the choice of optimization technique [145]. It is significantly substantial to carry out a systematic optimal solution process. The degree of precision and the realistic optimal result alters with the adopted technique. There are a lot of efforts that have been put down to develop such a technique that can be used to solve this kind of problem [115, 138], and [145]. The researchers generally agree that there are mainly two unique sorts of optimization approaches, namely; deterministic and stochastic approaches [146]. In this review paper, a third optimization approach is also introduced to solving more complicated optimization problems. Hereafter, a brief synopsis of the approaches is presented in **(Fig.5.2)**. An overview of the most recent approaches adopted in literature is discussed below.

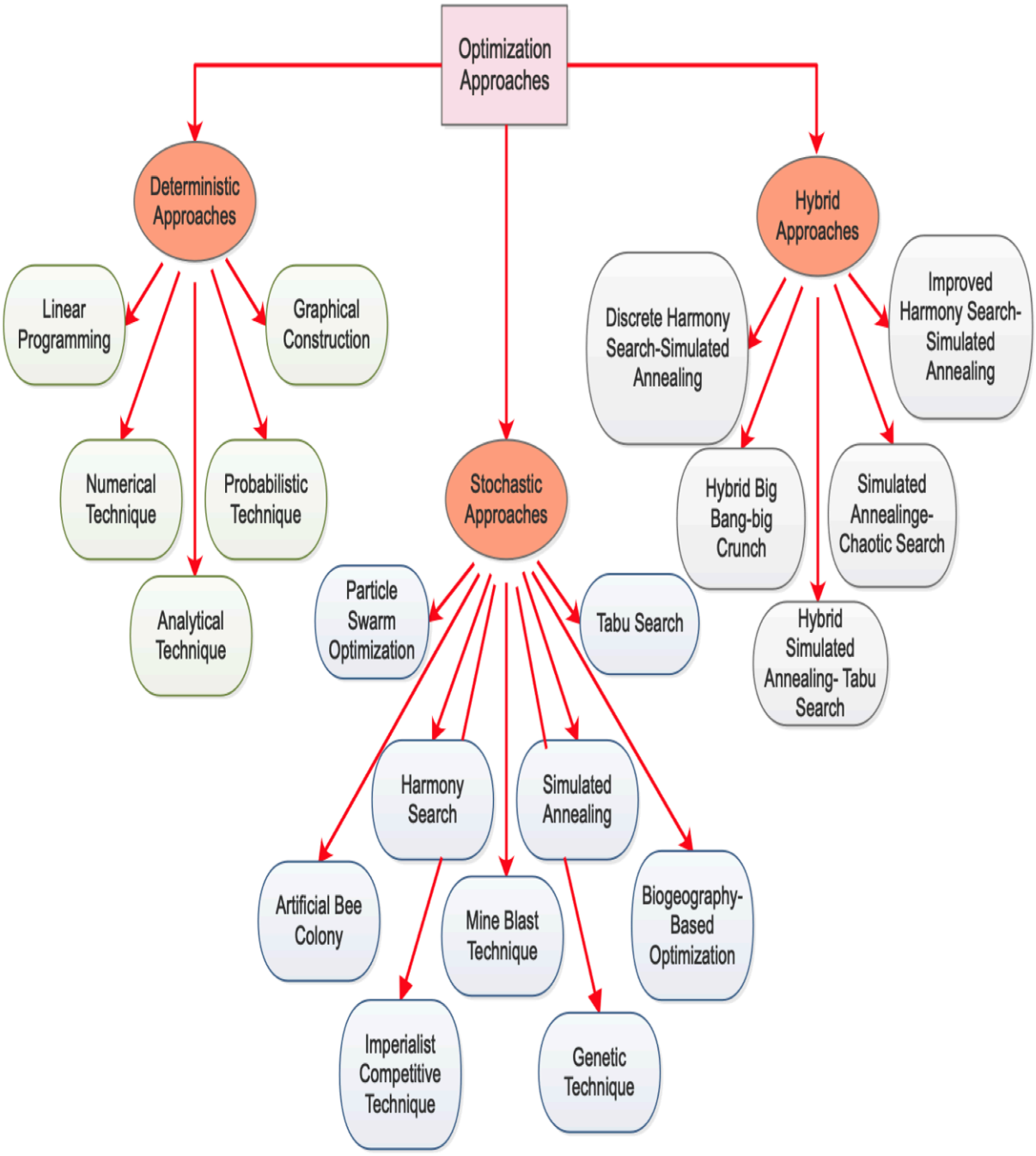


Figure 5.2: Diversity of Optimization Approaches.

I - Deterministic Approaches

The deterministic approaches consist of some techniques such as linear programming, graphical construction, numerical, probabilistic, and analytical techniques, etc. [146, 108], and [147]. The deterministic approaches apply the analytical characteristics of the problem to produce a positive definite sequence of points and converge in probability to a global minimum solution. The deterministic approaches always seek the local solution space based on a deterministic procedure and entirely employ the analytical characteristics of the problem, which effectively enhance computational efficiency [148]. The exhaustive technique is a deterministic approach that usually seeks in a discrete space by assessing all potential minimum solutions and choosing the most minimal or best one. This technique has been applied to in renewable energy system in order to lower the initial investment cost of the system in [149]. Due to a huge number of explanatory variables in the exhaustion optimization process, a large amount of time is needed. As a result of this study [149] and [148], the exhaustive method is not appropriate to large scale power problems. A research study has been compared two techniques in research study of distribution electric network optimization, namely, the deterministic voltage control and a novel meta-heuristic technique [150] and [151]. Moreover, a diversity research study in optimization techniques are widely discussed to effectively improve the shortcoming in the distributed energy systems [150]. A research study has been highlighted the most common distinction between a deterministic technique (Sequential Quadratic Programming) and a stochastic technique (Genetic Method)in the optimization of the model parameters of a smart grid energy storage [152].

In [153], an iterative simulation-optimization technique based on a deterministic approach has been considered to optimize a hybrid standalone solar energy, wind turbine, battery storage, and fuel system for four various sites in Iran's territory. The proposed problem was to minimize the overall system cost and reliability based on losses of the expected load indices. In a similar manner, the iterative optimization technique was considered to optimize a hybrid of standalone solar energy, wind turbine, and hydrogen hybrid system for a desalination unit [154]. The main target was to operate the combination of different power sources to meet the required loads at minimum power cost. However, these used techniques may be, in some cases, not adequate especially for problems with many local optima [147]. They are prone to local optima entrapment, meaning they may not be able to meet the point of the global solution. In order to evade entrapment, the techniques are iterated numerous times by randomly picking up an initial condition. Even with these iterations, the outcome result may possibly not be the best solution within a reasonable time due to the high intricacy of the problem [155]. A few research works have considered deterministic techniques and concluded that they have poor accuracy performance. Based on some recent research works, the principle advantages and the disadvantages of the deterministic techniques can be summarized in **Table.5.3**.

II - Stochastic Approaches

Recently, the use of stochastic approaches have been broadly considered in renewable energy operations; because of that renewable energy suffers from what is known as intermittency issues. They have also some advantages over the use of the deterministic approach [156]. These approaches have the ability to solve small or large scale power system operations [157] and [158]. The stochastic approaches have

a variety of methods that have been widely used; they are presented in **(Fig.5.2)**. In contrast with the deterministic approaches, the stochastic approaches only depend on utilizing random operators to avert entrapment in local optima. The stochastic approaches also have the ability to highly accurately locate the global optimum solution to a problem.

The particle swarm optimization is a population-based stochastic optimization technique improved by [42] and [159] in 1995, inspired by the social behavior of bird flocking or fish schooling, and is a swarm-based technique. The particle swarm optimization participates in many symmetries with evolutionary computation techniques such as genetic technique. The particle swarm optimization is rapid in convergence, simple and not complicated to apply [147]. This technique has been implemented in recent research work in terms of optimally operating renewable energy systems, where the system reliability is evaluated based on the probability of power supply loss [160]. A dynamic multi-objective particle swarm optimization is suggested for the operation of a hybrid standalone system. The main objective of this work is to keep the entire power system operating in the different subsystems in order to reduce fuel emission and the net present cost of the system. In this work, sensitivity analysis is performed on the system to examine the impact of changing input parameters on the optimal solutions obtained. Another research work considers the same method to operate a hybrid power system of wind turbines, solar, and hydrogen energies [161]. The principal goal of this research work is to ensure a highly reliable system that can power loads for an interval of twenty years. The proposed system is optimized based on both annualized cost of the system and loss of load expected, and it is found that the suggested approach yields a better outcome comparing to the deterministic approach.

The artificial bee colony method, in addition, has been developed to solve many real-life power system operation problems [162]. The idea of this method is motivated by the intelligent foraging behavior of honeybee swarms, suggested by [163] in 2005. In the artificial bee colony, a population-based method, the location of a food source depicts a potential solution to the optimization problem and the nectar amount of a food source corresponds to the quality (fitness) of the associated solution [164]. There are several research works that have employed the artificial bee colony method to a standalone hybrid power system [164]. The goal of this work is to integrate and optimize a multi-power system to economically provide energy and meet the loads. Another research work considers the multi-objective artificial bee colony method to locate the optimal operation of the power system with wind turbines, solar, and fuel cell energies [165]. The main target of the optimization is basically to reduce losses and the cost of the system while maximizing the voltage stability indices of a 33-bus distributed generation.

Moreover, another method is based on a music-based meta-heuristic optimization algorithm, known as a harmony search [166]. This kind of optimization algorithm was motivated by the realization that the purpose of music is to seek for the best situation of harmony [166]. The process of finding harmony in music is similar to the process of determining the optimal solution in optimization procedures. The search procedures in optimization can be contrasted to a jazz musician's improvisation procedures [166]. In [167], the harmony search method is proposed to optimize a distributed generating source consisting of some power system sources such as wind turbines, solar, and fuel cell energies. The main goal of this work is to reduce some objective functions such as the energy cost of the system, power losses, and carbon dioxide emission while maximizing the voltage

stability indices. This research work shows, as a result, that the used algorithm achieves better performance as contrasted with different algorithms [167].

Another optimization algorithm, the evolutionary algorithm, is inspired by imperialistic competition. Like other evolutionary ones, the proposed algorithm begins with an initial population of individuals which is known as a country [168]. The population individuals can be broken down into two types, namely, colonies and imperialists, that both define some empires. Imperialistic competition amidst these diverse empires forms the root of the evolutionary method. Throughout this competition, weak empires break down and robust ones take the property of their colonies [168]. There are several research works that have applied this imperialist competitive algorithm in terms of operating and planning such power systems. One of them is done by [169], where fuzzy logic and then imperialistic competition algorithm were used to optimize a hybrid standalone power system in order to reduce the air emission and net present cost while improving the reliability of power system. As a result of this proposed study, it demonstrates that it is likely cost-effective in grid-connected mode but not in standalone mode [169]. Based on some recent research works, comparison of the advantages and the disadvantages between both the stochastic and deterministic approaches is already summarized in **Table.5.3**.

Table 5.3: A synopsis of the advantages and disadvantages of deterministic and stochastic optimization methods.

Optimization Techniques	Advantages	Disadvantages
Deterministic Approaches	**A-** Efficient on single power systems. **B-** Not computationally expensive. **C-** Reliable in obtaining the same solution. **D-** Require fewer objective functions.	**A-** Not efficient on multi-power systems. **B-** High reliance on the initial solution. **C-** Low accuracy of locating the global optimum. **D-** Not effective for problems with computationally expensive derivation.
Stochastic Approaches	**A-** High efficiency in both single &multi-power systems. **B-** Avert local solutions. **C-** Low reliance on the initial solution. **D-** High accuracy of locating the global optimum solution.	**A-** Computationally expensive. **B-** Not fast on convergence. **C-** No exact answer is to be given for each iteration

III - Hybrid Approaches

As the complexity of power system operation grows, the hybrid technique is widely considered to solve non-convexity problems. Therefore, the hybrid approaches are highly required for more sophisticated and precise optimization techniques to be used in order to maintain pace with the swift progression on the use of renewable energy integration. Consequently, a lot of efforts have been recently made to develop such an optimization technique, called hybrid optimization approaches, to be applied in the renewable energy operation. Hybrid optimization approaches are basically a merging of two well-known stochastic optimization techniques. This association between two different methods offers a significant feature in such a way as to enhance or emphasize the qualities of both methods in terms of solving complicated optimization problems.

Recently, a new development on hybrid approaches, for instance, has been made by some research works such as Discrete Harmony Search-Simulated Annealing [170], Improved Harmony Search-Simulated Annealing [171], Hybrid Big Bang-Big Crunch [172], Hybrid Simulated Annealing-Tabu Search [173] and [147]. In [174], researchers determined the beneficial standalone hybrid system operation to provide electricity to a housing unit using different approaches separately simulated annealing-harmony search and simulated annealing-chaotic search techniques. In this work, the incorporation of three various renewable energy systems was considered: wind turbines, photovoltaic power generations, and hydrogen fuels. As a result of this study, the system was optimized for the purpose of maximizing the system reliability based on the probability of power generator losses. Therefore, the analysis result shows that the consideration of three renewable energy systems together can be cost-effective for generating electricity to the

housing unit. Using the simulated annealing harmony search technique can offer a more favorable solution in comparison to other techniques.

The novelty of developing the hybrid approach is to define multiple search strategies for enhancing the replacement of the worst solutions from two or/and three algorithms with the best solutions from the other algorithm with consideration of the uncertainty of different parameters. Therefore, the hybrid optimization approach will provide the decision-makers with an effective tool to achieve better management and operation for the power system. This new development of hybrid approaches offers some advantages as following: (1) it has greater success at finding the global optimal to a wide variety of functions; (2) it can be robust and it can rapidly discover and provide a good solution for many combinatorial problems; (3) it can be efficient for solving problems presenting difficulty to find accurate mathematical models; and (4) using the hybrid optimization approach an early convergence and immature solutions can be avoided. Finally, many researchers have recently studied and developed new algorithms to solve various power system operation problems using optimization techniques. However, new hybrid algorithms are highly needed to solve difficult and complicated real-world problems related to power system operation.

5.4 Conclusion

Optimization techniques are a critical key in power system operation, especially for systems with renewable energy. This article reviews the recent optimization approaches for hybrid energy systems with PV, diesel turbine generator, and energy storage systems. The general optimization formulation framework is first presented, including decision variables, constraints, and objective functions, for a better understanding of the operation problem. Then, the deterministic, stochastic, and hybrid approaches for energy system optimization are

reviewed and their advantages and disadvantages are compared. As deterministic methods are not efficient for the large power systems, stochastic methods are becoming more popular. As the complexity of power system operation grows, the hybrid technique is introduced to solve non-convexity problems. This review article sheds light on the important optimization techniques for the operation optimization of hybrid energy systems.

CHAPTER SIX

OPTIMAL POWER FLOW WITH ENERGY STORAGE

6.1 Notation

In this chapter, we first review the notation. A Graph $\mathcal{G}:=\{\mathcal{N},\mathcal{E}\}$ contains a set $\mathcal{N}$ of nodes and a set $\mathcal{E}$ of edges. Each line connects an ordered pair (n,j) of buses. If two buses n and j are connected by a tie line directly, we denote $(n,j)\in\mathcal{E}$ by $n\sim j$. For each bus $n\in\mathcal{N}$, $V_n(\kappa)$ represents its voltage. At each line let y_{nj} represent the conductance between bus $n\sim j$ from n to j. For each bus $n\in\mathcal{N}$, let $P_n^g(\kappa)$ denotes the generation, $P_n^d(\kappa)$ its load demand at time κ and $b_n(\kappa)$ the value of the energy storage at time κ. The energy storage elements are modeled by the difference equation (6.1). It can therefore be considered as the following collection of discrete linear time-varying models (one for each $\tau=\{1,...,(M)\}$), whose state at time κ (going backward in time) is $\kappa\in\tau$. It also can be assumed that T_s represents the time step of the time series. Moreover, $r_n(\kappa)$ represents the value of the power at time (κ) where it charges when $r_n(\kappa)$ has a negative value; $r_n^-<0$. Otherwise it discharges when $r_n(\kappa)$ has a positive value; $r_n^+\geq 0$. In addition, B_n^- and B_n^+ represent the minimum and maximum value of the energy storage, respectively.

6.2 The Optimal Power Flow with Energy Storage

An OPF problem optimizes both variables V and P over the feasible solutions of the bus injection model in (3.3). Additionally, all voltage magnitudes must satisfy (3.9) where the lower and upper bounds are represented by V_n^- and V_n^+. The lower bound of voltage magnitude is assumed to be greater than zero to avoid triviality in the system. The power injection is also bounded, as shown in (3.8), similar to the case of the voltage magnitudes, where P_n^- and P_n^+ are given

bounds on the injections at bus n. We now formulate an OPF with energy storage and time-varying generation costs and demands. As mentioned previously, $b_n(\kappa)$ represents the value of the energy storage at time κ at bus n. The amount of the energy storage is modeled to follow the first order difference equation.

$$b_n(\kappa+1) = b_n(\kappa) + \alpha_n r_n(\kappa), \quad \forall n \in \mathcal{N}, \quad \kappa \in \tau \tag{6.1}$$

where α_n denotes the time interval $[\kappa, \kappa+1]$. Assuming the initial energy stored is $b_n(0) \geq 0$ at each bus $n \in \mathcal{N}$

$$0 \leq B_n^- \leq b_n(\kappa) \leq B_n^+, \ \forall n \in \mathcal{N}, \ \ \kappa \in \tau \tag{6.2}$$

where B_n^- and B_n^+ represent the minimum and maximum value of the energy storage at bus n, respectively. Moreover, the charge rate of the battery are bounded by:

$$r_n^- \leq r_n(\kappa) \leq r_n^+, \quad \forall n \in \mathcal{N}, \quad \kappa \in \tau \tag{6.3}$$

where κ=$1, ..., (\tau+1)$. The power flow constraint at each bus $n \in N$ and time $\kappa \in \tau$ are thus:

$$P_n^g(\kappa) - P_n^d(\kappa) - r_n(\kappa) = \sum_{j:n\sim j}^{n\in\mathcal{N}} \Big(v_n(\kappa) - U_{nj}(\kappa) \Big) Y_{nj}, \forall n \in \mathcal{N}, \, \kappa \in \tau \tag{6.4}$$

where $P_n^g(\kappa)$ represents the generation at bus n at time κ and $P_n^d(\kappa)$ represents its load. Thus, OPF problem with energy storage in DC microgrid can be formulated

as follows:

$$\min_{P_n^g(\kappa),V_n(\kappa),b_n(\kappa),r_n(\kappa)} \quad \sum_{n\in\mathcal{N}}\left\{\sum_{\kappa=1}^{M} f_n(P_n^g(\kappa)) + h_n^{\kappa}(b_n(\tau))\right\}, \forall n\in\mathcal{N}, \kappa\in\tau \tag{6.5}$$

subj. to (6.6)

$$V_n^- \leq V_n(\kappa) \leq V_n^+, \ \forall n\in\mathcal{N}, \quad \kappa\in\tau \tag{6.7}$$

$$P_n^{g-} \leq P_n^g(\kappa) \leq P_n^{g+}, \ \forall n\in\mathcal{N}, \quad \kappa\in\tau \tag{6.8}$$

$$r_n^- \leq r_n(\kappa) \leq r_n^+, \quad \forall n\in\mathcal{N}, \quad \kappa\in\tau \tag{6.9}$$

$$b_n^- \leq b_n(\kappa) \leq b_n^+, \quad \forall n\in\mathcal{N}, \quad \kappa\in\tau \tag{6.10}$$

$$b_n(\kappa+1) = b_n(\kappa) + \alpha_n r_n(\kappa), \forall n\in\mathcal{N}, \kappa\in\tau \tag{6.11}$$

$$P_n^g(\kappa) - P_n^d(\kappa) - r_n(\kappa) = \sum_{j:n\sim j}^{n\in\mathcal{N}} \Big(V_n^2(\kappa) - V_n(\kappa)V_j(\kappa)\Big) y_{nj}, \forall n\in\mathcal{N}, \kappa\in\tau \tag{6.12}$$

- **The Initial Condition (I.C) of b_n at $\kappa = 0$**

$$b_n(0) = \mu_c, \quad \forall n\in\mathcal{N} \tag{6.13}$$

- **The Voltage Reference at bus n_{ref}**

$$V_{n_{ref}}^{ref}(\kappa) = V_0 \tag{6.14}$$

Now, we present the convex formulation of the OPF problem with energy storage:

$$\min_{P_n^g(\kappa),v_n(\kappa),b_n(\kappa),r_n(\kappa),U_n(\kappa)} \quad \sum_{n\in\mathcal{N}}\left\{\sum_{\kappa=1}^{M} f_n(P_n^g(\kappa)) + h_n^{\kappa}(b_n(\tau))\right\}, \forall n\in\mathcal{N}, \kappa\in\tau \tag{6.15}$$

subj. to (6.16)

$$v_n^- \leq v_n(\kappa) \leq v_n^+, \ \ \forall n\in\mathcal{N}, \quad \kappa\in\tau \tag{6.17}$$

$$P_n^{g-} \leq P_n^g(\kappa) \leq P_n^{g+}, \ \ \forall n\in\mathcal{N}, \quad \kappa\in\tau \tag{6.18}$$

$$r_n^- \leq r_n(\kappa) \leq r_n^+, \quad \forall n\in\mathcal{N}, \quad \kappa\in\tau \tag{6.19}$$

$$B_n^- \leq b_n(\kappa) \leq B_n^+, \quad \forall n\in\mathcal{N}, \quad \kappa\in\tau \tag{6.20}$$

$$b_n(\kappa+1) = b_n(\kappa) + \alpha_n r_n(\kappa), \forall n\in\mathcal{N}, \kappa\in\tau \tag{6.21}$$

$$P_n^g(\kappa) - P_n^d(\kappa) - r_n(\kappa) = \sum_{j:n\sim j}^{n\in\mathcal{N}} \Big(v_n(\kappa) - U_{nj}(\kappa)\Big) Y_{nj}, \forall n\in\mathcal{N}, \kappa\in\tau \tag{6.22}$$

$$M_{nj} = \begin{bmatrix} v_n & U_{nj} \\ U_{jn} & v_j \end{bmatrix} \succeq 0, \quad \forall n\sim j \tag{6.23}$$

$$\boldsymbol{Rank}(M_{nj}) = 1 \tag{6.24}$$

where $v_n{:=}V_n^2$ and $U_{nj}{:=}V_nV_j$ $\forall n\sim j$.

Since (6.24) is a non-convex constraint, it must be relaxed to arrive at the convex formulation. Also, f_n has to be a convex function.

- **The Initial Condition (I.C) of b_n at $\kappa = 0$**

$$b_n(0) = \mu_c, \quad \forall n\in\mathcal{N} \tag{6.25}$$

- **The Voltage Reference at bus n_{ref}**

$$V_{n_{ref}}^{ref}(\kappa) = V_0 \tag{6.26}$$

Equation (6.1) is often written in term of the State-of-Charge, $SOC_n(\kappa) := \frac{b_n(\kappa)}{E_{tot}}$, where E_{tot} is the total energy. Hence it is equivalent to

$$SOC_n(\kappa+1) = SOC_n(\kappa) + \alpha_n r_n(\kappa), \quad \forall n \in \mathcal{N}, \quad \kappa \in \tau \tag{6.27}$$

where, α_n is $\frac{T_s}{E_{tot}}$. With respect to SOC inequalities (6.20) became

$$SOC_n^- \leq SOC_n(\kappa) \leq SOC_n^+, \quad \forall n \in \mathcal{N}, \quad \kappa \in \tau \tag{6.28}$$

where

- $f_n(P_n^g)$ is a convex cost function, which represents generation.
- $h_n^\kappa(b_n(\tau))$ represents the terminal cost.

6.2.1 Optimal Power Flow with Line Constraints

It is also possible to limit the current going through any line $n \sim j$. Let I_{nj} be a threshold of the current flow through $n \sim j$, then the line constraint can be formulated as:

$$(v_n - U_{nj} - U_{jn} + v_j) y_{nj}^2 \leq I_{nj}^2 \tag{6.29}$$

which in terms of original voltage variables is:

$$(V_n - V_j)^2 y_{nj}^2 \leq I_{nj}^2 \tag{6.30}$$

Adding (6.29) to the constraints of the OPF problem leads to:

$$\min_{P_n^g(\kappa),v_n(\kappa),SOC_n(\kappa),r_n(\kappa),U_n(\kappa)} \quad \sum_{\kappa=1}^{M}\Big\{\sum_{n\in\mathcal{N}} f_n(P_n^g(\kappa)) + h_n^{\kappa}(b_n(\tau))\Big\},\ \forall n\in\mathcal{N},\quad \kappa(6.31)$$

$$\textbf{subj. to} \tag{6.32}$$

$$v_n^- \le v_n(\kappa) \le v_n^+,\ \forall n\in\mathcal{N},\quad \kappa\in\tau \tag{6.33}$$

$$P_n^{g-} \le P_n^g(\kappa) \le P_n^{g+},\ \forall n\in\mathcal{N},\quad \kappa\in\tau \tag{6.34}$$

$$r_n^- \le r_n(\kappa) \le r_n^+,\quad \forall n\in\mathcal{N},\quad \kappa\in\tau \tag{6.35}$$

$$B_n^- \le SOC_n(\kappa) \le B_n^+,\quad \forall n\in\mathcal{N},\quad \kappa\in\tau \tag{6.36}$$

$$SOC_n(\kappa+1) = SOC_n(\kappa) + \alpha_n r_n(\kappa),\quad \forall n\in\mathcal{N},\quad \kappa(6.37)$$

$$P_n^g(\kappa) - P_n^d(\kappa) - r_n(\kappa) = \sum_{j:n\sim j}^{n\in\mathcal{N}} \Big(v_n(\kappa) - U_{nj}(\kappa)\Big)Y_{nj}, \forall n\in\mathcal{N},\ \kappa\in\tau \tag{6.38}$$

$$\Big(v_n(\kappa) - U_{nj}(\kappa)\Big)Y_{nj} \le P_{nj} \tag{6.39}$$

$$\Big(v_j(\kappa) - U_{jn}(\kappa)\Big)Y_{jn} \le P_{jn} \tag{6.40}$$

$$M_{nj} = \begin{bmatrix} v_n & U_{nj} \\ U_{jn} & v_j \end{bmatrix} \succeq 0,\quad \forall n\sim j \tag{6.41}$$

One way to keep some of the theoretical equation is to force the line constraints in terms of power flows alternatively. In specific, $|I_{nj}| \le \hat{I}_{nj}$ is equivalent to $|P_{nj}| \le V_n\hat{I}_{nj}$. Assuming that V_n is near to its nominal value, then $|P_{nj}| \le V_n\hat{I}_{nj}$ can be proximated by $|P_{nj}| \le \hat{P}_{nj}$ for some $\hat{P}_{nj}\in\mathcal{R}$. Hence, the final formulation of the line constraints can be written as (6.39) and (6.41). (For detailed proofs, see ***Theorem − 7*** in [66]).

6.2.2 Modeling the Energy Storage

Presuming that bus n can have at most one battery device for energy storage, the SOC_n indicates the charge of the battery at bus n. The batteries were simplified by modeling them as discrete-time integrators:

$$SOC_n(\kappa+1) = SOC_n(\kappa) + \alpha_n r_n(\kappa), \quad SOC_n(0) \text{ given} \tag{6.42}$$

where α_n [h/KW] represents the event sampling and $r_n(\kappa)$ represents the rate of charge at bus n. This subsection explores how to demonstrate the dynamic formulations imposed by the battery as algebraic linear equations that are appropriate for integration in a non-dynamic optimization problem.

A discrete-time, causal linear, and time-invariant system with the state-space equations is expressed below

$$\begin{aligned} x(\kappa+1) &= Ax(\kappa) + Bu(\kappa), \quad x(0) = x_o \\ y(\kappa) &= Cx(\kappa) + Du(\kappa) \end{aligned} \tag{6.43}$$

where x indicates the state vector and u the input vector, and $x(0)$ represents the initial conditions of the system at time zero.

In general, the solution of the state-space formulations can be expressed as follows

$$x(\kappa) = A^{\kappa} x_o + \sum_{m=0}^{\kappa-1} A^{(\tau-1)-m} Bu(m), \quad \kappa \geq 0 \tag{6.44}$$

In the context of optimal power flow problems, τ defines the index of the planning epoch. Assume that the problem implies (M) epochs, beginning at $M = 1$. Then

(6.44) can be expressed in matrix form as:

$$x(M) - A^M x_o = \begin{bmatrix} A^{M-1}B & \cdots & AB & B \end{bmatrix} \begin{bmatrix} u(0) \\ u(1) \\ \vdots \\ u(M-1) \end{bmatrix} \tag{6.45}$$

We obtain the following linear algebraic equation by collecting all of the states at each epoch in a vector as follows:

$$\begin{bmatrix} x(1) \\ x(2) \\ \vdots \\ \vdots \\ x(M) \end{bmatrix} - \begin{bmatrix} A \\ A^2 \\ \vdots \\ \vdots \\ A^M \end{bmatrix} x_o = \begin{bmatrix} B & 0 & \cdots & \cdots & 0 \\ AB & B & \ddots & & 0 \\ & \ddots & \ddots & \ddots & \vdots \\ A^{M-2}B & & \ddots & B & 0 \\ A^{M-1}B & A^{M-2}B & \cdots & AB & B \end{bmatrix} \begin{bmatrix} u(0) \\ u(1) \\ \vdots \\ \vdots \\ u(M-1) \end{bmatrix} \tag{6.46}$$

From the above equations (6.46), the specific model of the battery in equation (6.42) can be reduced to

$$\begin{bmatrix} SOC_n(1) \\ SOC_n(2) \\ \vdots \\ \vdots \\ SOC_n(M) \end{bmatrix} - \begin{bmatrix} 1 \\ 1 \\ \vdots \\ \vdots \\ 1 \end{bmatrix} SOC_n(0) = \begin{bmatrix} \alpha_n & 0 & \cdots & \cdots & 0 \\ \vdots & \ddots & \ddots & & 0 \\ \vdots & & \ddots & \ddots & \vdots \\ \vdots & & & \ddots & 0 \\ \alpha_n & \cdots & \cdots & \cdots & \alpha_n \end{bmatrix} \begin{bmatrix} r_n(0) \\ r_n(1) \\ \vdots \\ \vdots \\ r_n(M-1) \end{bmatrix} \tag{6.47}$$

CHAPTER SEVEN

DEMONSTRATION AND ASSESSMENT OF THE PROPOSED OPF APPROACH INCLUDING ENERGY STORAGE

This chapter illustrates the DC-OPF problem with energy storage units by evaluating the effectiveness of the proposed polynomial convex approach, two different case studies, the IEEE 14 and 30 bus test systems, are used. This OPF problem is considered as a nonconvex optimization problem whose objective function has discontinuous first-order derivatives that we solved through a special CVX solver and ran on a Lenovo Intel Core i5 DDR3 SDRAM (2410M Cache, 2.30 GHz) with 8GB memory.

7.1 CASE STUDIES

7.1.1 The DC Microgrid Power System Test Case

The first case study considers a microgrid system of a 14 bus power system, with five distributed power sources — the DC network and four battery devices — directly attached to the microgrid over various buses. The battery devices are included in the grid to provide sufficient power to smoothly cover the demand loads, including during situations where the local power sources are not adequate or if a specific generator breaks down.

7.1.2 The Parameters and Results of the First Case Scenario-I

The microgrid is a system of fourteen buses shown in Fig. 7.1. The network consists of five power generators at buses 2, 5, 6, 8, and 14; five loads at buses 4, 5, 8, 11, and 13; eight link buses (i.e., without generation nor load); and nineteen transmission lines. An energy storage unit has been added to busses 3, 8, 10, and 12. Since the full life of a battery device is directly related to the number of charging and discharging cycles, there is a cost associated with it per charge cycle

[5]. The parameters and the boundary conditions associated with the power generators, the SOC, and the bus reference are given in Table. 7.1 and the power loads at different operational times are given in **APPENDIX A** Table. 1. The line constraints are given in Table. 7.2. The costs of power purchased from the generators are set to $P_2^g = 5\$/\text{MWh}$, $P_5^g = 7\$/\text{MWh}$, $P_6^g = 5\$/\text{MWh}$, $P_8^g = 7\$/\text{MWh}$, and $P_1 4^g = 5\$/\text{MWh}$. The voltage magnitude bounds for all buses are set between 350 V and 450 V, and the voltage magnitude at the first bus as defined as a reference bus, V_1^{ref}, is 380 V.

Table 7.1: The lower and upper bounds of the constraint parameters.

BUS	V_n^-	V_n^+	P_n^{g-}	P_n^{g+}	$V_{n_{ref}}^{ref}$	SOC_n^-	SOC_n^+	r_n^-	r_n^+
1	-	-	-	-	380	-	-	-	-
2	380	450	0	100K	-	-	-	-	-
3	380	450	-	-	-	0.2	0.8	-7K	7K
4	380	450	-	-	-	-	-	-	-
5	380	450	0	100K	-	-	-	-	-
6	380	450	0	100K	-	-	-	-	-
7	380	450	-	-	-	-	-	-	-
8	380	450	0	100K	-	0.2	0.8	-7K	7K
9	380	450	-	-	-	-	-	-	-
10	380	450	-	-	-	0.2	0.8	-7K	7K
11	380	450	-	-	-	-	-	-	-
12	380	450	-	-	-	0.2	0.8	-7K	7K
13	380	450	-	-	-	-	-	-	-
14	380	450	0	100K	-	-	-	-	-

Table 7.2: The power capacity bounds of the constraint parameters.

BUS	$\Delta V_{nj}(\kappa)^{-}$	$\Delta V_{nj}(\kappa)^{+}$
4 To 5	-2K	2K
5 To 4	-2K	2K
11 To 13	-2K	2K
13 To 11	-2K	2K

For power system protection and security, in this scenario, the transmission lines between buses 4 and ,5 and between buses 11 and 13, are restricted. The storage battery is constrained by a capacity $SOC_n(\kappa)^{-}$ and $SOC_n(\kappa)^{+}$ with a charge or discharge rate (discussed earlier) as $r_n(\kappa)^{-}$and $r_n(\kappa)^{+}$. The initial condition of the energy storage units is defined as 0.7 KWh. A total of 20 KWh of energy was proposed, as well as the sampling time of one hour, and the simulations were performed over one day. The simulation results explicate the merits of including energy storage units under low and high-demand circumstances. During low demand, the energy is stored in the storage unit and then released when the load starts rising, smoothing the total power injected into the power grid system.

7.1.3 Demonstration of the First Case Scenario-I

The system in **Fig. 7.1** includes four storage devices at buses $3, 8, 10$, and 12. To reiterate, the following description was mentioned earlier: power generations are represented by P_n^g, storage power is $r_n(\kappa)$, and the event sampling is α_n. The battery is modeled by its minimum and the maximum value of the energy storage $r_n(\kappa)^{-}$ and $r_n(\kappa)^{+}$, and the battery State of Charge SOC_n, is in the range of 0.2 and 0.8. This represents energy in this problem.

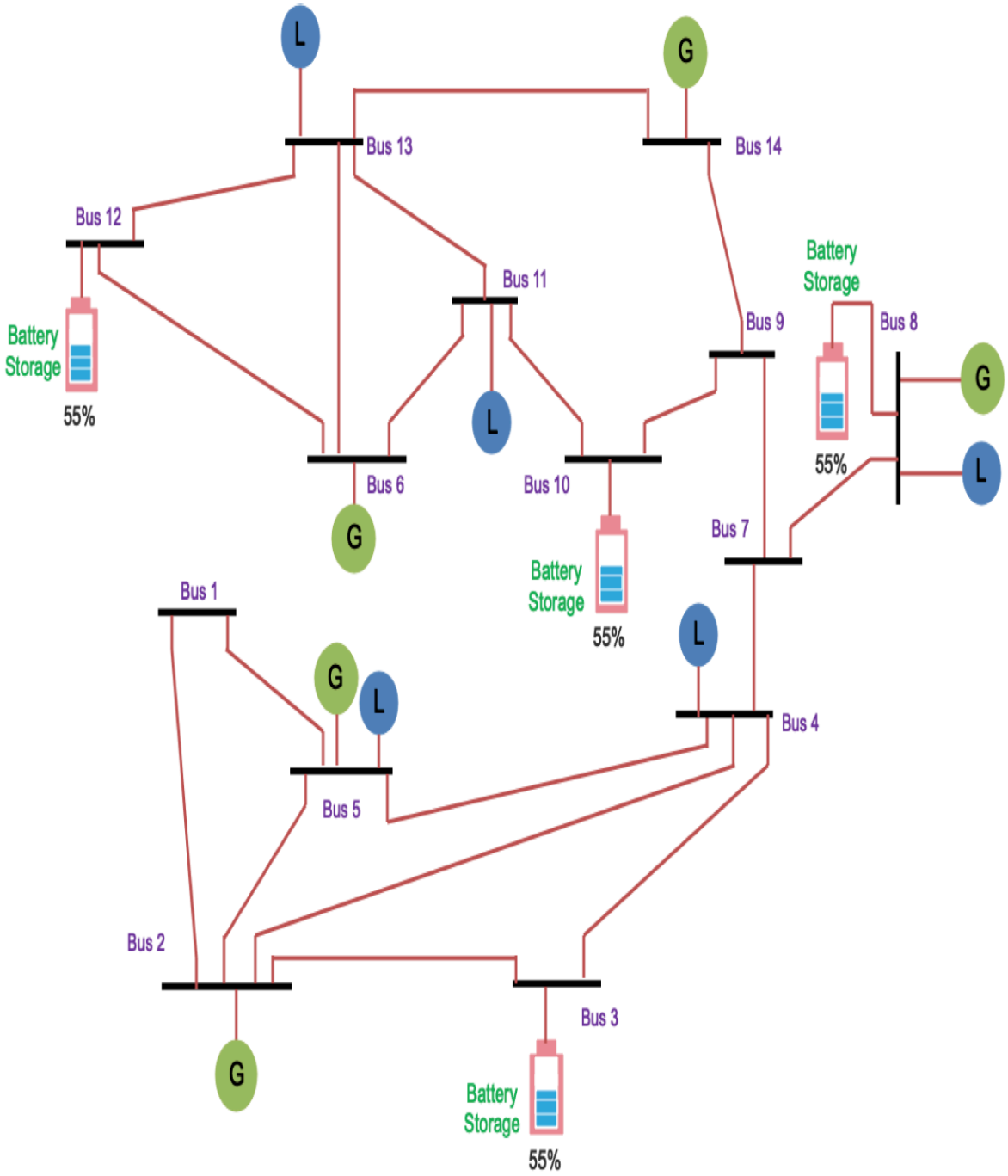


Figure 7.1: The first scenario-I: fourteen bus power system with energy storage units.

$$\min_{P_n^g(\kappa), v_n(\kappa), SOC_n(\kappa), r_n(\kappa), U_n(\kappa)} \quad \sum_{\kappa=1}^{24} \left\{ \sum_{n \in 14} f_n(5P_{2,6,14}^g(\kappa) + 7P_{5,8}^g(\kappa)) \right\} \tag{7.1}$$

$$\textbf{subj. to} \tag{7.2}$$

$$380 \leq v_n(\kappa) \leq 450, \ \ \forall n \in 14, \quad \kappa \in \tau \tag{7.3}$$

$$0 \leq P_2^g(\kappa) \leq 100K, \ \ \kappa \in \tau \tag{7.4}$$

$$0 \leq P_5^g(\kappa) \leq 100K, \ \ \kappa \in \tau \tag{7.5}$$

$$0 \leq P_6^g(\kappa) \leq 100K, \ \ \kappa \in \tau \tag{7.6}$$

$$0 \leq P_8^g(\kappa) \leq 100K, \ \ \kappa \in \tau \tag{7.7}$$

$$0 \leq P_{14}^g(\kappa) \leq 100K, \ \ \kappa \in \tau \tag{7.8}$$

$$-7K \leq r_{[3,8,10,12]}(\kappa) \leq 7K, \ \ \kappa \in \tau \tag{7.9}$$

$$0.2 \leq SOC_{[3,8,10,12]}(\kappa) \leq 0.8, \ \ \kappa \in \tau \tag{7.10}$$

$$SOC_{[3,8,10,12]}(\kappa + 1) = SOC_{[3,8,10,12]}(\kappa) + \alpha_{[3,8,10,12]} r_{[3,8,10,12]}(\kappa), \kappa \in \tau \tag{7.11}$$

$$P_{[2,5,6,8,14]}^g(\kappa) - P_{[4,5,8,11,13]}^d(\kappa) - r_{[3,8,10,12]}(\kappa) = \sum_{j:n \sim j}^{n \in 14} \Big\{ v_n(\kappa) - U_{nj}(\kappa) \Big\} Y_{nj}, \forall n \in 14, \kappa \in \tau \tag{7.12}$$

$$-2K \leq \Big\{ v_n(\kappa) - U_{nj}(\kappa) \Big\} Y_{nj} \leq 2K \tag{7.13}$$

$$-2K \leq \Big\{ v_j(\kappa) - U_{jn}(\kappa) \Big\} Y_{jn} \leq 2K \tag{7.14}$$

$$\boldsymbol{R} := \begin{bmatrix} \boldsymbol{M}_{nj} & & \\ & \ddots & \\ & & \boldsymbol{M}_{jn} \end{bmatrix} \succeq 0, \quad \forall n \sim j \tag{7.15}$$

- **The Initial Condition (I.C) of $SOC_{[3,8,10,12]}$ at $\kappa = 0$**

$$SOC_{[3,8,10,12]}(0) = 0.7 \tag{7.16}$$

- **The Voltage Reference at Bus n_{ref}**

$$V_{n_1}^{ref}(\kappa) = 380 \tag{7.17}$$

The problem was solved numerically using CVX. The results are summarized in Table. 7.3.

Table 7.3: The result of the first case scenario-I.

Optimization Methods	Opt. value	Comp. Time (s) w/ acceleration	Comp. Time (s) w/o acceleration
SP-Relaxation Algorithm	1.64665e+06	140.283	590.845
Mixed-Integer Programming Algorithm	1.65327e+06	320.743	1350.907
Interior-Point Algorithm	1.69653e+06	474.591	1998.885
Genetic Algorithm (GA)	1.97481e+06	758.8	3195.919
Particle Swarm Opt. Algorithm (PSO)	1.74653e+06	773.4	3257.4119

It was proven, subsequently, that the rank one conditions on $M_{nj}, \forall\ n \sim j$ were satisfied for the proposed technique. Hence the optimal value of the cost reported in the table is also a global optimum for the original OPF. The proposed optimization approach is compared with other existing techniques to ensure the proposed technique's performance. The numerical values of power injections and nodal voltages are listed in **APPENDIX A**, Tables. 2 and 3.

7.1.4 The Load Data of the First Case Scenario-I

The total power load of the DC microgrid for each hour is shown in **Fig. 7.2**. This includes the power loads at buses 4, 5, 8, 11, and 13. The power loads at buses 5 and 11 are constant during the operational time. However, the power loads at buses 4, 8, and 13 are unsteady, with an average hourly power load of around 12.704 KWh.

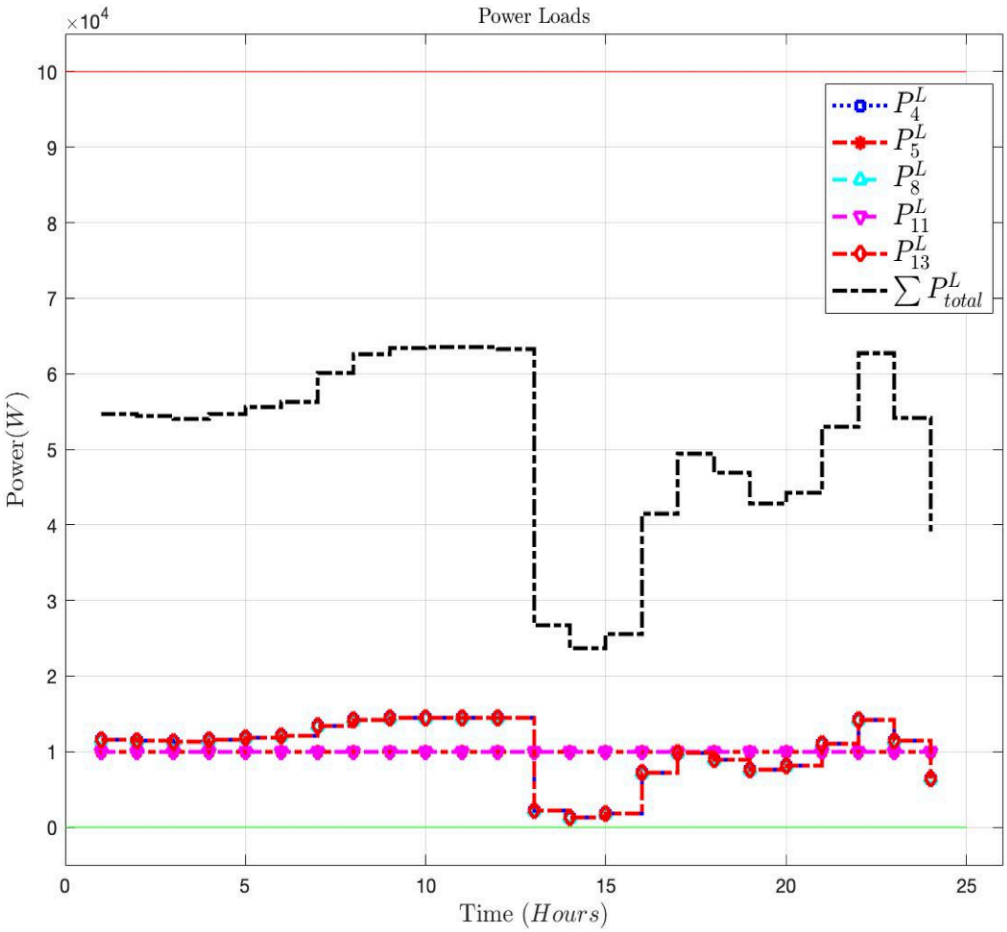


Figure 7.2: The power load profiles.

7.1.5 The Power Generation Data of the First Case Scenario-I

The power generator schedule for 24 hours is presented in **Fig. 7.3**, which illustrates that all generators during the operational time are within the boundaries and satisfied the constraints. It can be also seen that the power generator at bus 6 produces less energy compared to others, due to its location between two energy storage units, which are busses 10 and 12.

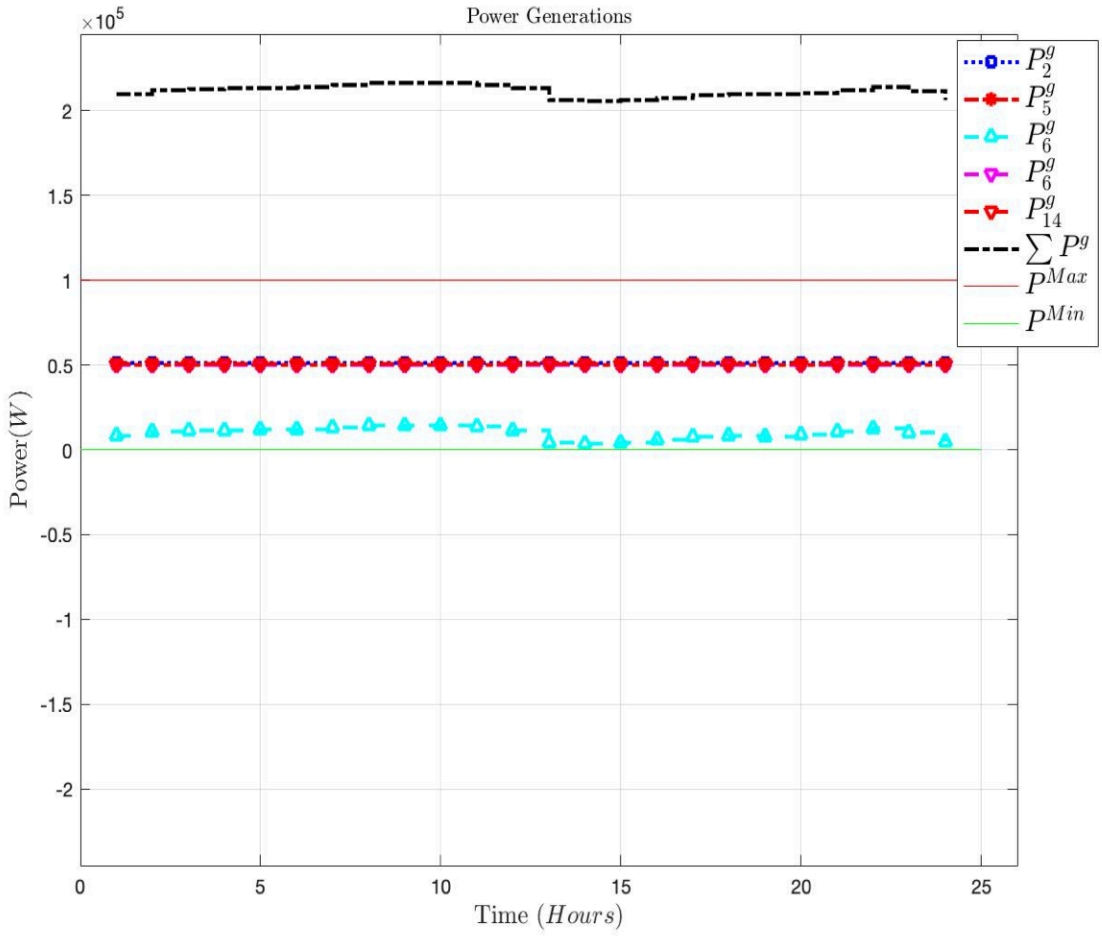


Figure 7.3: The hourly economic schedule of power generation.

7.1.6 The State-of-Charge (SOC) and Battery Rate (r) of Case Scenario-I

A dynamic OPF problem has been solved due to the dynamics of the state-of-charge (SOC) of the battery. As shown in Fig. 7.4, it can be seen experimentally when the battery is either charged fully $SOC = 100\%$ or discharged to $SOC = 0\%$.

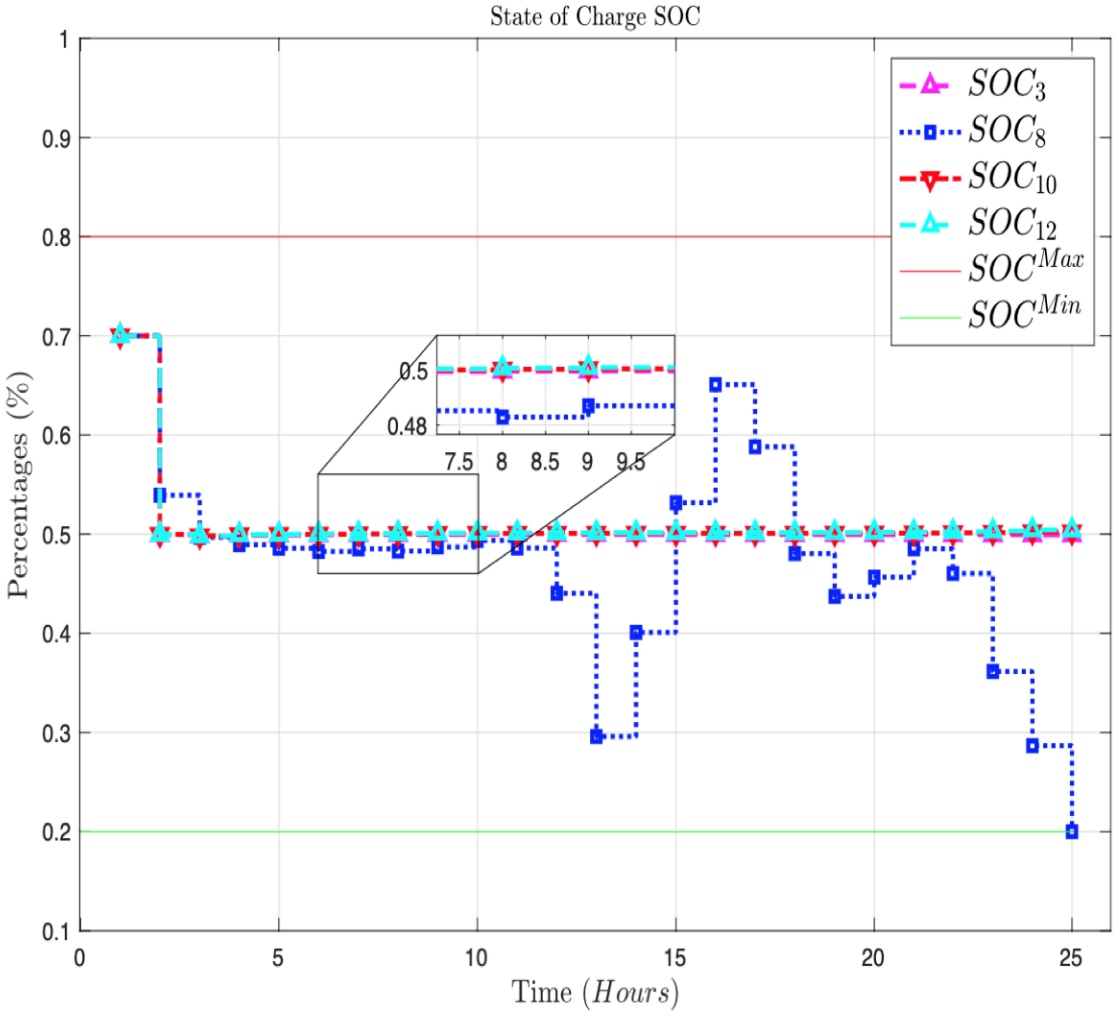


Figure 7.4: The hourly economic schedule for state-of-charge.

In **Fig. 7.5**, it can been seen that the battery schedule satisfied the constraints and boundaries during the operations. Moreover, battery charging and discharging occur during the production times, as can be seen by noting the graphs. The energy stored in the battery at bus 3 is charging during 2 to 5, 9 to 14, and between 17 and 24. It is also discharging during 1 to 2, 6 to 8, and between 15 and 16. In bus 8, the energy stored in the battery is charging during 2 to 6, 8 to 10, 13 to 16, and between 19 and 21. It is also discharging during 1 to 2, 7 to 8, 17 to 19, and between 22 and 24. The energy stored in the battery at bus 10 is charging during 2 to 6, 9 to 13, and between 17 to 23. It is also discharging during 1 to 2, 7 to 8, 14 to 16, and between 23 to 24. The energy stored in the battery at bus 12 is charging during 2 to 5, 9 to 14, and between 17 and 24. It is also discharging during 1 to 2, 6 to 8, and between 15 and 16. The stored power is utilized to feed nearby loads and avoid losses and the high cost on the system if the DC generations are used to feed these loads is far away. Since the batteries are not needed to hold any further power at the end of 25 hours, it is economically beneficial to discharge all the battery energy so the net battery energy is 0. The total optimal cost for supplying the load are given in Table. 7.3. A list of the standby power battery values are given in **APPENDIX A**, Table. 3. These values are required at each hour to support the system by providing energy necessary for the loads.

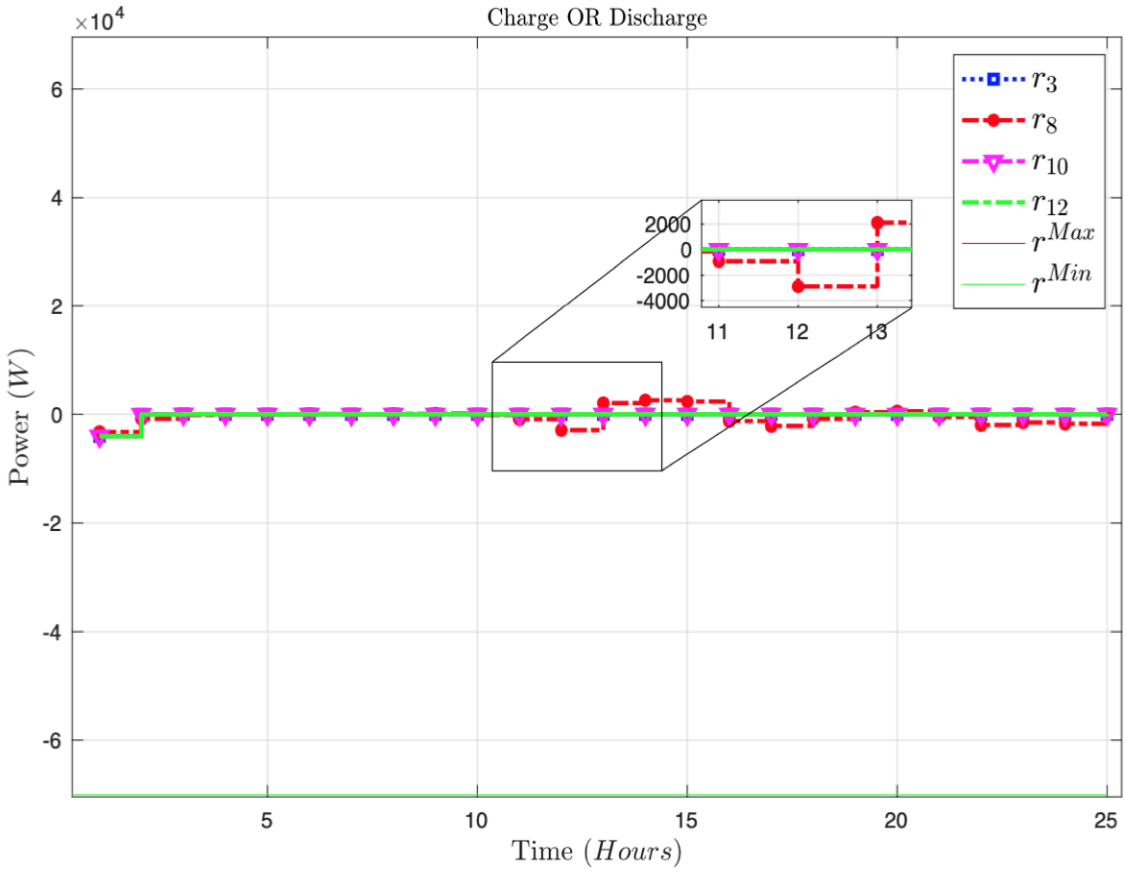


Figure 7.5: The hourly economic schedule for the battery units.

7.1.7 The Voltages Profile of the First Case Scenario-I

The optimal solution obtained by using the proposed algorithm of IEEE 14 bus system for the scenario is specified previously, and the voltage profiles for this scenario are shown in the following **Fig.7.6**. As can be seen, the voltage profiles for each bus are maintained within the limit during the operational time. There are two straight lines showing the maximum (red) and minimum (green) limit of voltages (i.e., 380 - 450 volt), respectively. Upon closer examination, it is noticed that the average voltage profiles at all times are within the system's limits.

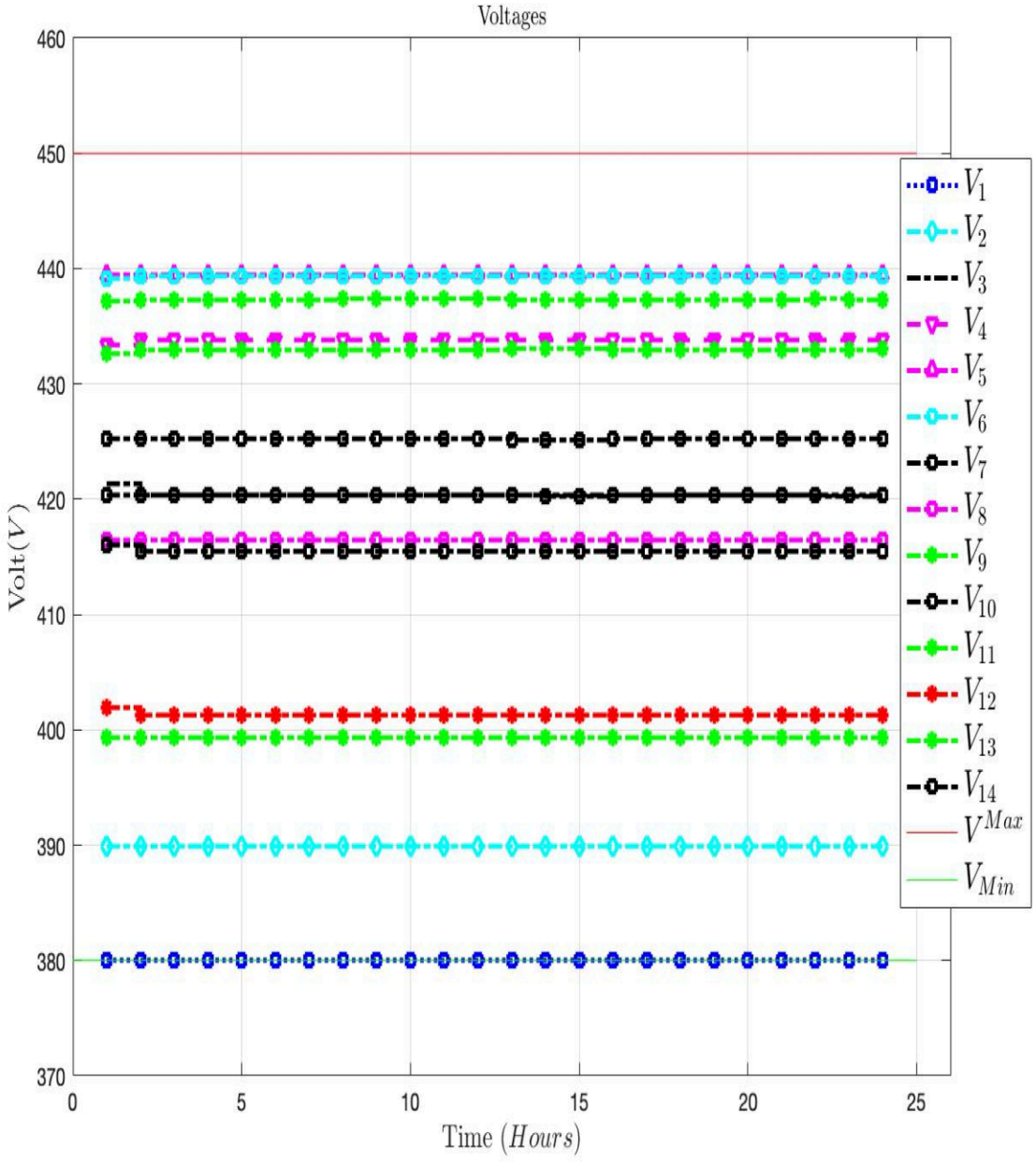


Figure 7.6: The voltage profile of the IEEE 14 bus system.

7.1.8 The Parameters and Results of the Second Case Scenario-II

In this scenario, the OPF formulation with energy storage dynamics is applied to examine the reliability and stability of the system. The power system of a DC microgrid is depicted in **Fig. 7.7**. The considered power network model consists of six power generators at buses 1, 2, 13, 22, 23, and 27; twelve distributed loads at buses 3, 4, 8, 11, 13, 14, 18, 21, 23, 26, 27, and 30; four link buses (i.e., without including generation nor load); and thirty one transmission lines. Furthermore, nine energy storage units have been applied in the network at buses 7, 8, 10, 11, 12, 19, 24, 28, and 30. The main aim of including battery device units distributed in this system is to increase system security and continuity of supporting the loads by acting as a standby when required. The parameters and the constraints in the power network associated with the power generators P_n^g, the state of charge (SOC), and the bus reference V_n^{ref} are summarized in Table. 7.4, and the power loads P_n^d at different operational times are also given in **APPENDIX B** Table. 1. Furthermore, to ensure system security, the line constraints have been taken into consideration in this case, as depicted in Table. 7.5. The costs of power purchased to the main grid throughout the operation are also set to $P_1^g = 5\$/\text{MWh}$, $P_2^g = 7\$/\text{MWh}$, $P_{13}^g = 8\$/\text{MWh}$, $P_{22}^g = 9\$/\text{MWh}$, $P_{23}^g = 10\$/\text{MWh}$, and $P_{27}^g = 10\$/\text{MWh}$. The voltage magnitude V_n bounds for all buses are set between 350 and 450 V and the voltage magnitude at the first bus is defined as a reference bus, $V_1^{ref} = 380V$.

In this scenario, the transmission lines between buses 3 and 4, and between buses 27 and 30, are tied between an upper and lower limit. The battery storage device units are constrained by a capacity $SOC_n(\kappa)^-$ and $SOC_n(\kappa)^+$ with a charge or discharge rate (discussed earlier) as $r_n(\kappa)^-$ and $r_n(\kappa)^+$. The initial condition of the storage battery was selected to be 0.7 KWh.

Table 7.4: The lower and upper bounds of the constraint parameters.

BUS	V_n^-	V_n^+	P_n^{g-}	P_n^{g+}	$V_{n_{ref}}^{ref}$	SOC_n^-	SOC_n^+	r_n^-	r_n^+
1	-	-	0	100K	380	-	-	-	-
2	380	450	0	100K	-	-	-	-	-
3	380	450	-	-	-	-	-	-	-
4	380	450	-	-	-	-	-	-	-
5	380	450	-	-	-	-	-	-	-
6	380	450	-	-	-	-	-	-	-
7	380	450	-	-	-	0.2	0.8	-7K	7K
8	380	450	-	-	-	0.2	0.8	-7K	7K
9	380	450	-	-	-	-	-	-	-
10	380	450	-	-	-	0.2	0.8	-7K	7K
11	380	450	-	-	-	0.2	0.8	-7K	7K
12	380	450	-	-	-	0.2	0.8	-7K	7K
13	380	450	0	100K	-	-	-	-	-
14	380	450	-	-	-	-	-	-	-
15	380	450	-	-	-	-	-	-	-
16	380	450	-	-	-	-	-	-	-
17	380	450	-	-	-	0.2	0.8	-7K	7K
18	380	450	-	-	-	-	-	-	-
19	380	450	-	-	-	0.2	0.8	-7K	7K
20	380	450	-	-	-	-	-	-	-
21	380	450	-	-	-	-	-	-	-
22	380	450	0	100K	-	-	-	-	-
23	380	450	0	100K	-	-	-	-	-
24	380	450	-	-	-	0.2	0.8	-7K	7K
25	380	450	-	-	-	-	-	-	-
26	380	450	-	-	-	-	-	-	-
27	380	450	0	100K	-	-	-	-	-
28	380	450	-	-	-	0.2	0.8	-7K	7K
29	380	450	-	-	-	-	-	-	-
30	380	450	-	-	-	0.2	0.8	-7K	7K

Table 7.5: The power capacity bounds of the constraint parameters.

BUS	$\Delta V_{nj}(\kappa)^{-}$	$\Delta V_{nj}(\kappa)^{+}$
3 To 4	-2K	2K
4 To 3	-2K	2K
27 To 30	-2K	2K
30 To 27	-2K	2K

A total of 20 KWh of energy was proposed as well as the sampling time of one hour, and the simulations were performed over one day. The simulation outcomes demonstrate the benefits of integrating energy storage devices under low and high-demand circumstances.

7.1.9 Demonstration of the Second Case Scenario-II

The power network system is elucidated in **Fig. 7.7** and comprises nine storage devices at buses 7, 8, 10, 11, 12, 19, 24, 28, and 30. During the power production, the energy is stored in the battery and released when the $r_n(\kappa)$, value of the power at time (κ), is $r_n(\kappa)^{+} \geq 0$ and $r_n(\kappa)^{-} \leq 0$, respectively.

The following illustration was given earlier: power generations are described by P_n^g, storage power is $r_n(\kappa)$, and the event sampling is α_n. The battery is modeled by minimum and maximum values of the energy storage $r_n(\kappa)^{-}$ and $r_n(\kappa)^{+}$, and the battery state-of-charge SOC_n, in the range 0.2 and 0.8, describes energy in this problem.

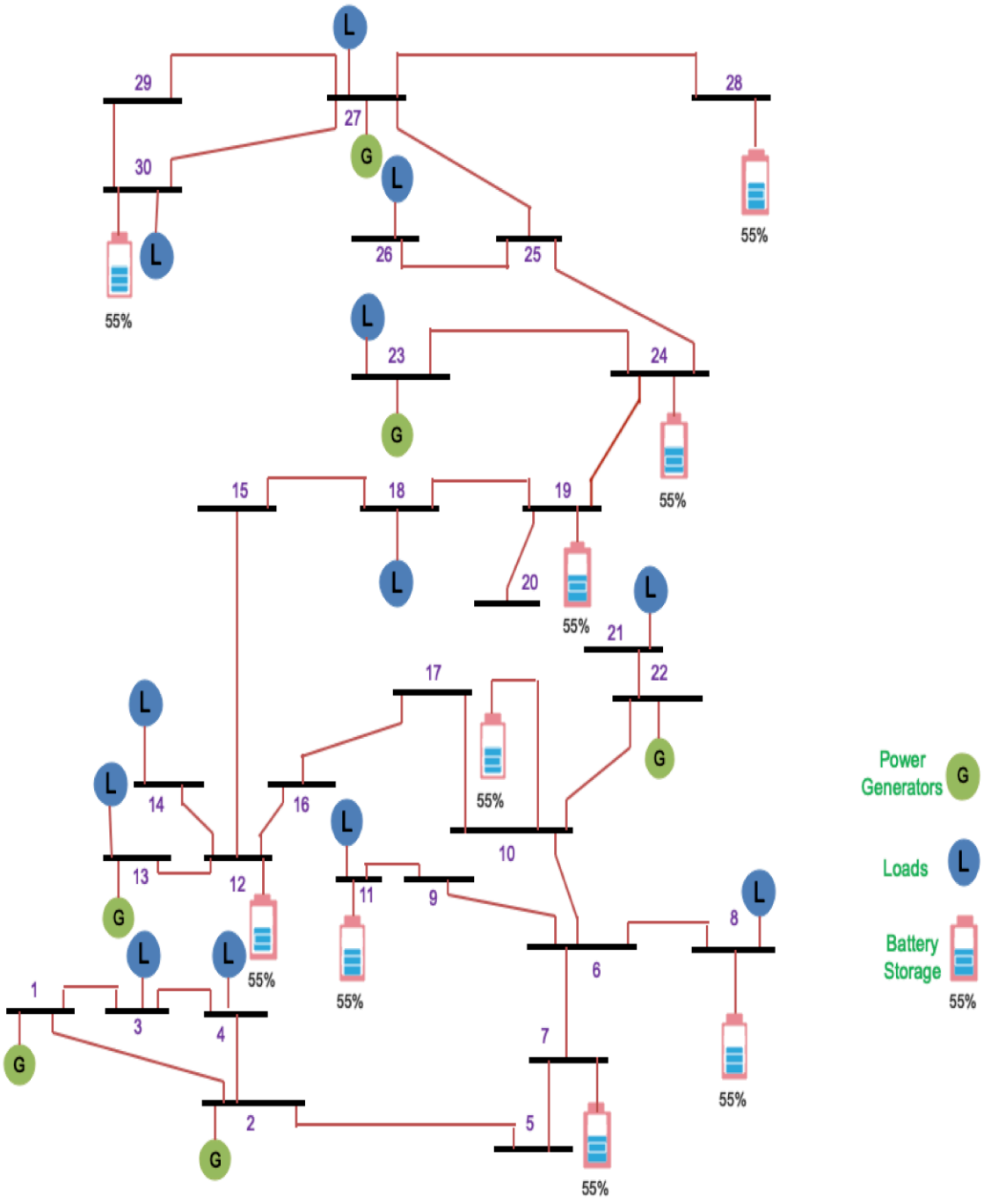


Figure 7.7: The second scenario-II: thirteen bus power system with nine energy storage units.

The optimization problem for this case is:

$$\min_{P_n^g(\kappa), v_n(\kappa), SOC_n(\kappa), r_n(\kappa), U_n(\kappa)} \quad \sum_{\kappa=1}^{24} \{ \sum_{n \in 30} f_n \} \tag{7.18}$$

$$\textbf{subj. to} \tag{7.19}$$

$$380 \leq v_n(\kappa) \leq 450, \ \ \forall n \in 30, \quad \kappa \in \boldsymbol{\tau} \tag{7.20}$$

$$0 \leq P_{1,2}^g(\kappa) \leq 100K, \ \ \kappa \in \boldsymbol{\tau} \tag{7.21}$$

$$0 \leq P_{13,22}^g(\kappa) \leq 100K, \ \ \kappa \in \boldsymbol{\tau} \tag{7.22}$$

$$0 \leq P_{23,27}^g(\kappa) \leq 100K, \ \ \kappa \in \boldsymbol{\tau} \tag{7.23}$$

$$-7K \leq r_n(\kappa) \leq 7K, \ \ \kappa \in \boldsymbol{\tau} \tag{7.24}$$

$$0.2 \leq SOC_n(\kappa) \leq 0.8, \ \ \kappa \in \boldsymbol{\tau} \tag{7.25}$$

$$SOC_n(\kappa + 1) = SOC_n(\kappa) + \alpha_n r_n(\kappa), \kappa \in \boldsymbol{\tau} \tag{7.26}$$

$$P_n^g(\kappa) - P_n^d(\kappa) - r_n(\kappa) = \sum_{j:n \sim j}^{n \in 30} \Big\{ v_n(\kappa) - U_{nj}(\kappa) \Big\} Y_{nj}, \forall n \in 30, \ \kappa \in \boldsymbol{\tau} \tag{7.27}$$

$$-2K \leq \Big\{ v_n(\kappa) - U_{nj}(\kappa) \Big\} Y_{nj} \leq 2K \tag{7.28}$$

$$-2K \leq \Big\{ v_j(\kappa) - U_{jn}(\kappa) \Big\} Y_{jn} \leq 2K \tag{7.29}$$

$$\boldsymbol{R} := \begin{bmatrix} \boldsymbol{M}_{nj} & & \\ & \ddots & \\ & & \boldsymbol{M}_{jn} \end{bmatrix} \succeq 0, \quad \forall n \sim j \tag{7.30}$$

- **The Initial Condition (I.C) of $SOC_{[7,8,10,11,12,19,24,28,30]}$ at $\kappa = 0$**

$$SOC_{[7,8,10,11,12,19,24,28,30]}(0) = 0.7 \tag{7.31}$$

- **The Voltage Reference at bus n_{ref}**

$$V_1^{ref}(\kappa) = 380 \tag{7.32}$$

The optimal value of the cost and the running time are shown in Table. 7.6.

Table 7.6: The result of the second case scenario-II.

Optimization Methods	Opt. value	Comp. Time (s) w/ acceleration	Comp. Time (s) w/o acceleration
SP-Relaxation Algorithm	1.64979e+07	214.83	904.822
Mixed-Integer Programming Algorithm	1.65989e+07	1423.773	5996.657
Interior-Point Algorithm	1.72437e+07	1592.58	6707.640
Genetic Algorithm (GA)	1.99864e+07	2575.2	10846.246
Particle Swarm Opt. Algorithm (PSO)	1.71218e+07	2672.4	11255.634

The numerical values of power injections and nodal voltages are listed in **APPENDIX B**, Tables 2 and 3.

7.1.10 The Load Data of the Second Case Scenario-II

Analogous to the previous scenario, the total power load of the DC microgrids for each hour are presented in **Fig. 7.8**. This includes the power loads at buses 3, 4, 8, 11, 13, 14, 18, 21, 23, 26, 27, and 30. The attached power load at buses 3 and 11 are constant throughout the operational time. However, the power load at buses 4, 8, 13, 14, 18, 21, 23, 26, 27, and 30 are unsteady with an average hourly power load of around 12.704 KWh.

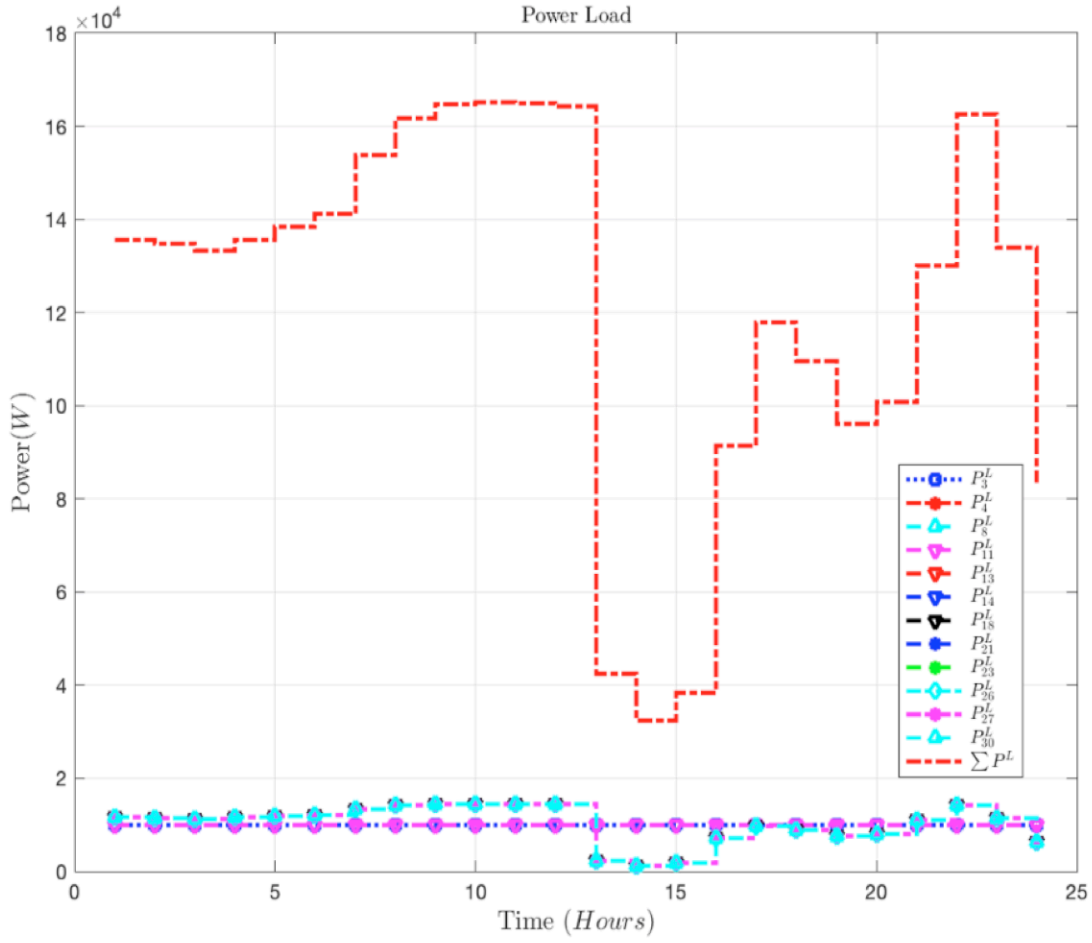


Figure 7.8: The power load profiles.

7.1.11 The Power Generation Data of the Second Case Scenario-II

The power generators' schedules for 24 hours are given in **Fig. 7.9**. From this figure, it can been observed that all generators through the operational time are retained inside the limits and they satisfied the system's constraints. It can be also noticed that the power productions are dropped around hour 14, due to the drop on required demand loads compared to other operational times.

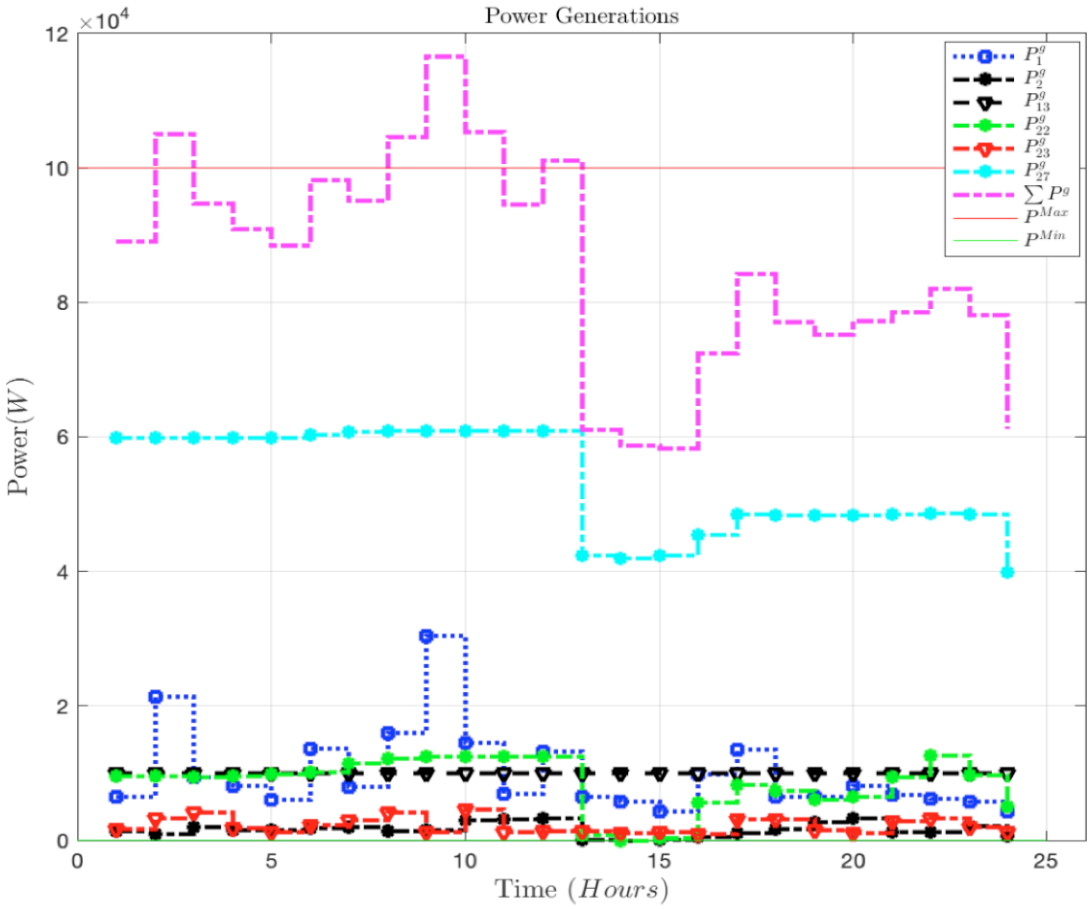


Figure 7.9: The hourly economic schedule of power generation.

7.1.12 The State-of-Charge (SOC) and Battery Rate (r) for Case Scenario-II

A dynamic OPF problem has been solved due to the dynamics of the state-of-charge (SOC) of the battery. As shown in Fig. 7.10, it can be seen experimentally when the battery is either fully charged $SOC = 100\%$ or fully discharged to $SOC = 0\%$. The battery rates are shown in **Fig. 7.11**. It can be observed that the battery schedules are within the limits and satisfied constraints throughout the operations. Furthermore, battery charging and discharging happens

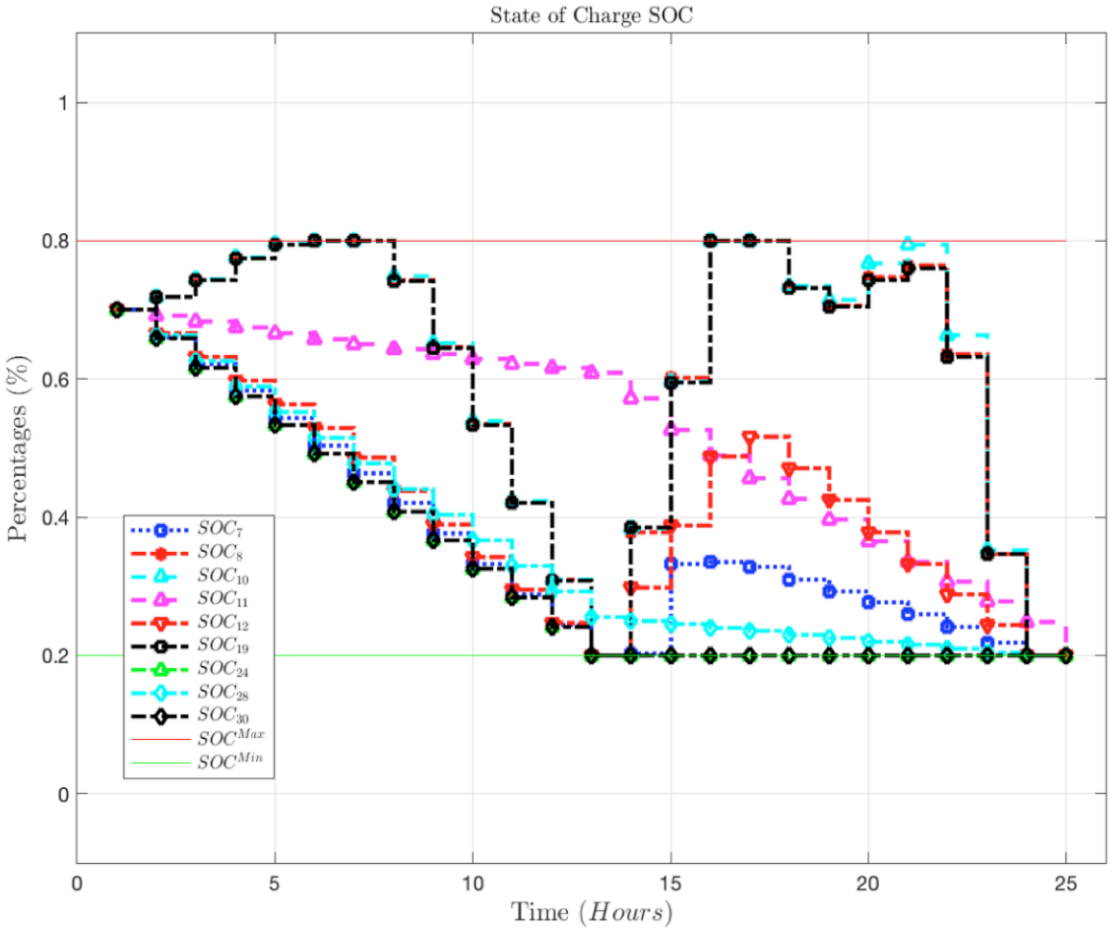


Figure 7.10: The hourly economic schedule for state-of-charge.

during the production time, as noted in the graphs. The energy stored in the battery at bus 7 is charging between 12 to 18. It is also discharging during 1 to 11 and between 19 and 24. The battery at this bus is charging most of the time and acts as a standby energy source due to a low required demand load at this location. In buses 8, 10, and 19, the battery behavior is nearly the same during the charging and discharging statuses. The energy stored in the batteries is charging between 1 to 7, 13 to 16, and between 19 and 21. Also, they are discharging during 8 to 12, 17 to 18, and between 22 and 24. The energy stored in the battery at bus 11 is

charging and discharging slightly due to its location between three battery devices, 7, 8 and 10, and they support the required demand load at bus 11. The energy stored in the battery at bus 12 is charging between 10 to 21. It is also discharging during 1 to 9 and between 22 and 24. Similarly, the battery at this bus is charging most of the time and acts as a standby energy source due to a low required demand load and its location between two power sources, the energy storage unit and the power generation at buses 10 and 13, respectively. In buses 24 and 30, the battery behavior is, again, nearly same during the charging and discharging statuses. The energy stored in the batteries is charging between 12 to 14, 16 to 17, and between 19 and 22. It is also discharging during 1 to 11, 15 to 16, and between 23 and 24. In bus 28, the battery starts to store at the beginning of the operation until hour 7, then it discharges from hours 8 to 13, then reverts back to restore the battery between 14 and 17, and thereafter the battery discharges during 18 to 22. In general, the energy storage behaves such as that when the energy at a specific bus is stored in the battery, and the battery at other buses is discharged from energy. The stored powers are utilized to feed nearby loads and avoid losses as well as the high cost on the system if faraway DC generations feed these loads. Since the battery is not needed to hold any further power at the end of 25 hours, it is economically beneficial to discharge all the battery energy so the net battery energy is 0. The total optimal cost for supplying the load is given in Table. 7.6. Also, a list of the standby power battery values are given in Table. 3.

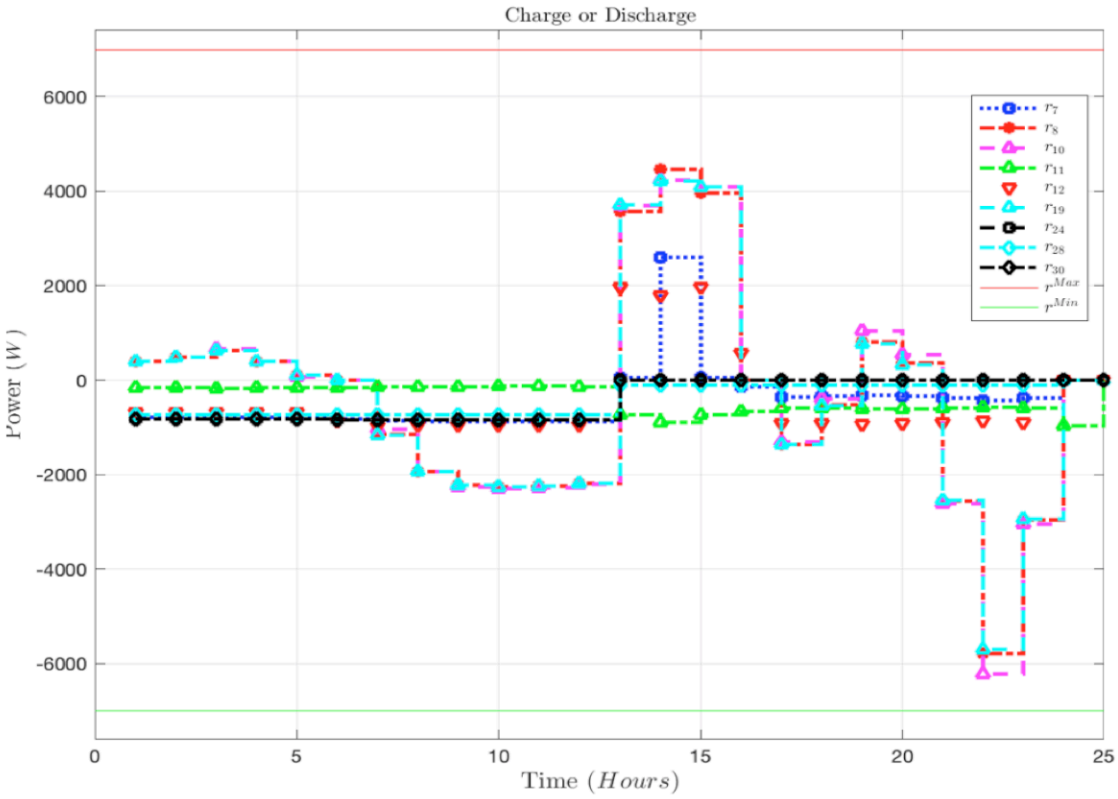


Figure 7.11: The hourly economic schedule for the battery units.

7.1.13 The Voltages Profile of the Second Case Scenario-II

The optimal solution obtained by using the proposed algorithm of the IEEE 30 bus system for the scenario was specified previously, and the voltage profiles for this scenario are shown in the following Fig.7.12. As can be observed, the voltage profiles for each bus are maintained within the boundary through the operational time. The two straight lines on the graph represent that the maximum (red) and minimum (green) boundary of voltages (i.e., 380 - 450 volt), respectively. Upon closer examination, it is noticed that the average voltage profiles at all times are within the system limits.

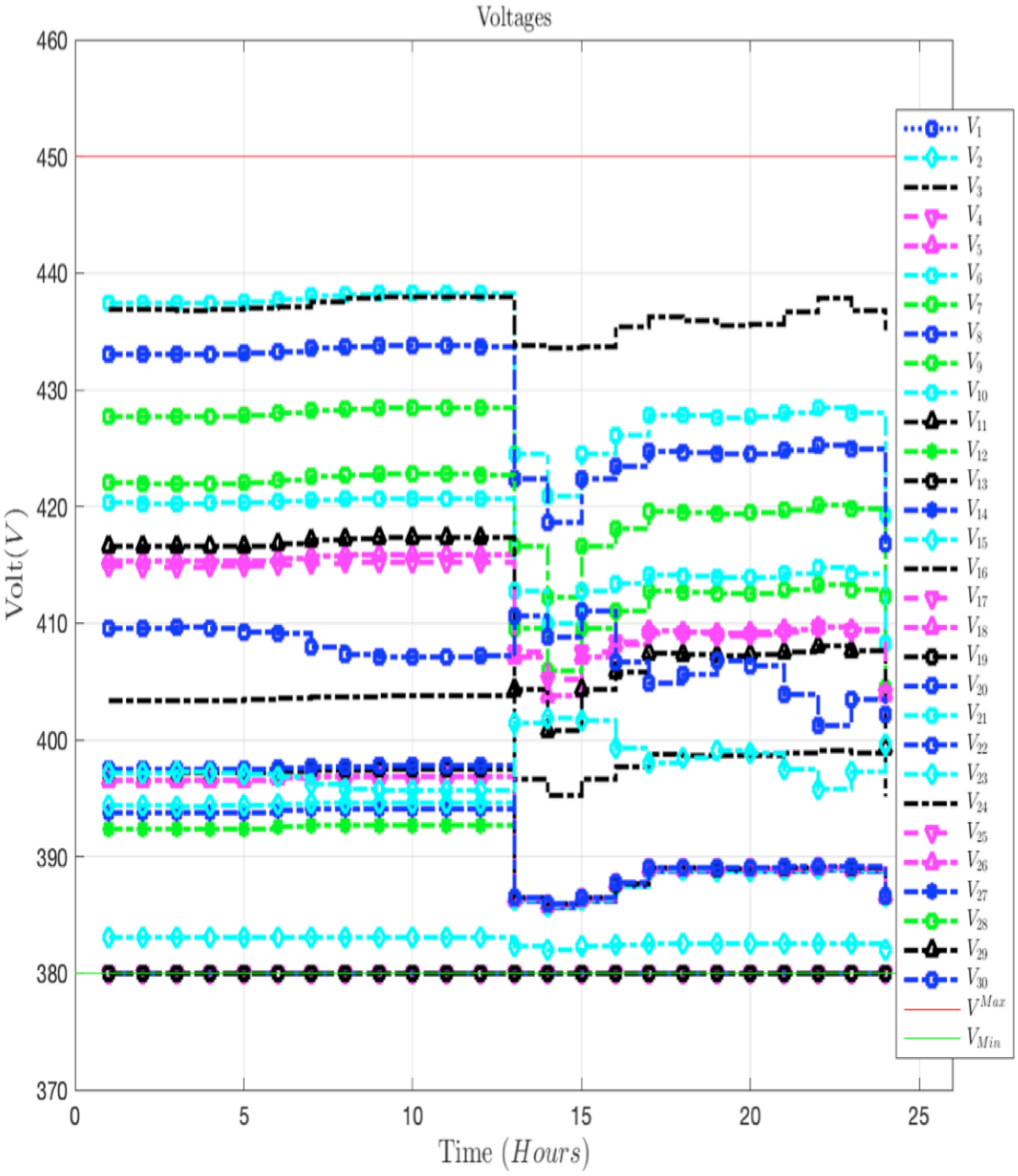


Figure 7.12: The voltage profile of the IEEE 30 bus system.

7.1.14 Analysis of Results

As can be seen from above scenarios, the SOCP is is exact, i.e. $\boldsymbol{Rank(M_{nj})} = 1$ holds, $\forall n \sim j$ and hence the solution found is also a global solution for the original OPF. However, the scale of the problems solved in this work is small. In practice, multi-bus DC systems may integrate a large number of buses. The results of computation time suggests that the proposed method may not be suitable for very large scale systems. Therefore, following flowchart summarizes the SOPC relaxation approach used to solve the OPF problem.

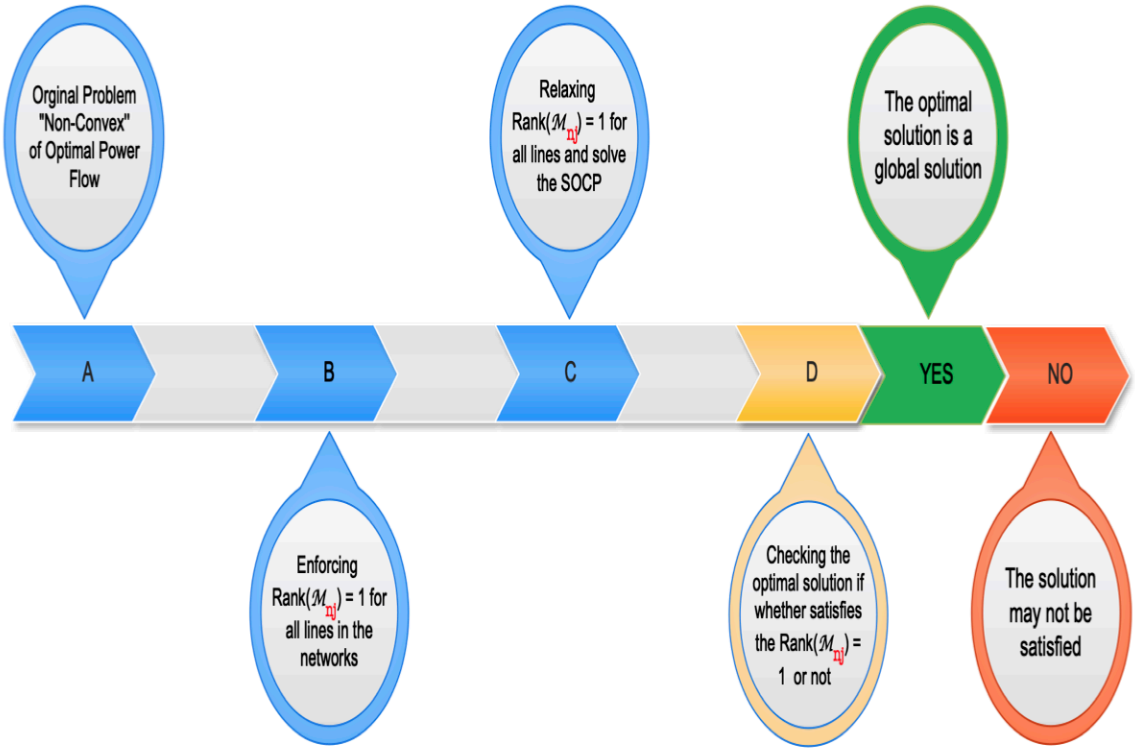


Figure 7.13: The flowchart of the convexification process.

The solution of the SOCP includes a set of 2×2 positive semidefinite matrices $M_{nj}, \forall\ n\ j$. Hence it is necessary to check the rank constraint a posteriory. If it is satisfied then the optimal solution is the global solution of the original OPF problem. If it is not satisfied then, in general, nothing can be said [6].

CHAPTER EIGHT

HYBRID AC-DC POWER GRIDS

In this chapter, an introduction is given based on recent literature reviews for consideration of the hybrid AC/DC optimal power flow problem. The proposed solution of the hybrid AC/DC optimal power flow problem with its formulation is illustrated and explained in this chapter. Thereafter, a set of equality and inequality constraints are illustrated. The original problem of hybrid AC/DC OPF is transformed to the positive semidefinite programming relaxation (SDP) format, and it is further relaxed by a finite number of second-order cone programming (SOCP) relaxations. Finally, the performance of the proposed algorithm has been examined on different electrical power networks with various power system sizes, such as IEEE 5, 14, and 30-bus. The outcomes of the experiments proved the adaptability of the algorithm when considering large-scale electrical power networks. In contrast, this proposed algorithm has been compared with existing optimization algorithms given in the literature for similar power systems, where it shows the effectiveness of the proposed method.

8.1 Introduction:

The transition from fully used AC power networks to hybrid AC/DC power networks is expeditious as a result of the improvement in power electronics and the boost of the applications for DC power networks. Several renewable energy resources, for instance, photovoltaic (PV) power systems, Wind turbines, generate DC power networks [175]. High Voltage Direct Current (HVDC) transmission lines ease transmitting power to or from rural areas [176]. Numerous electrical loads, for example, electrical appliances and lights inside the home, consume the energy inside the home[177]. The DC microgrid systems can be a feasible substitution as an

energy source for producing energy while covering the loads [178]. Another stimulus for shifting towards hybrid AC/DC power networks is the expansion of energy efficiency by eradicating losses associated with DC to AC and/or AC to DC conversions [179]. Besides, hybrid AC/DC power networks can be more reliable than only AC power networks since the supplementary conversion stages in AC power networks may produce potential faults [180].

As was already introduced in previous chapters, the optimal power flow (OPF) problem is critical and it plays a significant role in proper power system operation and planning. In OPF, the output power of the generators is defined by optimizing an objective function, for example, the overall cost and the power losses in the systems [181]. The OPF problem in AC power networks is subject to some physical and operating constraints, such as power balance constraints, voltage magnitude, power flow limits, and network constraints [181]. The OPF in AC power networks is introduced as a non-convex optimization problem and it is commonly quite intricate to solve. The non-convexity of the problem obviously emerges from both the nonlinear power flow equations and quadratic dependency on the set of bus voltages.

In most recent research studies [35, 182, 183], and [184], the consideration of OPF in hybrid AC/DC power networks does not guarantee the acquisition of the global optimal solution or the approximate optimal solution. In this chapter, the target is to effectively define the global optimal solution and/or the approximate optimal solution of the hybrid AC/DC OPF problem. The efficiency of positive semidefinite programming relaxation (SDP) in solving the AC and DC OPF problem has stimulated us to apply this method to solve the hybrid AC/DC OPF problem. In this chapter, the hybrid AC/DC are linked with each other via

three-phase AC/DC converters. The voltage source converter (VSC) is considered to model the AC/DC converters and is broadly utilized in practice [185].

One of the key elements of using the VSC in hybrid AC/DC power networks which has not been impartially addressed in the literature is its effect on enhancing the economic efficiency of the electricity industry. In terms of quantifying the economic efficiency of such systems, they have to be duly modeled in the OPF formulation. Generality OPF formulations considering hybrid AC/DC systems suggested in the literature have accounted for Current-Sourced Converter (CSC) - High Voltage Direct Current Transmission (HVDC) systems. For instance, the two sequential quadratic programming and sequential gradient-restoration algorithm approaches have been applied to solve the AC/DC OPF problem of AC systems with multiterminal DC systems constructed from current-sourced converters, respectively [186] and [187]. Moreover, this research study [35] has suggested a combination approach of heuristic and interior-point methods to solve the optimal reactive power flow problem in the AC/DC power networks, integrating current-sourced converters. In another study [188], a model of security-constrained unit commitment with current-sourced converter based AC/DC power networks utilizing benders decomposition is suggested. From this work, the proposed problem is split into two parts: main and subproblem, where the mixed-integer programming and Newton Raphson techniques are applied. However, since there is a number of essential variations between voltage source converters and current-sourced converters in both operation fundamental and structure, these suggested models cannot be implemented to the hybrid AC/DC integrating voltage source converters.

Given the nonconvex nature of the optimal power flow problem, it has been attempted in all the above-mentioned approaches to improve a convex optimization

problem, which in several cases, drives the loss of precision in solutions or intricacy of algorithms.

8.2 System Model and the Proposed Hybrid AC/DC OPF Formulation

This section illustrates the proposed hybrid AC/DC OPF formulation based on the branch flow model variables. The derived formulation is then modified as positive semidefinite programming relaxation (SDP) format, which is a convex optimization problem. Foremost, a set of hybrid AC/DC constraints are enhanced over the branch flow equations. In this research [189], the branch power flow model has been considered to define the optimal locations of thyristor controlled series capacitors utilizing mixed-integer programming. In this work, a number of equality constraints are substituted by inequality constraints in terms of solving problems with quadratic mixed-integer programming. Also, in terms of removing the nonlinearity from the formulation, the transmission line losses equations have been neglected. The transmission line losses equations are considered the master source of nonlinearity in power flow equations.

A few research studies have formulated these power line losses as a quadratic function of the variance phase angle between two linked buses and thereafter applied a linearized approximation of the power losses [190] and [191]. In this chapter of the dissertation, however, all the nonlinear equations related to both active and reactive power losses for all AC and DC lines are modeled as a function of branch power flow variables. An alternative of considering the linearized approximation of losses, the active and reactive power losses are converted to convex constraints. Additionally, all other AC and DC line capacity and thermal constraints, and generator/VSC capacity constraints, are turned into convex constraints.

In order to perform the precision of the proposed positive semidefinite programming relaxation (SDP) OPF, the numerical results are obtained in the

general algebraic modeling system (GAMS) utilizing MOSEK solver [192] and are contrasted to outcomes achieved in MATPOWER [193]. Four IEEE 5, 14, and 30 bus

8.2.1 The Model of Hybrid AC-DC Power Grids

In this subsection, an introduction to both the AC and DC models are illustrated. An AC line between nodes i and j is represented by a π-equivalent element consisting of a series impedance $Z_{ij} = R_{ij} + jX_{ij}$ of the branch and a shunt element of charging susceptance B_{ij}. If the branch also contains a transformer, it is specified by a tap ratio τ and a phase shift θ.

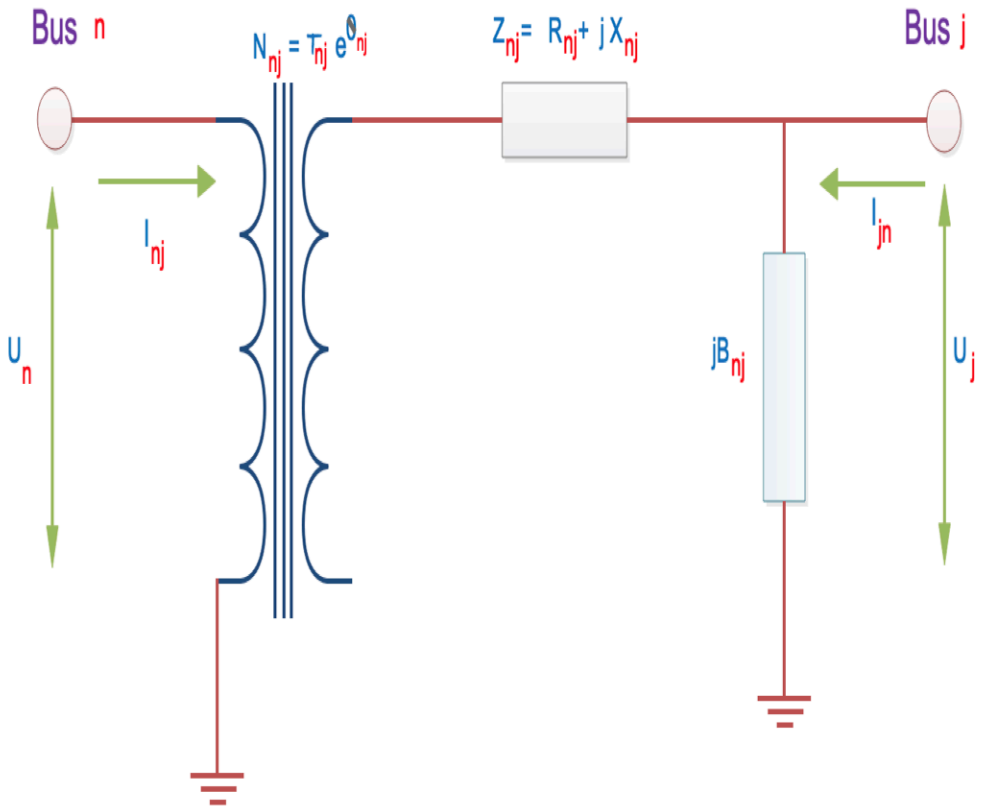


Figure 8.1: Model of an AC transmission branch.

An AC bus may have a number of generators, a load and a shunt element. A generator is modeled as a complex power injection:

$$S_n^g = P_n^g + jQ_n^g. \tag{8.1}$$

Several generators can be attached to the same bus. The total load at a bus is modeled as a consumed complex power quantity:

$$S_n^d = P_n^d + jQ_n^d. \tag{8.2}$$

Each bus has its own total load. The bus also may have a shunt element specified by its admittance

$$Y_n^{sh} = G_n^{sh} + jB_n^{sh}. \tag{8.3}$$

The DC bus can be specified by the power consumed from the DC grid P_{dc} and the voltage U_{dc}. The DC transmission line can be simply specified by its resistance R_s.

8.2.2 The Model of the Voltage Source Converter (VSC)

A voltage source converter (VSC) is used to convert energy between an AC grid and a DC grid so it is connecting an AC bus and a DC bus. As the name suggests, such a converter is controlling the output voltage either on the AC part or the DC part. It is the most used type of converter because it has many advantages over the alternative current source converter that was used previously. For the purpose of OPF computations, a VSC converter is modelled as a pair of coupled generators: an AC generator on the side of the AC grid and a DC generator on the side of the DC grid, as illustrated in **Fig.8.2**. In addition, the active power losses in the converter are best modelled as a quadratic function of the current magnitude

through the VSC converter:

$$P_{loss,c_n} = a_n + b_n I_{c_n} + (c_n + r_n) I_{c_n}^2, \quad \forall n \in \mathcal{N}, \tag{8.4}$$

where

$$I_{c_n} = \frac{\sqrt{P_{k_n}^2 + Q_{k_n}^2}}{U_{k_n}}, \quad \forall n \in \mathcal{N}, \tag{8.5}$$

The AC and DC sides of a converter are linked by the energy conservation principle as shown below

$$P_{loss,c_n} = P_{dc_n} - P_{k_n}, \quad \forall n \in \mathcal{N}, \tag{8.6}$$

If the converter losses are supposed to be proportional to passing active power through the converter (i.e. $P_{loss,c_n} = \beta P_{k,n}$), injected DC power at each DC bus can be defined as follows

$$P_{dc_n} = (1 + \beta) P_{k_n}, \quad \forall n \in \mathcal{N}, \tag{8.7}$$

From this, the inequality constraints can be defined for the VSC converter at each bus for both active and reactive power P_{k_n} and Q_{k_n}, respectively as follows:

$$P_{k_n}^- \leq P_{k_n}(\kappa) \leq P_{k_n}^+, \quad \forall n \in \mathcal{N}, \tag{8.8}$$

$$Q_{k_n}^- \leq Q_{k_n}(\kappa) \leq Q_{k_n}^+, \quad \forall n \in \mathcal{N}, \tag{8.9}$$

A more complicated model of a VSC converter that includes output impedance, filter, and transformers can be accommodated by introducing a "dummy generator or motor which either can absorb or inject active/reactive power to the AC network," an AC bus at the AC output of the converter, and a transmission line to the actual AC bus.

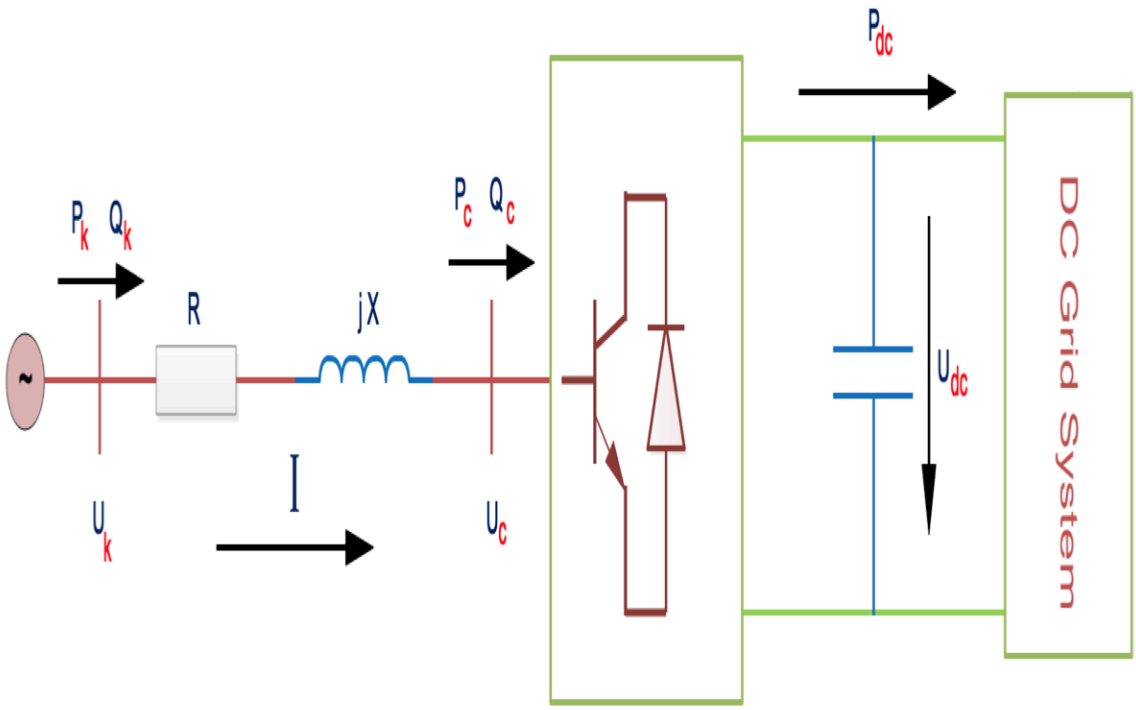


Figure 8.2: Modeling of a VSC AC/DC converter.

In the following subsection, we present the objective function and the constraints of the AC/DC OPF problem.

8.2.3 Objective Function

The general use of the OPF objective function is to reduce the overall cost of the produced power, occasionally taking into consideration the active transmission losses in the whole or a portion of the power network as well. For the convergence, the generation cost functions are considerably approximated by either linear or quadratic functions [99]. In some conditions, the cost is a function of both the active generation and reactive power in the network. The total fuel cost of production (f_1) for the real power of the interconnected generators is given by the

quadratic function.

$$f_1 = \min_{u} \sum_{n \in \mathcal{N}} (A_n + B_n P_n^g + C_n (P_n^g)^2) \tag{8.10}$$

where A_n, B_n and C_n are the fuel cost coefficients of the generating unit i, P_n^g is the generated active power at bus n and $\mathcal{N}$ is number of generators including the slack bus.

8.2.4 Constraints

Constraints are commonly considered an integral portion of a particular optimization problem and play a critical role in its categorization, for instance, convex vs non-convex. In the OPF problem, the network variables must be within admissible bounds, or else the electrical power network devices can be damaged or cause a malfunction. Typically, the constraints are classified as equality and inequality constraints [45] and [109].

In OPF problems, equality constraints are the power flow system equations [110]. Inequality constraints designate upper and lower bounds on the control and state the variables for the devices using the electrical power network, as well as the bounds required to guarantee network security and stability [111]. The inequality constraints on the state and control variables can be partitioned as follows: the state variables' bounds are on the magnitude angle of voltage and the power lines. The control variables' bounds are on the active and reactive power generation, voltage generation, and transformer tap position. Furthermore, the inequality constraints can also locate forbidden areas of branch flow boundaries, interface boundaries, active/reactive power reserve boundaries, power of the PV power source constraints [112], power of the diesel turbine source constraints, spinning reserve requirements, transient security, transient stability, transient contingencies, environment constraints, rotor angle stability, and more. [113].

8.2.4.1 Photovoltaic (PV) System

In this subsection, the photovoltaic system is discussed and its constraints are introduced. The photovoltaic power generation system consists of one or a set of solar panels incorporated with an inverter device, controller, and other electrical components. This kind of renewable energy is used to generate electricity through solar energy. The photovoltaic power generations are currently implemented on a wide range, with several energy investing companies promoting them. However, it requires a high level of expertise for enforcement, modeling, and improvements. Today, several countries are interested in harnessing their geographical position to install solar energy to help them reduce cost and support their electrical needs.

The photovoltaic power generation system is comprised of a photovoltaic array which transmutes the sunlight (photons) falling on it to electrons. This produces a direct current (DC) which can be enhanced with DC-DC converters and then reversed to give an AC power to the loads. Consequently, the most important device in terms of linking the PV to the grid is the power electronic device. Moreover, a particular maximum power point tracking system (MPPT) is needed to vest photovoltaic system to reduce maximum energy from the sun by changing the slanting angle of its beams all throughout the day-time. Lastly, the low-pass filter systems are required to be considered in terms of ignoring unwanted harmonics before it enters the grid.

Most photovoltaic power generation systems are made of semiconductor crystalline materials. Since there are several types of materials are used to design PV systems, a new material in designing PV systems was discovered to improve the power efficiency of the system, which is known as titanium-oxide coated PV cells. Thus, the PV cells are placed in a group to shape modules which can either be

electrically correlated in parallel and/or in series, shaping large systems with scaled voltages and improved power outputs. The MPPT systems are significantly substantial for optimal absorption of solar energy to maximize the efficiency and reliability of the transformation system. Although the solar insolation may differ naturally during the daytime, the MPPT system regulates the PV array output to produce the highest real power at a fixed voltage. Reactive power control is done by utilizing an inverter controller operating in fixed power factor mode. A silicon PV module output relies on numerous variables comprising the sort of material, temperature, and solar irradiation incident on the surface of the module [114]. Its output can be formulated as follows:

$$P_{out} = P_{rat} \times \frac{G_c \times [1 + \kappa(T_c - T_{rat})]}{G_{rat}} \tag{8.11}$$

where P_{out} represents the power output of the PV system in W; G_{rat} represents the solar insolation in Wm^{-2}; G_c represents the insolation of the operating point; κ represents the temperature coefficient of the power; and P_{rat} represents the rated output generated by the module under standard test conditions in watts [115]. The T_c represents the temperature and it can be obtained as following

$$T_c = T_a + \frac{(N_T - 20)}{0.8} \times S_g \tag{8.12}$$

where T_a represents ambient temperature, S_g represents the global solar insolation incident on a horizontal plane united as kWm^{-2}, and N_T represents the normal operating cell temperature, which is around $48C$. The Assumption that the PV system can be correlated in series and/or parallel was illustrated previously to improve the output of both the voltages and currents. A matrix of $\mathcal{N} \in (n_s \times n_p)$ represents that the number of models are connected in series (n_s) or parallel (n_p), respectively. The voltage outputs of the PV array V_{pva}, and power of the PV

systems P_{pv}, are expressed as follows:

$$V_{pva} = N_{pvs} V_{Pv} \tag{8.13}$$

$$P_{pv} = n_s \times n_p \times P_{sys} \times \eta_{MPPT} \times \eta_{loss} \tag{8.14}$$

where N_{pvs} represents the serial connection number of the PV modules, η_{MPPT} is the efficiency of the MPPT system, P_{sys} indicates the maximum power output delivered by the PV system, and η_{loss} is the factor which represents cable resistance and other losses [15]. The local observatories usually provide data on solar irradiance as incident on a horizontal plane. Hence, Hongxing et al. [116] employed the Perez model which helps to find the solar irradiance data for slanting planes with the aim of exploiting maximum η at any time.

8.2.4.2 Diesel Turbine Generator

In this subsection, the diesel turbine system is discussed and its constraints are introduced. To enhance clean energy, diesel turbine generators are now mainly utilized as standby resources in a hybrid power system. In the situation of failures on the renewable sources and battery systems to provide power to meet the required loads, the diesel turbine generator is brought into action. There are several crucial factors for operating diesel turbine generators, including demand loads, and the costs of both transportation and fuel, etc. have to be taken into consideration [117] and [114]. An example was considered by Deshmukh and Deshmukh, where they operated engine generators under two situations, one when the diesel turbine generator is directly connected to the demand load,and another when it is employed as a battery charger [118]. Overall, the diesel turbine generator efficiency can be expressed as

$$\eta_{\mathbf{total}} = \eta_{\mathbf{brake\ thermal}} \times \eta_{\mathbf{generator}} \tag{8.15}$$

where $\eta_{\textbf{brake thermal}}$ represents the brake power of a heat engine as a function of the thermal input from the fuel in the diesel engine and $\eta_{\textbf{generator}}$ is the power efficiency of the diesel engine. Indeed, the generator operation at $70-90\%$ of full load was discovered to be economical. Hence, diesel turbine generator is beneficial in promoting power during peak demand hours and later for energizing the energy storage units when desired. The power constraints for diesel turbine generators can be written as

$$k_{gen}P_{D_{gen}}^{-} \leq P_{D_{gen}} \leq P_{D_{gen}}^{+} \tag{8.16}$$

the value of k_{gen} is set at 0.3 based on the manufacturer's suggestion [115]. The minimum and maximum power constraints for the diesel turbine can be represented by $P_{D_{gen}}^{-}$ and $P_{D_{gen}}^{+}$, respectively.

8.2.4.3 Network Constraints

In this subsection, we present two mathematical models of the power system networks and show their equivalence. Let the set of buses be $\mathcal{N}$:=$\{1,2,3,..,n\}$, the set of transmission lines $\mathcal{E} \subseteq \{\mathcal{N} \times \mathcal{N}\}$ of edges. Then $n \sim j$ denotes a line between the buses n and j. The general bus injection model is defined by the following power flow equations that represent Kirchhoff's laws at each bus:

$$S_n = \sum_{j:n\sim j} V_n(V_n^H - V_j^H)y_{nj}^H, \forall n \in \mathcal{N} \tag{8.17}$$

the superscript H denotes hermitian transpose. Let the set of solutions of the power flow V for each S to be:

$$\mathcal{V} := \{V \in \mathcal{C}^{(n+1)} |\ V \ \text{ satisfies } (8.17)\} \tag{8.18}$$

The buses in the power networks can be divided into three classes: slack, generation, and load buses. The next quantities are generally identified at each bus:

voltage phase angles δ, voltage magnitudes $|V|$, active power output of the slack bus only P_s, and reactive power of all generations Q_n. Usually the voltage magnitudes and the angles are described by one complex variable V rather than real and imaginary variables. Let us now consider the general power network modeled by the subset of buses $\mathcal{N}:=\{1,2,3,..,n\}$, the set of transmission lines $\mathcal{E} \subseteq \{\mathcal{N} \times \mathcal{N}\}$ of edges, and the set of generation buses $\mathcal{G} \subset \mathcal{N}$.

- $P_n^d + iQ_n^d$: Complex power of the load connected to bus $n, \forall n \in \mathcal{N}$.
- $P_n^g + iQ_n^g$: Complex power output of the generator connected to bus $n, \forall n \in \mathcal{N}$
- V_n: Complex voltage at bus $n, \forall n \in \mathcal{N}$.
- y_{nj}: conductance of the transmission line $(n,j) \in \mathcal{E}$, $y_{nj} = g_{nj} + ib_{nj}$.

Define V, P^g, Q^g, P^d and Q^d as the vectors formed stacking, in lexicographical order the values at all the buses of the corresponding variables V_n, P_n^g, Q_n^g, P_n^d, and Q_n^d $\forall n \in \mathcal{N}$, respectively. Assume $f_n(\cdot)$ is a convex function representing the cost associated with bus $n \in \mathcal{N}$. The objective is to minimize the total cost of the system. This problem can then be formulated as follows:

$$\min_{P_n^g, V_n} \quad f = \sum_{n \in \mathcal{N}} f_n(P_n^g) \tag{8.19}$$

subj. to (8.20)

$$|V_n^-| \leq V_n(\kappa) \leq |V_n^+|, , \quad \forall n \in \mathcal{N}, \quad \kappa \in \tau \tag{8.21}$$

$$P_n^{g-} \leq P_n^g(\kappa) \leq P_n^{g+}, \quad \forall n \in \mathcal{N}, \quad \kappa \in \tau \tag{8.22}$$

$$Q_n^- \leq Q_n(\kappa) \leq Q_n^+, \quad \forall n \in \mathcal{N}, \quad \kappa \in \tau \tag{8.23}$$

$$V_{pv_n(\kappa)} = N_{pvs} V_{pv_n(\kappa)}, \quad \forall n \in \mathcal{N}, \quad \kappa \in \tau \tag{8.24}$$

$$k_{gen} P_{Dgen_n}^- \leq P_{Dgen_n}(\kappa) \leq P_{Dgen_n}^+, \quad \forall n \in \mathcal{N}, \quad \kappa \in \tau \tag{8.25}$$

$$P_{pv_n}(\kappa) = n_s \times n_p \times P_{sys_n}(\kappa) \times \eta_{MPPT}(\kappa) \times \eta_{loss}(\kappa), \forall n \in \mathcal{N}, \kappa \in \tau \tag{8.26}$$

$$P_{pv_n}^- \leq P_{pv_n}(\kappa) \leq P_{pv_n}^+, \quad \forall n \in \mathcal{N}, \quad \kappa \in \tau \tag{8.27}$$

$$|V_n(\kappa) - V_j(\kappa)| \leq \Delta V_{nj}^+(\kappa), \quad \forall (n,j) \in \mathcal{E} \tag{8.28}$$

$$P_n^g(\kappa) + Q_n^g(\kappa) = P_n^d(\kappa) + Q_n^d(\kappa) + r_n(\kappa) + P_{pv_n}(\kappa) +$$
$$P_{Dgen_n}(\kappa) + V_n(\kappa) \sum_{j:n\sim j}^{n \in \mathcal{N}} \Big\{ V_n(\kappa) - V_j^H(\kappa) \Big\} y_{nj}, \qquad \forall n \in \mathcal{N}, \qquad \kappa \in \tau \tag{8.29}$$

In this formulation P_n^g and Q_n^g are controllable variables, and P_n^d and Q_n^d are given external disturbances. The solution will give values of P_n^g and Q_n^g, at every bus, to minimize the cost and satisfy the physical and operational constraints of the network.

8.3 Performance Evaluation

In this section, we illustrate the performance of the optimization approach for solving the AC/DC OPF problem. The performance of the proposed algorithm has been examined on different electrical power networks with various power system sizes, such as IEEE 5 bus, IEEE 14 bus, and IEEE 30 bus. The outcomes of the

experiments proved the adaptability of the algorithm when considering large-scale electrical power networks. In contrast, this proposed algorithm has been compared with several exiting optimization algorithms given in the literature for similar consider power systems, where it shows the effectiveness of this proposed method.

8.3.1 Hybrid AC/DC Power Grid of IEEE 5 Bus Case Study

In this case study, an IEEE of 5 bus system test is selected and modified from [194]. The five bus power system is illustrated in Figure 8.3. The power system consists of 2 AC power buses attached at bus 1 and bus 2, three DC buses, five AC branches, three DC branches, and three load sides attached at buses $3, 4$ and 5. Three AC/DC converters are embedded in this system as follows: the converter $VSC-1$ that is connected to bus 2 controls the DC voltage at DC bus $D-1$. Also, the converter $VSC-2$ that is connected to bus 3 controls the DC voltage at DC bus $D-2$. The converters $VSC-3$ that is connected to bus 5 controls the DC voltage at DC bus $D-3$. In bus $D-G$, the renewable energy source (i.e., photovoltaic power system) has been considered to support the demand loads in the system.

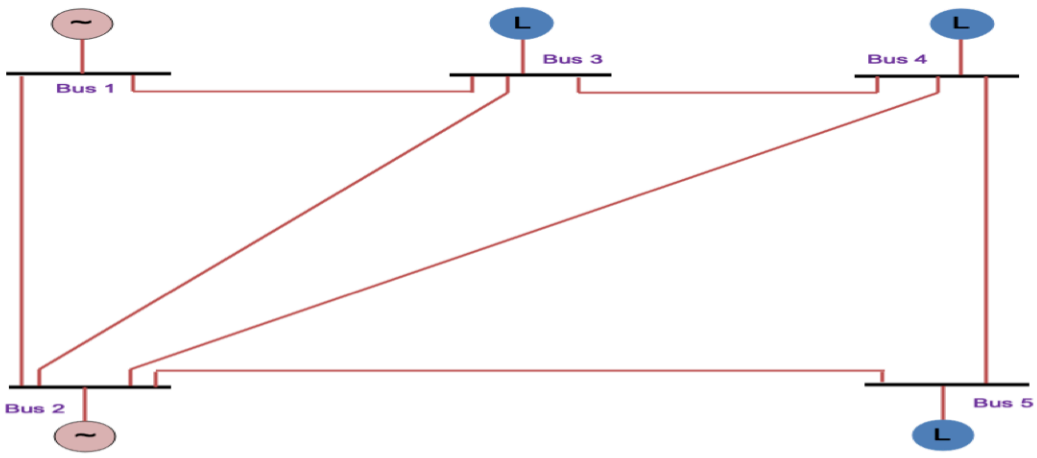


Figure 8.3: An AC power system of IEEE 5 bus.

To the AC power grid, we add a DC power grid connected through VSC converters as shown in **Fig.8.4**, where the DC part of the grid was indicated in a different color. The optimal value of the cost and the running time are shown in

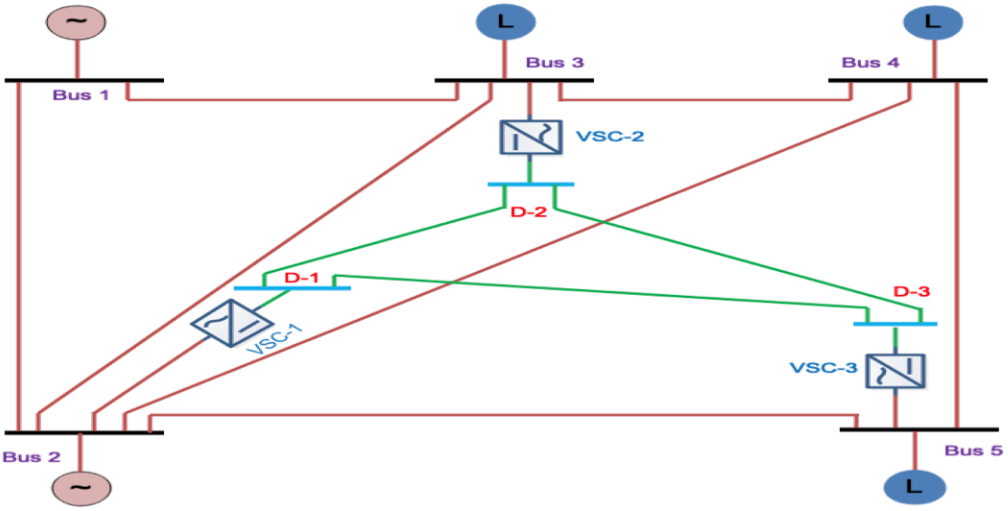


Figure 8.4: A hybrid AC/DC power grid with five AC buses and three DC buses.

Table. 8.1. The data and results for this case are presented in **APPENDIX C**, Tables 1 and 2, respectively.

Table 8.1: The result of the hybrid AC/DC power grid of the IEEE 5 bus.

Optimization Methods	Opt. value	Comp. Time (s) w/ acceleration	Comp. Time (s) w/o acceleration
SP-Relaxation Algorithm	1.5510e+03	0.1510	0.332
Mixed-Integer Programming Algorithm	1.6552e+04	0.5714	0.9714
Interior-Point Algorithm	1.7553e+04	0.6028	1.5028
Genetic Algorithm (GA)	1.7551e+04	93.0323	122.81
Particle Swarm Opt. Algorithm (PSO)	1.7552e+04	90.212	120.701

8.3.2 Hybrid AC/DC Power Grid of IEEE 14 Bus Case Study

In this case, five hybrid power system terminals are adopted to modify IEEE 14-bus system, as represented in **Fig.8.5**. The power system consists of 14 AC power buses, five DC buses, five generators, 20 AC branches, seven DC branches, three HNSs, one renewable energy source (i.e., photovoltaic power system), and 11 load sides. Four AC/DC converters are embedded in this system as follows: the converter $VSC-1$ that is connected to bus 1 controls the DC voltage at DC bus $D-1$. Also, the converter $VSC-3$ that is connected to bus 3 controls the DC voltage at DC bus $D-3$. The converters $VSC-9$ and $VSC-13$ that are connected to bus 9 and 13 controls the DC voltage at DC bus $D-9$ and $D-13$, respectively. In bus $D-G$, the renewable energy source (i.e., photovoltaic power system) has been attached to support the demand loads in the system.

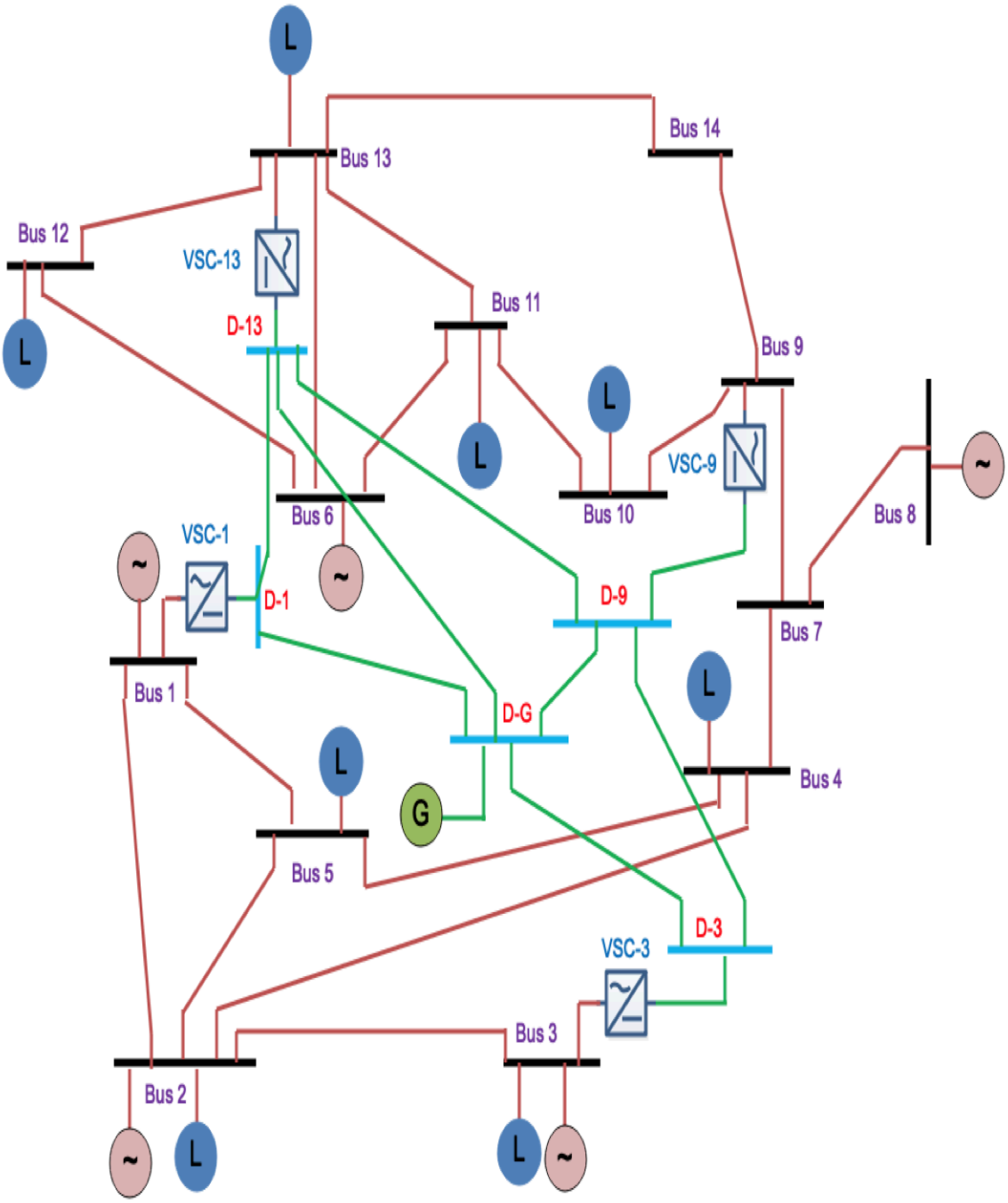


Figure 8.5: A hybrid AC/DC power grid based on the IEEE 14 bus case.

The fully used data for this system are provided in **APPENDIX D**, Tables 1, 2 and 3. The running of power flow results are also given in **APPENDIX D**, Tables 4, 5 and 6. The optimal value of the cost and the running time are shown in Table. 8.2.

Table 8.2: The result of the hybrid AC/DC power grid of the IEEE 14 bus.

Optimization Methods	Opt. value	Comp. Time (s) w/ acceleration	Comp. Time (s) w/o acceleration
SP-Relaxation Algorithm	1.0234e+05	95.27	401.267
Mixed-Integer Programming Algorithm	1.3752e+05	281.32	903.545
Interior-Point Algorithm	1.4652e+05	361.93	1615.28
Genetic Algorithm (GA)	1.4352e+05	661.32	2998.12
Particle Swarm Opt. Algorithm (PSO)	1.4152e+05	698.09	3092.85

8.3.3 Hybrid AC/DC Power Grid of IEEE 30 Bus Case Study

A large-scale power system has to be considered to validate the practicability of the proposed approach. An IEEE 30-bus power system (see **Fig.8.6**) is modified to effectively cover the loads in the system. In this power grid system, four renewable power sources (i.e., photovoltaic systems) are connected to the main power grid at buses 1, 2, 5, 6, 15, and 30 through a HVDC line. The power system consists of 30 AC power buses, five DC buses, six distributed power generators, three main power feeders, 41 AC branches, eleven DC branches, and 20 load sides.

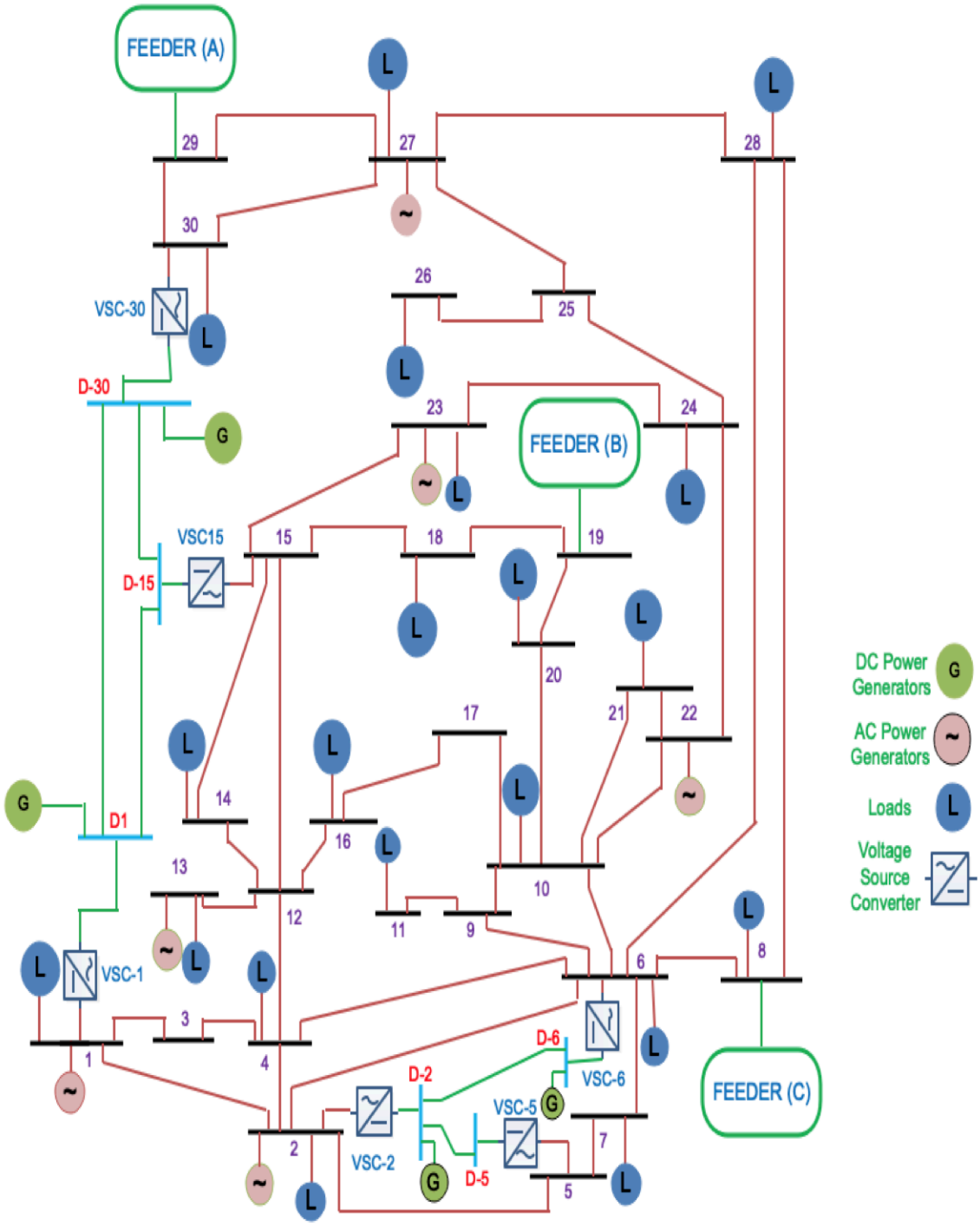


Figure 8.6: A hybrid AC/DC power grid based on the IEEE 30 bus case.

The fully used data for this system is presented in **Appendix E**, Tables 1, 2 and 3. The optimal value of the cost and the running time are shown in Table. 8.3.

Table 8.3: The result of the hybrid AC/DC power grid of the IEEE 30 bus.

Optimization Methods	Opt. value	Comp. Time (s) w/ acceleration	Comp. Time (s) w/o acceleration
SP-Relaxation Algorithm	0.8356e+06	188.25	635.31
Mixed-Integer Programming Algorithm	1.23059e+07	1210.773	4146.201
Interior-Point Algorithm	1.33145e+07	1303.3	5163.04
Genetic Algorithm (GA)	1.40148e+07	2641.6	9846.246
Particle Swarm Opt. Algorithm (PSO)	1.21892e+07	2783.1.4	9943.942

8.4 Analysis of Simulation Results

In terms of assessing the performance of the suggested proposed optimization approach, different electrical power networks with various power system sizes, such as IEEE 5, 14, and 30 buses, have been considered for this study. In this work, converters associated with a hybrid AC/DC power system have been implemented and compared with other existing techniques, with and without using the Matlab acceleration technique.

The proposed optimization approach has been examined for a small power system size, such as IEEE 5 bus test systems. The performance of the proposed optimization approach is compared against existing approaches, where the results of this system are presented in table 8.1. As can be observed, the SP-Relaxation

algorithm offers a better performance, e.g. minimize objective value with a short computational time, as compared with other approaches, even when it is a small power network size.

The outputs of the proposed optimization approach are applied to IEEE 14 bus test power systems and then compared and summarized in table 8.2. Notice the SP-Relaxation algorithm provides the lowest objective value and it takes about 95.27 seconds when we do not consider the acceleration technique. However, while considering the acceleration technique, it provides a better computational time. This proposed optimization approach is compared with other existing techniques. For example, when we use the mixed-integer technique, as can be seen, the objective value is slightly high compared to the proposed approach but it takes more computational time to reach this value. Similarly, while applying the interior-point technique, the computational time is increased, as well as the objective value. However, these two techniques have shown better solutions and computational times as compared to other well-known techniques, namely the genetic algorithm (GA) and particle swarm optimization algorithm (PSO). The genetic algorithm (GA) takes less computational time compared to the particle swarm optimization algorithm (PSO) to achieve the objective value. However, the particle swarm optimization algorithm (PSO) gives less objective value as compared to the genetic algorithm (GA).

For the full implementation, the IEEE 30 bus case study was modified with six terminal DC power systems, as illustrated in **Fig.8.6**. These DC power systems can be set in two different sorts of configurations such as V and Δ. The converters have been connected as follows: $VSC-1$, $VSC-2$, $VSC-5$, $VSC-6$, $VSC-15$, and $VSC-30$ are connected to AC buses 1, 2, 5, 6, 15, and 30, respectively. The product range of the DC voltage levels is modified according to

the ABB High Voltage Cable (HVC) technical report [195]. In this simulation, the converter power ratings are chosen to be 100 (MVA).

For this hybrid power system, the constraints strategies have been considered on the converter variables instead of using some control strategies. The converters are set to be within upper and lower constraints. Therefore, the best value will be chosen based on which one the objective function has minimized. The output results are summarized in tables 8.4, 8.5 and 8.6

Table 8.4: The result of the IEEE 30 test system including the DC converters.

DC	P_n^g(MW)	Q_n^g(MVRA)
DG1	156.36	0
DG2	140.00	4.72
DG5	0.00	6.24
DG8	0.00	27.62
DG11	0.00	9.53
DG13	0.00	12.43

Table 8.5: The result of the IEEE 30 test system including the DC converters rated at 100 MVA.

Parameters	Total value
P_{loss}	3.82 MW
Q_{loss}	14.19 MVAR
P^g	289.92 MW
Q^g	36.16 MVAR
Q_{Shant}	61.19 MVAR
Q_{conv}	43.00 MVAR
P_{loss}^{dc}	2.10 MW

Table 8.6: The result of the IEEE 30 test system including the DC converters rated at 100 MVA.

DC bus parameters	Voltage (p.u)	$P_{conv}(MW)$	$Q_{conv}(MVAR)$
$D-2$	1.060	-79.962	17.310
$D-6$	1.045	25.741	2.682
$D-5$	1.040	52.529	26.898
$D-1$	1.060	-59.910	-17.454
$D-15$	1.045	40.444	10.071
$D-30$	1.052	18.453	3.499

As can be seen from the outputs, the total losses of the AC power system are minimized, which leads to a reduction in the generated power and analogous reduction of generation cost due to the optimization values of converter variables. Moreover, the reactive power generations have also been lowered due to local reactive powers injected by converters.

From the other side of the analysis, the rating powers of the converter have been set to a lower value of 100 (MVA). The reason for this is to observe its influence on both total generation cost and converter variables. The corresponding results are already summarized in tables 8.5 and 8.6. As a summary of outputs obtained for the IEEE 5, 14, and 30 bus test power systems, the proposed optimization approach is effectively performed with a hybrid AC/DC power system associated with converters and it proves the accuracy of the proposed relaxation OPF formulation. Notably, the solution can be reached with less computational time compared to other existing approaches.

CHAPTER NINE

CONCLUSION AND FUTURE WORK

9.1 Conclusions

In this dissertation, the polynomial optimization problem (POP) relaxation based on optimization approaches has been introduced to solve the nonlinear equation of the optimal power flow problem in standalone DC-microgrids and hybrid AC/DC microgrids. The first objective of this dissertation was to formulate the optimal power flow problem in a standalone DC-microgrid in order to economically reduce the cost and network losses during the operational time. The second objective was to formulate the optimal power flow (OPF) problem with dynamic energy storage as a static optimization problem. Furthermore, the optimal power flow (OPF) problem of a hybrid AC/DC power system associated with converters has been formulated to deal with non-convexity present in the hybrid AC/DC power system.

Since this problem leads to a nonlinear programming problem, it was converted to a problem with constraints over the cone of positive semidefinite matrices and required the introduction of a rank suitable constraint. The rank constraint was ignored, resulting in an SOPC problem that can be solved numerically as using SDP solvers. This approach was tested in various scenarios, for example standalone DC-microgrids, power grid including energy storage device units, and hybrid AC/DC microgrids. Analysis of the numerical results for these scenarios shows that the optimal solution can be obtained, (i.e. $\boldsymbol{Rank(M_{nj})} = 1$ holds, $\forall n \sim j$). In cases where the energy storage devices were considered, it can be observed that, as expected, the energy stored was scheduled to balance the power of

loads and generation sources. It can be noticed that energy storage provides additional flexibility to the power grid for tackling load variations and power limits, with the potential of providing improved power quality, stability, load following, peak reduction, and reliability.

Moreover, in this dissertation, a comparison of various exiting optimization algorithms was considered in terms of showing the robustness and effectiveness of the polynomial optimization problem (POP) relaxation based on the optimization approach. As an achievement for this comparison, it can be seen that the proposed approach can solve the nonconvexity of large-scale networks while minimizing the energy expenses and network system losses. It can be also noted that the objective value can be reached with a low computational time compared to other exiting optimization considered algorithms in this dissertation.

9.2 Future Work

This dissertation offers numerous future research directions that have been exposed as a result of ordinary work. Below is a summary of the most promising possible trends to be carried out and investigated in future iterations:

- It is significant to understand how to convert such challenging problems into straightforward ones by merging the most recent techniques that efficiently impose the relaxation of the rank constraint to its tractable convex envelope, rather than neglecting it. Good techniques for further investigation are based on the consideration of the Schatten quasi-norm minimization (SQNM) technique and holder inequality for Schatten norms (HISN) [196] and [197], respectively.

- Another research trend to make this study valuable is to consider both the transient and small signal stability in terms of guaranteeing that the power networks' stability is not being affected by the circuit breakers when they are turned "on" and "off" during the operational time.

- Future research in this area could evaluate the performance of the proposed approach by considering a large-scale problem with multi-objective functions such as minimizing the quadratic fuel cost function, fuel cost with value-point loadings, real power losses of transmission, and fuel cost emission. Doing so will offer a better evaluation for our proposed technique and then compared it to other exiting techniques.

9.2.1 Other Possible Topics for Future Research

In contrast to the OPF problem for AC grids that was extensively studied over many years, DC grids have not received as much attention. In fact, we could only identify two papers that are exclusively devoted to the OPF problem for DC grids and both are fairly recent. This is undoubtedly due to the fact that DC grids are encountered far less often than the ubiquitous AC grids, providing many possibilities for future research. Many problems, though not all, that were tackled in the case of AC grids, can and should be considered for DC microgrids as well.

9.2.1.1 Local Approximations

As opposed to relaxation that calls for eliminating or weakening constraints, approximating the problem around an operating point may transform the problem into a Linear Programming problem that is readily solvable using the Simplex Algorithm. An interesting extension of Linear Programming that was used in the solution of the OPF problem [198] is Sequential Linear Programming which uses

multiple linearization points to obtain the optimal solution. The cited reference [198] introduces Sequential Quadratic Programming that uses a quadratic approximation of the original problem.

9.2.1.2 Iterative Methods

The classical methods have proven their usefulness for the OPF problem in the past and they may be interesting for DC microgrids as well, especially since the size of such grids is usually moderate. First order methods, like the Gradient Method, and second order methods, like Newton-Raphson, may be very useful, especially if some information is available for an adequate initialization. Versions of these methods can be used such as Reduced Gradient (e.g., [29]) which take advantage of the fact that most constraints are linear to obtain even better results.

9.2.1.3 Duality Methods

A powerful alternative to relaxation for transforming a non-convex problem into a convex one is duality. The duality of a non-convex optimization problem is a convex problem itself, and its value is a lower bound of the value of the original (primal) problem. The difference between the values of the two problems is called the duality gap. If the duality gap is zero, it is possible to obtain the solution of the primal problem, by solving the dual problem.

This approach was pursued in [199] for AC power grids and it would be interesting to see how it can be adapted to DC grids.

9.2.1.4 Convex Relaxation Methods

The paper analyzed here uses second-order conic relaxation which is a very special relaxation type. There are other relaxation types that were used in the

literature, specifically semidefinite programming (SDP) relaxations, such as in [200] and [37] and many others. In fact, the two part tutorial [40] and [41] gives a detailed overview of all the convex relaxation approaches utilized at the time for solving the OPF problem for AC grids. The interest of studying different convex relaxation methods, other than second-order conic, is that they may prove to be exact even for the case of line currents constraints. This advantage may come with an execution time penalty since second-order conic problems are easier to solve numerically than other convex problems, such as SDP problems.

9.2.1.5 Distributed Processing Methods

Due to the enormous size of AC grids and the interest in operating them as efficiently as possible, there was a great interest in devising optimization methods that use distributed data processing such as [201, 202, 203]. In the future, it could be interesting to examine such methods for DC grids as well, although the current opportunities to do so are relatively sparse.

9.2.1.6 Dynamic Networks with Discrete Elements

Although the OPF problem is referring to the optimal steady-state operation of a network, the solution may change dynamically over time as new loads and/or generators are coming online. Some networks have the ability to switch on and off certain lines, depending on the power production and network demand. In this case, the configuration of the network may be changed to improve the operation, and therefore the OPF problem becomes a mixed integer optimization problem. This case was extensively studied for AC grids, e.g., [81], but has not yet been studied for DC power networks.

This area of research may potentially be of great interest in the future. After all, the decisive advantage of AC grids over DC grids is the limitation of switches

and circuit breakers, one of AC energy's major advantages over DC energy. Thus, the robust optimization of DC grids with switches should take such constraints into account.

9.2.1.7 New Problem Formulations

There are many formulations for the OPF problem for AC grids. This is due to specific characteristics of AC grids that require the control of reactive power, for example. Balancing the efficiency of utilizing active power with the need to avoid losses due to reactive power has motivated many versions of the OPF problem that have been studied over the years. The situation is entirely different for DC grids and the few contributions in this area have used the same formulation, based on power generated and consumed over the grid. However, DC power grids have their own characteristics. As aforementioned, one of them refers to switches and circuit breakers. Another aspect is related to the change of voltage levels that is more difficult in the case of DC energy. These and other aspects should be taken into account to formulate more realistic versions of the OPF problem for DC power grids that will likely present different challenges and may require the development of new methods entirely different from those used in the AC case.

APPENDIX A

Power Load Data of the First Scenario

A.3 APPENDIX A

Table A.1: The power load data for the first case scenario-I.

Time (hrs)	$P^{d}_{5,11}$	$P^{d}_{4,8,13}$	$\sum P^{\text{Loads}}$
1	10K	11566.88	54700.64
2	10K	11475.32	54425.96
3	10K	11322.26	53966.78
4	10K	11560.44	54681.32
5	10K	11850.9	55552.7
6	10K	12109.52	56328.56
7	10K	13375.81	60127.43
8	10K	14178.95	62536.85
9	10K	14462.95	63388.85
10	10K	14506.92	63520.76
11	10K	14488.38	63465.14
12	10K	14422.6	63267.8
13	10K	2236.89	26710.69
14	10K	1248.72	23746.17
15	10K	1845.20	25535.61
16	10K	7148.93	41446.80
17	10K	9794.53	49383.59
18	10K	8951.72	46855.17
19	10K	7615.88	42847.65
20	10K	8071.939	44215.81
21	10K	11004.78	53014.34
22	10K	14248.72	62746.17
23	10K	11393.01	54179.04
24	10K	6354.01	39062.03

Table A.2: The power generation data for the first case scenario-I.

Time (hrs)	P_2^g	P_5^g	P_6^g	P_8^g	P_{14}^g	$\sum P_n^g$
1	51167.58	49818.81	8353.78	49818.81	50862.45	210021.42
2	51244.40	49821.38	10626.93	49821.38	50890.91	212405.00
3	51243.96	49821.51	11170.41	49821.51	50891.27	212948.65
4	51243.12	49821.44	11491.95	49821.44	50890.89	213268.84
5	51242.81	49821.37	11781.87	49821.37	50890.67	213558.10
6	51242.51	49821.32	12164.78	49821.32	50890.51	213940.45
7	51242.20	49821.09	13328.92	49821.09	50890.41	215103.71
8	51241.91	49820.95	14262.07	49820.95	50890.31	216036.18
9	51241.65	49820.89	14594.33	49820.89	50890.21	216367.98
10	51241.45	49820.88	14357.21	49820.88	50890.13	216130.56
11	51241.30	49820.89	13571.88	49820.89	50890.07	215345.02
12	51241.19	49820.90	11535.10	49820.90	50890.03	213308.12
13	51240.84	49823.05	4338.91	49823.05	50889.62	206115.48
14	51240.81	49823.22	3861.26	49823.22	50889.59	205638.10
15	51240.88	49823.12	4228.54	49823.12	50889.63	206005.28
16	51241.12	49822.20	5894.98	49822.20	50889.84	207670.34
17	51241.41	49821.73	7642.37	49821.73	50890.00	209417.25
18	51241.75	49821.87	8086.94	49821.87	50890.09	209862.53
19	51242.24	49822.10	8002.45	49822.10	50890.21	209779.10
20	51242.94	49822.01	8646.21	49822.01	50890.43	210423.60
21	51243.87	49821.47	10505.88	49821.47	50890.79	212283.48
22	51244.95	49820.87	12272.00	49820.87	50891.23	214049.93
23	51246.29	49821.37	9896.78	49821.37	50891.60	211677.41
24	51247.82	49822.19	4619.78	49822.19	50891.74	206403.73

Table A.3: The power load data and the battery charging rate for the first case scenario-I.

Time (hrs)	r_3	r_8	r_{10}	r_{12}	$\sum r_n$
1	-4004.39	-3213.10	-4006.79	-4004.02	-15228.29
2	-30.61	-848.39	-29.81	-30.63	-939.44
3	25.01	-151.85	23.29	25.55	-77.99
4	6.66	-68.49	5.48	6.96	-49.40
5	6.23	-69.03	5.22	6.46	-51.12
6	6.90	55.26	5.83	7.13	75.13
7	6.05	-46.89	4.92	6.28	-29.65
8	4.62	83.12	3.49	4.82	96.06
9	3.32	131.38	2.23	3.47	140.40
10	2.35	-149.71	1.33	2.42	-143.61
11	1.67	-916.50	0.74	1.67	-912.42
12	1.19	-2887.50	0.35	1.08	-2884.88
13	0.86	2102.01	0.10	0.68	2103.65
14	0.59	2612.53	-0.07	0.31	2613.36
15	0.46	2383.33	-0.13	0.13	2383.79
16	0.52	-1253.95	-0.05	0.20	-1253.27
17	0.96	-2152.16	0.30	0.73	-2150.17
18	1.95	-864.78	1.03	1.92	-859.89
19	3.56	386.56	2.19	3.83	396.15
20	5.55	574.27	3.57	6.13	589.52
21	7.19	-498.90	4.60	7.84	-479.26
22	9.10	-1976.72	5.60	9.72	-1952.30
23	20.20	-1496.23	12.97	23.05	-1440.01
24	1.46	-1734.23	-2.47	-3.66	-1738.90
25	0.00	0.00	0.00	0.00	0.00

APPENDIX B

Power Load Data of the Second Scenario

B.4 APPENDIX B

Table B.1: The power load data for the second case scenario-II.

Time (hrs)	$P^{d}_{3,11}$	$P^{d}_{4,8,13,14,18,21,23,26,27}$	$\sum P^{\text{Loads}}_{n}$
1	10K	11566.88	124101.92
2	10K	11475.32	123277.88
3	10K	11322.26	121900.34
4	10K	11560.44	124043.96
5	10K	11850.9	126658.1
6	10K	12109.52	128985.68
7	10K	13375.81	140382.29
8	10K	14178.95	147610.55
9	10K	14462.95	150166.55
10	10K	14506.92	150562.28
11	10K	14488.38	150395.42
12	10K	14422.6	149803.4
13	10K	2236.89	40132.07
14	10K	1248.72	31238.51
15	10K	1845.20	36606.83
16	10K	7148.93	84340.42
17	10K	9794.53	108150.79
18	10K	8951.72	100565.51
19	10K	7615.88	88542.97
20	10K	8071.939	92647.45
21	10K	11004.78	119043.03
22	10K	14248.72	148238.51
23	10K	11393.01	122537.12
24	10K	6354.01	77186.10

Table B.2: The power generation data for the second case scenario-II.

Time (hrs)	P_1^g	P_2^g	P_{13}^g	P_{22}^g	P_{23}^g	P_{27}^g	$\sum P_n^g$
1	6502.54	1372.01	10000.00	9604.06	1666.67	59823.40	88968.68
2	21364.26	990.93	10000.00	9512.93	3333.33	59819.92	105021.37
3	9345.97	2034.91	10000.00	9360.58	4166.67	59814.18	94722.30
4	8084.22	1499.63	10000.00	9597.65	1851.85	59823.24	90856.60
5	5983.48	1544.80	10000.00	9886.73	1190.48	59834.75	88440.23
6	13689.68	1810.23	10000.00	10137.29	2272.73	60234.61	98144.54
7	7997.06	2034.07	10000.00	11390.78	2941.18	60777.67	95140.76
8	16004.19	1451.11	10000.00	12189.30	4166.67	60815.91	104627.17
9	30415.03	1558.95	10000.00	12471.59	1282.05	60830.05	116557.67
10	14483.87	2979.83	10000.00	12515.30	4545.45	60832.27	105356.73
11	6912.65	3124.22	10000.00	12496.87	1190.48	60831.33	94555.54
12	13223.48	3271.44	10000.00	12431.49	1428.57	60828.00	101182.98
13	6421.81	117.92	10000.00	731.12	1315.79	42383.96	60970.61
14	5816.44	0.00	9937.50	0.00	1104.17	41878.40	58736.50
15	4238.20	80.89	10000.00	339.72	1282.05	42382.00	58322.85
16	9859.08	581.69	10000.00	5584.23	1000.00	45351.76	72376.76
17	13447.46	1020.88	10000.00	8167.02	3125.00	48410.85	84171.21
18	6539.03	1665.32	10000.00	7327.43	3125.00	48388.81	77045.59
19	6534.91	2725.47	10000.00	5996.04	1515.15	48358.35	75129.92
20	8061.36	3225.33	10000.00	6450.66	1136.36	48368.16	77241.87
21	6728.69	1201.55	10000.00	9372.07	2777.78	48446.58	78526.67
22	6226.41	1285.57	10000.00	12598.60	3333.33	48566.00	82009.91
23	5768.93	2121.41	10000.00	9758.49	1923.08	48458.98	78030.87
24	4339.94	661.28	10000.00	5025.74	1190.48	39927.41	61144.84

Table B.3: The power load data and the battery charging rate for the second case scenario-II.

Time (hrs)	r_7	r_8	r_{10}	r_{11}	r_{12}	r_{19}	r_{24}	r_{28}	r_{30}	$\sum r$
1	-783.66	388.27	387.29	-169.42	-684.86	388.51	-832.65	-740.04	-832.65	-2879.22
2	-782.19	479.21	487.31	-169.94	-685.70	477.94	-832.64	-740.03	-832.64	-2598.69
3	-779.75	631.23	654.35	-170.81	-687.08	627.49	-832.63	-740.02	-832.63	-2129.85
4	-783.55	394.72	394.35	-169.46	-684.93	394.81	-832.65	-740.04	-832.65	-2859.41
5	-788.33	106.45	76.68	-167.76	-682.26	111.24	-832.68	-740.07	-832.68	-3749.41
6	-816.14	-0.04	0.02	-157.90	-855.00	-0.01	-833.33	-740.65	-833.33	-4236.38
7	-860.36	-1144.16	-1038.62	-142.23	-963.12	-1161.50	-833.79	-741.05	-833.79	-7718.63
8	-876.34	-1940.26	-1931.93	-136.57	-954.14	-1941.66	-833.89	-741.14	-833.89	-10189.83
9	-882.25	-2221.66	-2249.23	-134.48	-950.81	-2217.16	-833.93	-741.18	-833.93	-11064.63
10	-883.19	-2265.22	-2298.42	-134.15	-950.29	-2259.80	-833.94	-741.18	-833.94	-11200.12
11	-882.80	-2246.86	-2277.68	-134.29	-950.51	-2241.82	-833.93	-741.18	-833.93	-11143.00
12	-881.43	-2181.69	-2204.10	-134.78	-951.29	-2178.03	-833.93	-741.17	-833.93	-10940.34
13	55.18	3573.65	3684.74	-741.35	1977.40	3701.36	2.30	-102.73	2.79	12153.33
14	2593.21	4461.22	4232.47	-901.65	1793.04	4207.07	1.51	-101.61	1.83	16287.10
15	55.96	3965.12	4082.78	-741.70	1979.97	4091.57	1.03	-101.33	1.24	13334.63
16	-143.81	-0.00	0.00	-671.24	580.02	0.00	0.66	-101.58	0.79	-335.16
17	-357.13	-1357.19	-1303.79	-596.23	-911.90	-1367.18	0.32	-101.91	0.39	-5994.61
18	-346.16	-517.83	-395.29	-600.09	-917.20	-540.58	0.00	-101.55	0.00	-3418.69
19	-331.02	813.24	1031.66	-605.41	-924.83	772.86	-0.31	-101.19	-0.38	654.62
20	-335.89	358.74	546.29	-603.70	-921.30	324.01	-0.65	-100.83	-0.78	-734.12
21	-374.88	-2561.81	-2619.62	-590.01	-898.73	-2551.25	-1.03	-100.45	-1.24	-9699.02
22	-434.34	-5787.04	-6214.64	-569.16	-864.59	-5707.52	-1.52	-99.97	-1.83	-19680.61
23	-381.11	-2948.09	-3044.61	-587.85	-891.88	-2930.34	-2.31	-99.08	-2.81	-10888.08
24	-0.02	-0.01	-0.00	-969.84	-0.00	-0.00	-0.00	-0.00	-0.00	-969.87
25	0.00	0.00	0.00	0.00	0.00	0.00	0.00	0.00	0.00	0.00

APPENDIX C

Power Load Data for the IEEE 5 Bus Power System

C.5 APPENDIX C

Table C.1: The data profile for the IEEE 5 bus power system.

(a) The data profile for the generators of the IEEE 5 bus power system.

Bus	P_g	Q_g	Q_{max}	Q_{min}	V_g	P_{max}	P_{min}
1	0	0	500	-500	1.06	250	10
2	40	0	300	-300	1	300	10

(b) The data profile for the buses of the IEEE 5 bus power system.

No	Type	P_d	Q_d	G_s	B_s	V_m	V_a	V_{max}	V_{min}
1	3	0	0	0	0	1.06	0	1.1	0.9
2	2	20	10	0	0	1	0	1.1	0.9
3	1	45	15	0	0	1	0	1.1	0.9
4	1	40	5	0	0	1	0	1.1	0.9
5	1	60	10	0	0	1	0	1.1	0.9

(c) The data profile for the branches of the IEEE 5 bus power system.

From	To	R
1	2	0.052

(d) The data profile for the DC buses of the IEEE 5 bus power system.

Bus_{DC}	Bus_{AC}	P_{dc}	V_{dc}	$V_{c,max}$	$V_{c,min}$
1	2	0	1	1.1	0.9
2	3	0	1	1.1	0.9

(e) The data profile for the DC lines of the IEEE 5 bus power system.

Bus_{DC}	P_s	Q_s,	V_{tar}	BasekV	$V_{m,max}$	$V_{m,min}$	a	b	c	r
1	-60	-40	1	345	1.1	0.9	1.103	0.887	4.371	2.885
2	0	0	1	345	1.1	0.9	1.103	0.887	4.371	2.885

Table C.2: The optimal power flow results of the IEEE 5 bus power system.

(a) The AC buses of the IEEE 5 bus power system

Bus	V_n
1	1.018
2	1.007
3	0.993
4	0.992
5	0.992

(b) The AC generators of the IEEE 5 bus power system

Bus	P_n^g	Q_n^g
1	128.3	-7.8
2	80	20

(c) The result of DC the grid buses

Bus_{DC}	Bus_{AC}	P_{dc}	V_{dc}
1	2	37.35	1.015
2	3	-12.34	1.094
3	5	-24.87	1.008

(d) The result of DC the grid lines

From	To	P_n^{DC}	P_j^{DC}
1	2	19.04	18.95
1	3	18.30	-18.19
2	3	6.60	-6.58

(e) The converter results

Bus_{DC}	P_{conv}	Q_{conv}, V_{conv}	$V_{m,c}$	$\delta_{m,c}$	$P_{c,loss}$
1	-37.49	-40 1	1.06	-9.03	0.023
2	12.31	-40 1	1.01	, -2.95	0.018
3	24.69	-40 1	0.92216	-1.54	0.016

APPENDIX D

Power Load Data for the IEEE 14 Bus Power System

D.6 APPENDIX D

Table D.1: The data profile for the IEEE 14 bus of AC power system.

(a) The data profile for the generators of the IEEE 14 bus power system.

Bus	P_g	Q_g	Q_{max}	Q_{min}	V_g	P_{max}	P_{min}
1	232.4	-16.9	10	0	1.06	332.4	0
2	40	42.4	50	-40	1.045	140	0
3	0	23.4	40	0	1.01	100	0
6	0	12.2	24	-6	1.07	100	0
8	0	17.4	24	-6	1.09	100	0

(b) The data profile for the buses of the IEEE 14 bus power system.

No	Type	P_d	Q_d	G_s	B_s	V_m	V_a	V_{max}	V_{min}
1	3	0	0	0	0	1.06	0	1.06	0.94
2	2	21.7	12.7	0	0	1.045	-4.98	1.06	0.94
3	2	94.2	19	0	0	1.01	-12.72	1.06	0.94
4	1	47.8	-3.9	0	0	1.019	-10.33	1.06	0.94
5	1	7.6	1.6	0	0	1.02	-8.78	1.06	0.94
6	2	11.2	7.5	0	0	1.07	-14.22	1.06	0.94
7	1	0	0	0	0	1.062	-13.37	1.06	0.94
8	2	0	0	0	0	1.09	-13.36	1.06	0.94
9	1	29.5	16.6	0	19	1.056	-14.94	1.06	0.94
10	1	9	5.8	0	0	1.051	-15.1	1.06	0.94
11	1	3.5	1.8	0	0	1.057	-14.79	1.06	0.94
12	1	6.1	1.6	0	0	1.055	-15.07	1.06	0.94
13	1	13.5	5.8	0	0	1.05	-15.16	1.06	0.94
14	1	14.9	5	0	0	1.036	-16.04	1.06	0.94

Table D.2: The data profile for the IEEE 14 bus of AC power system.

(a) The data profile for the branches of the IEEE 14 bus power system.

From	To	r	x	b
1	2	0.01938	0.05917	0.0528
1	5	0.05403	0.22304	0.0492
2	3	0.04699	0.19797	0.0438
2	4	0.05811	0.17632	0.034
2	5	0.05695	0.17388	0.0346
3	4	0.06701	0.17103	0.0128
4	5	0.01335	0.04211	0
4	7	0	0.20912	0
4	9	0	0.55618	0
5	6	0	0.25202	0
6	11	0.09498	0.1989	0
6	12	0.12291	0.25581	0
6	13	0.06615	0.13027	0
7	8	0	0.17615	0
7	9	0	0.11001	0
9	10	0.03181	0.0845	0
9	14	0.12711	0.27038	0
10	11	0.08205	0.19207	0
12	13	0.22092	0.19988	0
13	14	0.17093	0.34802	0

Table D.3: The data profile for the IEEE 14 bus of DC power system.

(a) The data profile for the DC buses of the IEEE 14 bus power system.

Bus_{DC}	Bus_{AC}	P_{dc}	V_{dc}	$V_{c,max}$	$V_{c,min}$
1	1	20	1	1.1	0.9
2	3	20	1	1.1	0.9
3	9	20	1	1.1	0.9
4	14	20	1	1.1	0.9
5	0	-5	1	1.1	0.9

(b) The data profile for the DC lines of the IEEE 14 bus power system.

From	To	R
1	4	0.38
1	5	0.25
2	5	0.38
2	3	0.32
3	4	0.51
3	5	0.51
4	5	0.51

(c) The data profile for the converters of the IEEE 14 bus power system.

Bus_{DC}	P_s	Q_s	V_{tar}	Base (kV)	$V_{m,max}$	$V_{m,min}$	a	b	c	r
1	-60	-40	1	100	1.1	0.9	0.01	0	0	0.02
2	-60	-40	1	100	1.1	0.9	0.01	0	0	0.02
3	-60	-40	1	100	1.1	0.9	0.01	0	0	0.02
4	-60	-40	1	100	1.1	0.9	0.01	0	0	0.02

Table D.4: The power flow results of the IEEE 14 bus of AC power system.

(a) The results of generator for the IEEE 14 bus power system

Bus	P_g	Q_g	V_g
1	307.8432	13.1492	1.06
2	40	147.8076	1.045
3	0	122.6089	1.01
6	0	105.5845	1.07
8	0	66.5951	1.09

(b) The results of buses for the IEEE 14 bus power system

No	Type	P_d	Q_d	V_m	V_a
1	3	0	0	1.06	0
2	2	21.7	12.7	1.045	-10.2081
3	2	94.2	19	1.01	-24.4862
4	1	47.8	-3.9	0.96765	-20.0293
5	1	7.6	1.6	0.97611	-17.4385
6	2	11.2	7.5	1.07	-31.1678
7	1	0	0	0.98238	-29.3317
8	2	0	0	1.09	-29.3317
9	1	29.5	16.6	0.92216	-34.5665
10	1	9	5.8	0.93895	-34.1806
11	1	3.5	1.8	0.9985	-32.6886
12	1	6.1	1.6	1.0277	-32.8943
13	1	13.5	5.8	0.99051	-33.26
14	1	14.9	5	0.79046	-40.1509

Table D.5: The power flow results for the IEEE 14 bus of AC power system.

(a) The results of branches for the IEEE 14 bus power system.

From	To	P_{from}	Q_{from}	P_{to}	Q_{to}
1	2	316.3443	-50.0736	-298.7007	98.0928
1	5	145.3173	23.2227	-134.8381	14.9283
2	3	132.3263	1.1433	-124.7862	25.9976
2	4	104.3675	17.9974	-98.3615	-3.2219
2	5	80.3069	17.874	-76.7399	-10.5208
3	4	-29.4138	37.6113	30.9439	-34.9581
4	5	-97.074	13.613	98.444	-9.2917
4	7	75.132	9.4407	-75.132	2.8081
4	9	41.5596	19.0263	-41.5596	-7.374
5	6	105.534	3.2841	-105.534	22.3296
6	11	26.6389	25.9309	-25.4924	-23.5299
6	12	17.5055	9.4787	-17.0801	-8.5932
6	13	50.1895	40.3454	-47.7936	-35.6271
7	8	6.1062e-14	-60.0198	-5.5511e-14	66.5951
7	9	75.132	57.2117	-75.132	-47.0459
9	10	-12.0804	-13.7554	12.2058	14.0885
9	14	39.272	27.7325	-35.8171	-20.3833
10	11	-21.2058	-19.8885	21.9924	21.7299
12	13	10.9801	6.9932	-10.6256	-6.6725
13	14	44.9192	36.4996	-39.0829	-24.6167

Table D.6: The power flow results for the IEEE 14 bus of DC power system.

(a) The results of DC buses for the IEEE 14 bus power system.

Bus_{DC}	Bus_{AC}	P_{dc}	V_{dc}
1	1	153.8434	1
2	3	-59.99	1.1948
3	9	-59.99	1.188
4	14	-59.99	1.129
5	0	0	1.1075

(b) The results of DC lines for the IEEE 14 bus power system.

From	To	P^{DC}_{from}	P^{DC}_{to}
1	4	-67.8699	76.6219
1	5	-85.9735	95.2129
2	5	54.9176	-50.9035
2	3	5.0724	-5.0436
3	4	27.5118	-26.1443
3	5	37.5218	-34.978
4	5	9.5124	-9.3313

(c) The results of converters for the IEEE 14 bus power system.

Bus_{DC}	P_{conv}	Q_{conv}	V_{conv}	$V_{m,c}$	$\delta_{m,c}$	$P_{c,loss}$
1	153.8185	-40	1	1.06	2.0397e-07	0.024988
2	-60	-40	1	1.01	-24.4862	0.01
3	-60	-40	1	0.92216	-34.5665	0.01
4	-60	-40	1	0.79046	-40.1509	0.01

APPENDIX E

Power Load Data for the IEEE 30 Bus Power System

E.7 APPENDIX E

Table E.1: The data profile of the AC generators and buses for the IEEE 30 bus power system.

(a) The data profile for the generators of IEEE 30 bus power system.

Bus	P_g	Q_g	Q_{max}	Q_{min}	V_g	P_{max}	P_{min}
1	260.2	-16.1	10	0	1.06	360.2	0
2	40	50	50	-40	1.045	140	0
5	0	37	40	-40	1.01	100	0
8	0	37.3	40	-10	1.01	100	0
11	0	16.2	24	-6	1.082	100	0
13	0	10.6	24	-6	1.071	100	0
102	10	0	10	0	1	10	0
103	15	0	15	0	1	15	0

(b) The data profile for the buses of the IEEE 30 bus power system

No	Type	P_d	Q_d	G_s	B_s	V_m	V_a	V_{max}	V_{min}
1	3	0	0	0	0	1.06	0	1.06	0.94
2	2	21.7	12.7	0	0	1.043	-5.48	1.06	0.94
3	1	2.4	1.2	0	0	1.021	-7.96	1.06	0.94
4	1	7.6	1.6	0	0	1.012	-9.62	1.06	0.94
5	2	94.2	19	0	0	1.01	-14.37	1.06	0.94
6	1	0	0	0	0	1.01	-11.34	1.06	0.94
7	1	22.8	10.9	0	0	1.002	-13.12	1.06	0.94
8	2	30	30	0	0	1.01	-12.1	1.06	0.94
9	1	0	0	0	0	1.051	-14.38	1.06	0.94
10	1	5.8	2	0	19	1.045	-15.97	1.06	0.94
11	2	0	0	0	0	1.082	-14.39	1.06	0.94
12	1	11.2	7.5	0	0	1.057	-15.24	1.06	0.94
13	2	0	0	0	0	1.071	-15.24	1.06	0.94
14	1	6.2	1.6	0	0	1.042	-16.13	1.06	0.94
15	1	8.2	2.5	0	0	1.038	-16.22	1.06	0.94
16	1	3.5	1.8	0	0	1.045	-15.83	1.06	0.94
17	1	9	5.8	0	0	1.04	-16.14	1.06	0.94
18	1	3.2	0.9	0	0	1.028	-16.82	1.06	0.94
19	1	9.5	3.4	0	0	1.026	-17	1.06	0.94
20	1	2.2	0.7	0	0	1.03	-16.8	1.06	0.94
21	1	17.5	11.2	0	0	1.033	-16.42	1.06	0.94
22	1	0	0	0	0	1.033	-16.41	1.06	0.94
23	1	3.2	1.6	0	0	1.027	-16.61	1.06	0.94
24	1	8.7	6.7	0	4.3	1.021	-16.78	1.06	0.94
25	1	0	0	0	0	1.017	-16.35	1.06	0.94
26	1	3.5	2.3	0	0	1	-16.77	1.06	0.94
27	1	0	0	0	0	1.023	-15.82	1.06	0.94
28	1	0	0	0	0	1.007	-11.97	1.06	0.94
29	1	2.4	0.9	0	0	1.003	-17.06	1.06	0.94
30	1	0	0	0	0	0.992	-17.94	1.06	0.94
101	1	0	0	0	0	0.992	-17.94	1.06	0.94
102	1	0	0	0	0	0.992	-17.94	1.06	0.94
103	1	0	0	0	0	0.992	-17.94	1.06	0.94

Table E.2: The data profile of the AC branches and buses for the IEEE 30 bus power system.

(a) The data profile for the branches of the IEEE 30 bus power system.

From	To	r	x	b
1	2	0.0192	0.0575	0.0528
1	3	0.0452	0.1652	0.0408
2	4	0.057	0.1737	0.0368
3	4	0.0132	0.0379	0.0084
2	5	0.0472	0.1983	0.0418
2	6	0.0581	0.1763	0.0374
4	6	0.0119	0.0414	0.009
5	7	0.046	0.116	0.0204
6	7	0.0267	0.082	0.017
6	8	0.012	0.042	0.009
6	9	0	0.208	0
6	10	0	0.556	0
9	11	0	0.208	0
9	10	0	0.11	0
4	12	0	0.256	0
12	13	0	0.14	0
12	14	0.1231	0.2559	0
12	15	0.0662	0.1304	0
12	16	0.0945	0.1987	0
14	15	0.221	0.1997	0
16	17	0.0524	0.1923	0
15	18	0.1073	0.2185	0
18	19	0.0639	0.1292	0
19	20	0.034	0.068	0
10	20	0.0936	0.209	0
10	17	0.0324	0.0845	0
10	21	0.0348	0.0749	0
10	22	0.0727	0.1499	0
21	22	0.0116	0.0236	0
15	23	0.1	0.202	0
22	24	0.115	0.179	0
23	24	0.132	0.27	0
24	25	0.1885	0.3292	0
25	26	0.2544	0.38	0
25	27	0.1093	0.2087	0
28	27	0	0.396	0
27	29	0.2198	0.4153	0
27	30	0.3202	0.6027	0
29	30	0.2399	0.4533	0
8	28	0.0636	0.2	0.0428
6	28	0.0169	0.0599	0.013
102	101	0.2399	0.4533	0
103	102	0.2399	0.4533	0

Table E.3: The data profile of the DC power system for the IEEE 30 bus power system.

(a) The data profile of DC buses for the IEEE 30 bus power system.

Bus_{DC}	Bus_{AC}	P_{dc}	V_{dc}	$V_{c,max}$	$V_{c,min}$
100	101	20	1	1.1	0.9
105	27	20	1	1.1	0.9
200	11	20	1	1.1	0.9
300	0	-5	1	1.1	0.9
400	0	-5	1	1.1	0.9

(b) The data profile of DC lines for the IEEE 30 bus power system.

From	To	R
300	200	0.052
400	200	0.052
100	105	0

(c) The data profile of converters for the IEEE 30 bus power system.

Bus_{DC}	P_s	Q_s	V_{tar}	$V_{m,max}$	$V_{m,min}$	a	b	c	r
200	-60	-40	1	1.1	0.9	1.103	0.887	4.371	2.885
100	-60	-40	1	1.1	0.9	1.103	0.887	4.371	2.885
105	-60	-40	1	1.1	0.9	1.103	0.887	4.371	2.885

REFERENCES

[1] M. H. Albadi and E. F. El-Saadany, "Demand response in electricity markets: An overview," in *2007 IEEE power engineering society general meeting*, pp. 1–5, IEEE, 2007.

[2] B. N. Silva, M. Khan, and K. Han, "Futuristic sustainable energy management in smart environments: a review of peak load shaving and demand response strategies, challenges, and opportunities," *Sustainability*, vol. 12, no. 14, p. 5561, 2020.

[3] J. Carpentier, "Contribution to the economic dispatch problem," *Bulletin de la Societe Francoise des Electriciens*, vol. 3, no. 8, pp. 431–447, 1962.

[4] S. H. Low, "Convex relaxation of optimal power flow—part ii: Exactness," *IEEE Transactions on Control of Network Systems*, vol. 1, no. 2, pp. 177–189, 2014.

[5] K. M. Chandy, S. H. Low, U. Topcu, and H. Xu, "A simple optimal power flow model with energy storage," in *Decision and Control (CDC), 2010 49th IEEE Conference on*, pp. 1051–1057, IEEE, 2010.

[6] S. H. Low, "Convex relaxation of optimal power flow—part i: Formulations and equivalence," *IEEE Transactions on Control of Network Systems*, vol. 1, no. 1, pp. 15–27, 2014.

[7] Q. Qdr, "Benefits of demand response in electricity markets and recommendations for achieving them," *US Dept. Energy, Washington, DC, USA, Tech. Rep*, vol. 5, 2006.

[8] J. Torriti, "A review of time use models of residential electricity demand," *Renewable and Sustainable Energy Reviews*, vol. 37, pp. 265–272, 2014.

[9] U. E. I. Administration, "How many smart meters are installed in the united states, and who has them?." `https://www.eia.gov/tools/faqs/faq.php?id=108&t=3t=blank`, 2017.

[10] D. J. Unger, "Digital journal, michigan, illinois lead the midwest in smart-meter installations." `https://energynews.us/2017/02/06/midwest/michigan-illinois-lead-the-midwest-in-smart-meter-installations/#:~:text=Two%20states%20%E2%80%94%20Michigan%20and%20Illinois,over%20the%20five%20years%20prior.`, 2017.
.

[11] F. Shariatzadeh, P. Mandal, and A. K. Srivastava, "Demand response for sustainable energy systems: A review, application and implementation strategy," *Renewable and Sustainable Energy Reviews*, vol. 45, pp. 343–350, 2015.

[12] A. Rabiee, A. Soroudi, B. Mohammadi-Ivatloo, and M. Parniani, "Corrective voltage control scheme considering demand response and stochastic wind power," *IEEE Transactions on Power Systems*, vol. 29, no. 6, pp. 2965–2973, 2014.

[13] S. Annala *et al.*, "Households' willingness to engage in demand response in the finnish retail electricity market: an empirical study," -, 2015.

[14] P. Cappers, A. Mills, C. Goldman, R. Wiser, and J. H. Eto, "Mass market demand response and variable generation integration issues: A scoping study," tech. rep., Lawrence Berkeley National Lab.(LBNL), Berkeley, CA (United States), 2011.

[15] P. Bertoldi, P. Zancanella, B. Boza-Kiss, *et al.*, "Demand response status in eu member states," *EUR 27998 EN*, pp. 1–140, 2016.

[16] Z. Zhao, C. Yu, M. Yew, and M. Liu, "Demand side management: A green way to power beijing," *Journal of Renewable and Sustainable Energy*, vol. 7, no. 4, p. 041505, 2015.

[17] M. S. Modarresi, L. Xie, and C. Singh, "Reserves from controllable swimming pool pumps: Reliability assessment and operational planning," in *Proceedings of the 51st Hawaii International Conference on System Sciences*, 2018.

[18] M. Braun and P. Strauss, "A review on aggregation approaches of controllable distributed energy units in electrical power systems," *International Journal of Distributed Energy Resources*, vol. 4, no. 4, pp. 297–319, 2008.

[19] S. Burger, J. P. Chaves-Ávila, C. Batlle, and I. J. Pérez-Arriaga, "A review of the value of aggregators in electricity systems," *Renewable and Sustainable Energy Reviews*, vol. 77, pp. 395–405, 2017.

[20] T. Samad, E. Koch, and P. Stluka, "Automated demand response for smart buildings and microgrids: The state of the practice and research challenges," *Proceedings of the IEEE*, vol. 104, no. 4, pp. 726–744, 2016.

[21] S. Braithwait and K. Eakin, "The role of demand response in electric power market design," *Edison Electric Institute*, pp. 1–57, 2002.

[22] K. Xie and Y. Song, "Dynamic optimal power flow by interior point methods," *IEE Proceedings-Generation, Transmission and Distribution*, vol. 148, no. 1, pp. 76–84, 2001.

[23] T. Niknam, M. R. Narimani, and M. Jabbari, "Dynamic optimal power flow using hybrid particle swarm optimization and simulated annealing," *International Transactions on Electrical Energy Systems*, vol. 23, no. 7, pp. 975–1001, 2013.

[24] S. Gill, I. Kockar, and G. W. Ault, "Dynamic optimal power flow for active distribution networks," *IEEE Transactions on Power Systems*, vol. 29, no. 1, pp. 121–131, 2014.

[25] D. Das, "A fuzzy multiobjective approach for network reconfiguration of distribution systems," *IEEE transactions on power delivery*, vol. 21, no. 1, pp. 202–209, 2005.

[26] J. Hazra and A. Sinha, "A multi-objective optimal power flow using particle swarm optimization," *European transactions on electrical power*, vol. 21, no. 1, pp. 1028–1045, 2011.

[27] K. Teeparthi and D. V. Kumar, "Multi-objective hybrid pso-apo algorithm based security constrained optimal power flow with wind and thermal generators," *Engineering Science and Technology, an International Journal*, vol. 20, no. 2, pp. 411–426, 2017.

[28] E. Davoodi, E. Babaei, and B. Mohammadi-ivatloo, "An efficient covexified sdp model for multi-objective optimal power flow," *International Journal of Electrical Power & Energy Systems*, vol. 102, pp. 254–264, 2018.

[29] H. W. Dommel and W. F. Tinney, "Optimal power flow solutions," *IEEE Transactions on power apparatus and systems*, no. 10, pp. 1866–1876, 1968.

[30] C. L. Sulzberger, "Triumph of ac. 2. the battle of the currents," *IEEE Power and Energy Magazine*, vol. 1, no. 4, pp. 70–73, 2003.

[31] P. Fairley, "Dc versus ac: The second war of currents has already begun [in my view]," *IEEE Power and energy magazine*, vol. 10, no. 6, pp. 104–103, 2012.

[32] M. Huneault and F. Galiana, "A survey of the optimal power flow literature," *IEEE transactions on Power Systems*, vol. 6, no. 2, pp. 762–770, 1991.

[33] S. Frank, I. Steponavice, and S. Rebennack, "Optimal power flow: a bibliographic survey i," *Energy Systems*, vol. 3, no. 3, pp. 221–258, 2012.

[34] S. Frank, I. Steponavice, and S. Rebennack, "Optimal power flow: a bibliographic survey ii," *Energy Systems*, vol. 3, no. 3, pp. 259–289, 2012.

[35] J. Yu, W. Yan, W. Li, C. Chung, and K. Wong, "An unfixed piecewise-optimal reactive power-flow model and its algorithm for ac-dc systems," *IEEE Transactions on Power Systems*, vol. 23, no. 1, pp. 170–176, 2008.

[36] R. Wiget and G. Andersson, "Optimal power flow for combined ac and multi-terminal hvdc grids based on vsc converters," in *2012 IEEE Power and Energy Society General Meeting*, pp. 1–8, IEEE, 2012.

[37] S. Bahrami, F. Therrien, V. W. Wong, and J. Jatskevich, "Semidefinite relaxation of optimal power flow for ac–dc grids," *IEEE Transactions on Power Systems*, vol. 32, no. 1, pp. 289–304, 2016.

[38] J. Li, F. Liu, Z. Wang, S. H. Low, and S. Mei, "Optimal power flow in stand-alone dc microgrids," *IEEE Transactions on Power Systems*, vol. 33, no. 5, pp. 5496–5506, 2018.

[39] L. Gan and S. H. Low, "Optimal power flow in direct current networks," *IEEE Transactions on Power Systems*, vol. 29, no. 6, pp. 2892–2904, 2014.

[40] S. H. Low, "Convex relaxation of optimal power flow-part i: Formulations and equivalence," *IEEE Transactions on Control of Network Systems*, vol. 1, no. 1, pp. 15–27, 2014.

[41] S. H. Low, "Convex relaxation of optimal power flow-part ii: Exactness," *IEEE Transactions on Control of Network Systems*, vol. 1, no. 2, pp. 177–189, 2014.

[42] J. Kennedy and R. Eberhart, "Particle swarm optimization," in *Proceedings of ICNN'95-International Conference on Neural Networks*, vol. 4, pp. 1942–1948, IEEE, 1995.

[43] R. Poli, J. Kennedy, and T. Blackwell, "Particle swarm optimization," *Swarm intelligence*, vol. 1, no. 1, pp. 33–57, 2007.

[44] M. Clerc, *Particle swarm optimization*, vol. 93. John Wiley & Sons, 2010.

[45] M. Abido, "Optimal power flow using particle swarm optimization," *International Journal of Electrical Power & Energy Systems*, vol. 24, no. 7, pp. 563–571, 2002.

[46] I. Oumarou, D. Jiang, and C. Yijia, "Particle swarm optimization applied to optimal power flow solution," in *2009 Fifth International Conference on Natural Computation*, vol. 3, pp. 284–288, IEEE, 2009.

[47] U. Leeton, D. Uthitsunthorn, U. Kwannetr, N. Sinsuphun, and T. Kulworawanichpong, "Power loss minimization using optimal power flow based on particle swarm optimization," in *ECTI-CON2010: The 2010 ECTI International Confernce on Electrical Engineering/Electronics, Computer, Telecommunications and Information Technology*, pp. 440–444, IEEE, 2010.

[48] M. Abido, "Multiobjective particle swarm optimization for optimal power flow problem," in *Handbook of swarm intelligence*, pp. 241–268, Springer, 2011.

[49] C. Suchetha and J. Ramprabhakar, "Optimal power flow controller for a hybrid renewable energy system using particle swarm optimization," in *2019 National Power Electronics Conference (NPEC)*, pp. 1–6, IEEE, 2019.

[50] A. G. Bakirtzis, P. N. Biskas, C. E. Zoumas, and V. Petridis, "Optimal power flow by enhanced genetic algorithm," *IEEE Transactions on power Systems*, vol. 17, no. 2, pp. 229–236, 2002.

[51] M. Osman, M. A. Abo-Sinna, and A. Mousa, "A solution to the optimal power flow using genetic algorithm," *Applied mathematics and computation*, vol. 155, no. 2, pp. 391–405, 2004.

[52] V. Suresh and P. Janik, "Optimal power flow in microgrids using genetic algorithm," in *2019 2nd International Conference on Power and Embedded Drive Control (ICPEDC)*, pp. 483–487, IEEE, 2019.

[53] T. Srihari, M. Boppa, S. A. Kumar, and H. Pulluri, "The application of genetic algorithm with multi-parent crossover to optimal power flow problem," in *Innovations in Electrical and Electronics Engineering*, pp. 417–427, Springer, 2020.

[54] S. Kirkpatrick, C. D. Gelatt, and M. P. Vecchi, "Optimization by simulated annealing," *science*, vol. 220, no. 4598, pp. 671–680, 1983.

[55] R. Chibante, *Simulated Annealing: Theory with Applications*. BoD–Books on Demand, 2010.

[56] C. Roa-Sepulveda and B. Pavez-Lazo, "A solution to the optimal power flow using simulated annealing," in *2001 IEEE Porto Power Tech Proceedings (Cat. No. 01EX502)*, vol. 2, pp. 5–pp, IEEE, 2001.

[57] C. Roa-Sepulveda and B. Pavez-Lazo, "A solution to the optimal power flow using simulated annealing," *International journal of electrical power & energy systems*, vol. 25, no. 1, pp. 47–57, 2003.

[58] T. Sousa, J. Soares, Z. Vale, H. Morais, and P. Faria, "Simulated annealing metaheuristic to solve the optimal power flow," in *2011 IEEE Power and Energy Society General Meeting*, pp. 1–8, IEEE, 2011.

[59] K. M. Passino, "Biomimicry of bacterial foraging for distributed optimization and control," *IEEE control systems magazine*, vol. 22, no. 3, pp. 52–67, 2002.

[60] M. Tripathy and S. Mishra, "Bacteria foraging-based solution to optimize both real power loss and voltage stability limit," *IEEE Transactions on power systems*, vol. 22, no. 1, pp. 240–248, 2007.

[61] M. S. Li, W. J. Tang, W. H. Tang, Q. H. Wu, and J. R. Saunders, "Bacterial foraging algorithm with varying population for optimal power flow," in *Applications of Evolutionary Computing* (M. Giacobini, ed.), (Berlin, Heidelberg), pp. 32–41, Springer Berlin Heidelberg, 2007.

[62] W. Tang, M. Li, S. He, Q. Wu, and J. Saunders, "Optimal power flow with dynamic loads using bacterial foraging algorithm," in *2006 International Conference on Power System Technology*, pp. 1–5, IEEE, 2006.

[63] W. Tang, M. Li, Q. H. Wu, and J. Saunders, "Bacterial foraging algorithm for optimal power flow in dynamic environments," *IEEE Transactions on Circuits and Systems I: Regular Papers*, vol. 55, no. 8, pp. 2433–2442, 2008.

[64] L. Xie, J. Zeng, and Z. Cui, "General framework of artificial physics optimization algorithm," in *2009 World Congress on Nature & Biologically Inspired Computing (NaBIC)*, pp. 1321–1326, IEEE, 2009.

[65] L. Xie, J. Zeng, and Z. Cui, "On mass effects to artificial physics optimisation algorithm for global optimisation problems," *International Journal of Innovative Computing and Applications*, vol. 2, no. 2, p. 69, 2009.

[66] J. Li, F. Liu, Z. Wang, S. H. Low, and S. Mei, "Optimal power flow in stand-alone dc microgrids," *arXiv preprint arXiv:1708.05140*, 2017.

[67] N. Z. Shor, "Class of global minimum bounds of polynomial functions," *Cybernetics and Systems Analysis*, vol. 23, no. 6, pp. 731–734, 1987.

[68] Y. Nesterov, "Squared functional systems and optimization problems," in *High performance optimization*, pp. 405–440, Springer, 2000.

[69] J. B. Lasserre, "Global optimization with polynomials and the problem of moments," *SIAM Journal on Optimization*, vol. 11, no. 3, pp. 796–817, 2001.

[70] M. Putinar, "Positive polynomials on compact semi-algebraic sets," *Indiana University Mathematics Journal*, vol. 42, no. 3, pp. 969–984, 1993.

[71] H. Waki, S. Kim, M. Kojima, and M. Muramatsu, "Sums of squares and semidefinite program relaxations for polynomial optimization problems with structured sparsity," *SIAM Journal on Optimization*, vol. 17, no. 1, pp. 218–242, 2006.

[72] M. Laurent, "Semidefinite representations for finite varieties," *Mathematical Programming*, vol. 109, no. 1, pp. 1–26, 2007.

[73] H. Markowitz, "Portfolio selection," *Journal of Finance 7 (1), March*, 1952.

[74] A. Roberts and M. Newmann, "Polynomial optimization of stochastic feedback control for stable plants," *IMA Journal of Mathematical Control and Information*, vol. 5, no. 3, pp. 243–257, 1988.

[75] A. Barmpoutis, B. Jian, B. C. Vemuri, and T. M. Shepherd, "Symmetric positive 4th order tensors & their estimation from diffusion weighted mri," in *Biennial International Conference on Information Processing in Medical Imaging*, pp. 308–319, Springer, 2007.

[76] T. G. Kolda and B. W. Bader, "Tensor decompositions and applications," *SIAM review*, vol. 51, no. 3, pp. 455–500, 2009.

[77] B. Mariere, Z.-Q. Luo, and T. N. Davidson, "Blind constant modulus equalization via convex optimization," *IEEE Transactions on Signal Processing*, vol. 51, no. 3, pp. 805–818, 2003.

[78] L. Qi and K. L. Teo, "Multivariate polynomial minimization and its application in signal processing," *Journal of Global Optimization*, vol. 26, no. 4, pp. 419–433, 2003.

[79] A. M. Alzahrani, "Convex optimization approach to the optimal power flow problem in dc-microgrids with energy storage," -, 2018.

[80] M. Kumar, M. Babu, and R. K. Shaik, "Voltage profile improvement for 16 bus distribution systems with dfig wind turbine using psat by fvsi index," in *SIGDOC*, pp. 87–95, 01 2017.

[81] C.-T. Su and C.-S. Lee, "Network reconfiguration of distribution systems using improved mixed-integer hybrid differential evolution," *IEEE Transactions on Power Delivery*, vol. 18, no. 3, pp. 1022–1027, 2003.

[82] R. Madani, S. Sojoudi, and J. Lavaei, "Convex relaxation for optimal power flow problem: Mesh networks," *IEEE Transactions on Power Systems*, vol. 30, no. 1, pp. 199–211, 2014.

[83] M. Farivar and S. H. Low, "Branch flow model: Relaxations and convexification-part i," *IEEE Transactions on Power Systems*, vol. 28, no. 3, pp. 2554–2564, 2013.

[84] M. Farivar and S. H. Low, "Branch flow model: Relaxations and convexification - part ii," *IEEE Transactions on Power Systems*, vol. 28, pp. 2565–2572, Aug 2013.

[85] A. G. Expósito and E. R. Ramos, "Reliable load flow technique for radial distribution networks," *IEEE Transactions on Power Systems*, vol. 14, no. 3, pp. 1063–1069, 1999.

[86] J. Heller and T. Pajdla, "Gposolver: a matlab/c++ toolbox for global polynomial optimization," *Optimization Methods and Software*, vol. 31, no. 2, pp. 405–434, 2016.

[87] J. Löfberg, "Yalmip: A toolbox for modeling and optimization in matlab," in *Proceedings of the CACSD Conference*, vol. 3, Taipei, Taiwan, 2004.

[88] D. P. Kaundinya, P. Balachandra, and N. H. Ravindranath, "Grid-connected versus stand-alone energy systems for decentralized power—a review of literature," *Renewable and Sustainable Energy Reviews*, vol. 13, no. 8, pp. 2041–2050, 2009.

[89] T. Ackermann, G. Andersson, and L. Söder, "Distributed generation: a definition," *Electric power systems research*, vol. 57, no. 3, pp. 195–204, 2001.

[90] M. Barnes, J. Kondoh, H. Asano, J. Oyarzabal, G. Ventakaramanan, R. Lasseter, N. Hatziargyriou, and T. Green, "Real-world microgrids-an overview," in *System of Systems Engineering, 2007. SoSE'07. IEEE International Conference on*, IEEE, 2007, 1–8.

[91] N. Pogaku, M. Prodanovic, and T. C. Green, "Modeling, analysis and testing of autonomous operation of an inverter-based microgrid," *IEEE Transactions on power electronics*, vol. 22, no. 2, pp. 613–625, 2007.

[92] O. Palizban and K. Kauhaniemi, "Energy storage systems in modern grids—matrix of technologies and applications," *Journal of Energy Storage*, vol. 6, pp. 248–259, 2016.

[93] H. Chen, T. N. Cong, W. Yang, C. Tan, Y. Li, and Y. Ding, "Progress in electrical energy storage system: A critical review," *Progress in Natural Science*, vol. 19, no. 3, pp. 291–312, 2009.

[94] S. Abu-Sharkh, R. Arnold, J. Kohler, R. Li, T. Markvart, J. Ross, K. Steemers, P. Wilson, and R. Yao, "Can microgrids make a major contribution to UK energy supply?," *Renewable and Sustainable Energy Reviews*, vol. 10, no. 2, pp. 78–127, 2006.

[95] M. Basu, "Economic environmental dispatch using multi-objective differential evolution," *Applied soft computing*, vol. 11, no. 2, pp. 2845–2853, 2011.

[96] N. Kok, N. Miller, and P. Morris, "The economics of green retrofits," *Journal of Sustainable Real Estate*, vol. 4, no. 1, pp. 4–22, 2012.

[97] T. Markvart, *Solar electricity*, vol. 6. John Wiley & Sons, 2000.

[98] P. K. Mishra and P. Tiwari, "Solar photovoltaic technology—a review," *Advanced Science, Engineering and Medicine*, vol. 12, no. 1, pp. 5–10, 2020.

[99] Q. Jiang, H.-D. Chiang, C. Guo, and Y. Cao, "Power–current hybrid rectangular formulation for interior-point optimal power flow," *IET generation, transmission & distribution*, vol. 3, no. 8, pp. 748–756, 2009.

[100] S. Frank, I. Steponavice, and S. Rebennack, "Optimal power flow: a bibliographic survey I," *Energy Systems*, vol. 3, no. 3, pp. 221–258, 2012.

[101] T. Tezer, R. Yaman, and G. Yaman, "Evaluation of approaches used for optimization of stand-alone hybrid renewable energy systems," *Renewable and Sustainable Energy Reviews*, vol. 73, pp. 840–853, 2017.

[102] A. Chauhan and R. Saini, "A review on integrated renewable energy system based power generation for stand-alone applications: Configurations, storage options, sizing methodologies and control," *Renewable and Sustainable Energy Reviews*, vol. 38, pp. 99–120, 2014.

[103] M. Amer, A. Namaane, and N. M'sirdi, "Optimization of hybrid renewable energy systems (hres) using pso for cost reduction," *Energy Procedia*, vol. 42, pp. 318–327, 2013.

[104] W. Li *et al.*, *Reliability assessment of electric power systems using Monte Carlo methods*. Springer Science & Business Media, 2013.

[105] I. A. Ibrahim, T. Khatib, and A. Mohamed, "Optimal sizing of a standalone photovoltaic system for remote housing electrification using numerical algorithm and improved system models," *Energy*, vol. 126, pp. 392–403, 2017.

[106] A. Maleki, M. G. Khajeh, and M. Ameri, "Optimal sizing of a grid independent hybrid renewable energy system incorporating resource uncertainty, and load uncertainty," *International Journal of Electrical Power & Energy Systems*, vol. 83, pp. 514–524, 2016.

[107] T. Khatib, I. A. Ibrahim, and A. Mohamed, "A review on sizing methodologies of photovoltaic array and storage battery in a standalone photovoltaic system," *Energy Conversion and Management*, vol. 120, pp. 430–448, 2016.

[108] S. Upadhyay and M. Sharma, "A review on configurations, control and sizing methodologies of hybrid energy systems," *Renewable and Sustainable Energy Reviews*, vol. 38, pp. 47–63, 2014.

[109] M. Modiri-Delshad, S. Koohi-Kamali, E. Taslimi, S. H. A. Kaboli, and N. Rahim, "Economic dispatch in a microgrid through an iterated-based algorithm," in *2013 IEEE Conference on Clean Energy and Technology (CEAT)*, pp. 82–87, IEEE, 2013.

[110] H. Bouchekara, M. Abido, and M. Boucherma, "Optimal power flow using teaching-learning-based optimization technique," *Electric Power Systems Research*, vol. 114, pp. 49–59, 2014.

[111] W. Zhang, F. Li, and L. M. Tolbert, "Review of reactive power planning: objectives, constraints, and algorithms," *IEEE transactions on power systems*, vol. 22, no. 4, pp. 2177–2186, 2007.

[112] L. M. Leon, A. S. Bretas, and S. Rivera, "Quadratically constrained quadratic programming formulation of contingency constrained optimal power flow with photovoltaic generation," *Energies*, vol. 13, no. 13, p. 3310, 2020.

[113] I. Farhat and M. El-Hawary, "Optimization methods applied for solving the short-term hydrothermal coordination problem," *Electric Power Systems Research*, vol. 79, no. 9, pp. 1308–1320, 2009.

[114] A. H. Fathima and K. Palanisamy, "Optimization in microgrids with hybrid energy systems–a review," *Renewable and Sustainable Energy Reviews*, vol. 45, pp. 431–446, 2015.

[115] B. Zhao, X. Zhang, J. Chen, C. Wang, and L. Guo, "Operation optimization of standalone microgrids considering lifetime characteristics of battery energy storage system," *IEEE transactions on sustainable energy*, vol. 4, no. 4, pp. 934–943, 2013.

[116] H. Yang, L. Lu, and W. Zhou, "A novel optimization sizing model for hybrid solar-wind power generation system," *Solar energy*, vol. 81, no. 1, pp. 76–84, 2007.

[117] A. Kwasinski, V. Krishnamurthy, J. Song, and R. Sharma, "Availability evaluation of micro-grids for resistant power supply during natural disasters," *IEEE Transactions on Smart Grid*, vol. 3, no. 4, pp. 2007–2018, 2012.

[118] M. Deshmukh and S. Deshmukh, "Modeling of hybrid renewable energy systems," *Renewable and sustainable energy reviews*, vol. 12, no. 1, pp. 235–249, 2008.

[119] E. Biyik and A. Kahraman, "A predictive control strategy for optimal management of peak load, thermal comfort, energy storage and renewables in multi-zone buildings," *Journal of Building Engineering*, p. 100826, 2019.

[120] B. Zhao, X. Zhang, P. Li, K. Wang, M. Xue, and C. Wang, "Optimal sizing, operating strategy and operational experience of a stand-alone microgrid on dongfushan island," *Applied Energy*, vol. 113, pp. 1656–1666, 2014.

[121] J. Faraji, A. Ketabi, and H. Hashemi-Dezaki, "Optimization of the scheduling and operation of prosumers considering the loss of life costs of battery storage systems," *Journal of Energy Storage*, vol. 31, p. 101655, 2020.

[122] Y. Liu, X. Wu, J. Du, Z. Song, and G. Wu, "Optimal sizing of a wind-energy storage system considering battery life," *Renewable Energy*, vol. 147, pp. 2470–2483, 2020.

[123] L. Wang and C. Singh, "Multicriteria design of hybrid power generation systems based on a modified particle swarm optimization algorithm," *IEEE Transactions on Energy Conversion*, vol. 24, no. 1, pp. 163–172, 2009.

[124] B. O. Bilal, V. Sambou, P. Ndiaye, C. Kébé, and M. Ndongo, "Multi-objective design of pv-wind-batteries hybrid systems by minimizing the annualized cost system and the loss of power supply probability (lpsp)," in *2013 IEEE International Conference on Industrial Technology (ICIT)*, IEEE, 2013, 861–868.

[125] A. Maheri, "Multi-objective design optimisation of standalone hybrid wind-pv-diesel systems under uncertainties," *Renewable Energy*, vol. 66, pp. 650–661, 2014.

[126] M. Sharafi and T. Y. ELMekkawy, "Multi-objective optimal design of hybrid renewable energy systems using pso-simulation based approach," *Renewable Energy*, vol. 68, pp. 67–79, 2014.

[127] M. Hassan and M. Abido, "Optimal design of microgrids in autonomous and grid-connected modes using particle swarm optimization," *IEEE Transactions on power electronics*, vol. 26, no. 3, pp. 755–769, 2010.

[128] S. A. Arefifar, A.-R. M. Yasser, and T. H. El-Fouly, "Optimum microgrid design for enhancing reliability and supply-security," *IEEE Transactions on Smart Grid*, vol. 4, no. 3, pp. 1567–1575, 2013.

[129] K. Bhumkittipich and W. Phuangpornpitak, "Optimal placement and sizing of distributed generation for power loss reduction using particle swarm optimization," *Energy Procedia*, vol. 34, pp. 307–317, 2013.

[130] M. V. Kirthiga, S. A. Daniel, and S. Gurunathan, "A methodology for transforming an existing distribution network into a sustainable autonomous micro-grid," *IEEE Transactions on Sustainable Energy*, vol. 4, no. 1, pp. 31–41, 2012.

[131] E. Afzalan, M. Taghikhani, and M. Sedighizadeh, "Optimal placement and sizing of dg in radial distribution networks using sfla," *international journal of energy engineering*, vol. 2, no. 3, pp. 73–77, 2012.

[132] H. Dagdougui, R. Minciardi, A. Ouammi, M. Robba, and R. Sacile, "A dynamic decision model for the real-time control of hybrid renewable energy production systems," *IEEE Systems Journal*, vol. 4, no. 3, pp. 323–333, 2010.

[133] X. Bai, H. Wei, K. Fujisawa, and Y. Wang, "Semidefinite programming for optimal power flow problems," *International Journal of Electrical Power & Energy Systems*, vol. 30, no. 6, pp. 383–392, 2008.

[134] J. K. Felder and I. A. Hiskens, "Optimal power flow with storage," in *Power Systems Computation Conference (PSCC), 2014*, pp. 1–7, IEEE, 2014.

[135] H. Kakigano, Y. Miura, and T. Ise, "Low-voltage bipolar-type dc microgrid for super high quality distribution," *IEEE transactions on power electronics*, vol. 25, no. 12, pp. 3066–3075, 2010.

[136] S. Dasgupta, S. N. Mohan, S. K. Sahoo, and S. K. Panda, "A plug and play operational approach for implementation of an autonomous-micro-grid system," *IEEE Transactions on Industrial Informatics*, vol. 8, no. 3, pp. 615–629, 2012.

[137] W. Al-Saedi, S. W. Lachowicz, D. Habibi, and O. Bass, "Power quality enhancement in autonomous microgrid operation using particle swarm optimization," *International Journal of Electrical Power & Energy Systems*, vol. 42, no. 1, pp. 139–149, 2012.

[138] W. Al-Saedi, S. W. Lachowicz, D. Habibi, and O. Bass, "Power flow control in grid-connected microgrid operation using particle swarm optimization under variable load conditions," *International Journal of Electrical Power & Energy Systems*, vol. 49, pp. 76–85, 2013.

[139] A. Baziar and A. Kavousi-Fard, "Considering uncertainty in the optimal energy management of renewable micro-grids including storage devices," *Renewable Energy*, vol. 59, pp. 158–166, 2013.

[140] M. Hemmati, B. Mohammadi-Ivatloo, M. Abapour, and A. Anvari-Moghaddam, "Day-ahead profit-based reconfigurable microgrid scheduling considering uncertain renewable generation and load demand in the presence of energy storage," *Journal of Energy Storage*, vol. 28, p. 101161, 2020.

[141] A. K. Basu, A. Bhattacharya, S. Chowdhury, and S. Chowdhury, "Planned scheduling for economic power sharing in a chp-based micro-grid," *IEEE Transactions on Power systems*, vol. 27, no. 1, pp. 30–38, 2011.

[142] S. Conti, R. Nicolosi, S. Rizzo, and H. Zeineldin, "Optimal dispatching of distributed generators and storage systems for mv islanded microgrids," *IEEE Transactions on Power Delivery*, vol. 27, no. 3, pp. 1243–1251, 2012.

[143] G.-C. Liao, "Solve environmental economic dispatch of smart microgrid containing distributed generation system–using chaotic quantum genetic algorithm," *International Journal of Electrical Power & Energy Systems*, vol. 43, no. 1, pp. 779–787, 2012.

[144] P. Jiang, J. Dong, and H. Huang, "Optimal integrated demand response scheduling in regional integrated energy system with concentrating solar power," *Applied Thermal Engineering*, vol. 166, p. 114754, 2020.

[145] M. D. Al-Falahi, S. Jayasinghe, and H. Enshaei, "A review on recent size optimization methodologies for standalone solar and wind hybrid renewable energy system," *Energy Conversion and Management*, vol. 143, pp. 252–274, 2017.

[146] X.-S. Yang, *Nature-inspired metaheuristic algorithms*. Luniver press, 2010.

[147] S. Sinha and S. Chandel, "Review of recent trends in optimization techniques for solar photovoltaic–wind based hybrid energy systems," *Renewable and Sustainable Energy Reviews*, vol. 50, pp. 755–769, 2015.

[148] Y. Xu, C. Yan, H. Liu, J. Wang, Z. Yang, and Y. Jiang, "Smart energy systems: A critical review on design and operation optimization," *Sustainable Cities and Society*, p. 102369, 2020.

[149] Y. Sun, "Sensitivity analysis of macro-parameters in the system design of net zero energy building," *Energy and Buildings*, vol. 86, pp. 464–477, 2015.

[150] P. Wang, J. Yi, M. Zangiabadi, P. Lyons, and P. Taylor, "Evaluation of voltage control approaches for future smart distribution networks," *Energies*, vol. 10, no. 8, p. 1138, 2017.

[151] A. M. Fathollahi-Fard, M. Hajiaghaei-Keshteli, and R. Tavakkoli-Moghaddam, "Red deer algorithm (rda): a new nature-inspired meta-heuristic," *Soft Computing*, pp. 1–29, 2020.

[152] D. Gallo, C. Landi, M. Luiso, and R. Morello, "Optimization of experimental model parameter identification for energy storage systems," *Energies*, vol. 6, no. 9, pp. 4572–4590, 2013.

[153] R. Hosseinalizadeh, H. Shakouri, M. S. Amalnick, and P. Taghipour, "Economic sizing of a hybrid (pv–wt–fc) renewable energy system (hres) for stand-alone usages by an optimization-simulation model: case study of iran," *Renewable and Sustainable Energy Reviews*, vol. 54, pp. 139–150, 2016.

[154] M. Smaoui, A. Abdelkafi, and L. Krichen, "Optimal sizing of stand-alone photovoltaic/wind/hydrogen hybrid system supplying a desalination unit," *Solar Energy*, vol. 120, pp. 263–276, 2015.

[155] F. Shen, L. Zhao, W. Du, W. Zhong, and F. Qian, "Large-scale industrial energy systems optimization under uncertainty: A data-driven robust optimization approach," *Applied Energy*, vol. 259, p. 114199, 2020.

[156] F. S. Gazijahani, S. N. Ravadanegh, and J. Salehi, "Stochastic multi-objective model for optimal energy exchange optimization of networked microgrids with presence of renewable generation under risk-based strategies," *ISA transactions*, vol. 73, pp. 100–111, 2018.

[157] Z. Zhou, J. Zhang, P. Liu, Z. Li, M. C. Georgiadis, and E. N. Pistikopoulos, "A two-stage stochastic programming model for the optimal design of distributed energy systems," *Applied Energy*, vol. 103, pp. 135–144, 2013.

[158] O. Hafez and K. Bhattacharya, "Optimal planning and design of a renewable energy based supply system for microgrids," *Renewable Energy*, vol. 45, pp. 7–15, 2012.

[159] R. Eberhart and J. Kennedy, "A new optimizer using particle swarm theory," in *MHS'95. Proceedings of the Sixth International Symposium on Micro Machine and Human Science*, IEEE, 1995, 39–43.

[160] V. M. Sanchez, A. Chavez-Ramirez, S. M. Duron-Torres, J. Hernandez, L. Arriaga, and J. M. Ramirez, "Techno-economical optimization based on swarm intelligence algorithm for a stand-alone wind-photovoltaic-hydrogen power system at south-east region of mexico," *International journal of hydrogen energy*, vol. 39, no. 29, pp. 16646–16655, 2014.

[161] H. Baghaee, M. Mirsalim, G. Gharehpetian, and H. Talebi, "Reliability/cost-based multi-objective pareto optimal design of stand-alone wind/pv/fc generation microgrid system," *Energy*, vol. 115, pp. 1022–1041, 2016.

[162] D. Karaboga and B. Basturk, "On the performance of artificial bee colony (abc) algorithm," *Applied soft computing*, vol. 8, no. 1, pp. 687–697, 2008.

[163] D. Karaboga, "An idea based on honey bee swarm for numerical optimization," tech. rep., Technical report-tr06, Erciyes university, engineering faculty, computer , 2005.

[164] A. Maleki and A. Askarzadeh, "Artificial bee swarm optimization for optimum sizing of a stand-alone pv/wt/fc hybrid system considering lpsp concept," *Solar Energy*, vol. 107, pp. 227–235, 2014.

[165] H. Nasiraghdam and S. Jadid, "Optimal hybrid pv/wt/fc sizing and distribution system reconfiguration using multi-objective artificial bee colony (moabc) algorithm," *Solar Energy*, vol. 86, no. 10, pp. 3057–3071, 2012.

[166] Z. W. Geem, J. H. Kim, and G. V. Loganathan, "A new heuristic optimization algorithm: harmony search," *simulation*, vol. 76, no. 2, pp. 60–68, 2001.

[167] M. D. Brinda, A. Suresh, and M. Rashmi, "Optimal sizing and distribution system reconfiguration of hybrid fc/wt/pv system using cluster computing based on harmony search algorithm," *Cluster Computing*, pp. 1–6, 2018.

[168] E. Atashpaz-Gargari and C. Lucas, "Imperialist competitive algorithm: an algorithm for optimization inspired by imperialistic competition," in *2007 IEEE congress on evolutionary computation*, IEEE, 2007, 4661–4667.

[169] H. Gharavi, M. Ardehali, and S. Ghanbari-Tichi, "Imperial competitive algorithm optimization of fuzzy multi-objective design of a hybrid green power system with considerations for economics, reliability, and environmental emissions," *Renewable Energy*, vol. 78, pp. 427–437, 2015.

[170] A. Askarzadeh, "A discrete chaotic harmony search-based simulated annealing algorithm for optimum design of pv/wind hybrid system," *Solar Energy*, vol. 97, pp. 93–101, 2013.

[171] W. Zhang, A. Maleki, M. A. Rosen, and J. Liu, "Optimization with a simulated annealing algorithm of a hybrid system for renewable energy including battery and hydrogen storage," *Energy*, vol. 163, pp. 191–207, 2018.

[172] S. Ahmadi and S. Abdi, "Application of the hybrid big bang–big crunch algorithm for optimal sizing of a stand-alone hybrid pv/wind/battery system," *Solar Energy*, vol. 134, pp. 366–374, 2016.

[173] R. Siddaiah and R. Saini, "A review on planning, configurations, modeling and optimization techniques of hybrid renewable energy systems for off grid applications," *Renewable and Sustainable Energy Reviews*, vol. 58, pp. 376–396, 2016.

[174] A. Maleki, F. Pourfayaz, and M. A. Rosen, "A novel framework for optimal design of hybrid renewable energy-based autonomous energy systems: a case study for namin, iran," *Energy*, vol. 98, pp. 168–180, 2016.

[175] M. Sechilariu, B. Wang, and F. Locment, "Building integrated photovoltaic system with energy storage and smart grid communication," *IEEE Transactions on Industrial Electronics*, vol. 60, no. 4, pp. 1607–1618, 2012.

[176] J. Liang, T. Jing, O. Gomis-Bellmunt, J. Ekanayake, and N. Jenkins, "Operation and control of multiterminal hvdc transmission for offshore wind farms," *IEEE Transactions on Power Delivery*, vol. 26, no. 4, pp. 2596–2604, 2011.

[177] B. T. Patterson, "Dc, come home: Dc microgrids and the birth of the" enernet"," *IEEE Power and Energy Magazine*, vol. 10, no. 6, pp. 60–69, 2012.

[178] D. Salomonsson, L. Soder, and A. Sannino, "An adaptive control system for a dc microgrid for data centers," in *Industry Applications Conference, 2007. 42nd IAS Annual Meeting. Conference Record of the 2007 IEEE*, pp. 2414–2421, IEEE, 2007.

[179] D. Chen, L. Xu, and L. Yao, "Dc voltage variation based autonomous control of dc microgrids," *IEEE transactions on power delivery*, vol. 28, no. 2, pp. 637–648, 2013.

[180] A. Bracale, P. Caramiaa, G. Carpinelli, F. Mottola, and D. Proto, "A hybrid ac/dc smart grid to improve power quality and reliability," in *2012 IEEE International Energy Conference and Exhibition (ENERGYCON)*, pp. 507–514, IEEE, 2012.

[181] J. Zhu, *Optimization of power system operation*. John Wiley & Sons, 2015.

[182] A. Pizano-Martinez, C. R. Fuerte-Esquivel, H. Ambriz-Pérez, and E. Acha, "Modeling of vsc-based hvdc systems for a newton-raphson opf algorithm," *IEEE Transactions on Power Systems*, vol. 22, no. 4, pp. 1794–1803, 2007.

[183] M. Baradar, M. R. Hesamzadeh, and M. Ghandhari, "Second-order cone programming for optimal power flow in vsc-type ac-dc grids," *IEEE Transactions on Power Systems*, vol. 28, no. 4, pp. 4282–4291, 2013.

[184] C. Liu, B. Zhang, Y. Hou, F. F. Wu, and Y. Liu, "An improved approach for ac-dc power flow calculation with multi-infeed dc systems," *IEEE Transactions on Power Systems*, vol. 26, no. 2, pp. 862–869, 2010.

[185] D. O. Neacsu, *Switching Power Converters: Medium and High Power*. CRC Press, 2014.

[186] C. Lu, S. Chen, and C. Ing, "The incorporation of hvdc equations in optimal power flow methods using sequential quadratic programming techniques," *IEEE Transactions on Power Systems*, vol. 3, no. 3, pp. 1005–1011, 1988.

[187] U. De Martinis, F. Gagliardi, A. Losi, V. Mangoni, and F. Rossi, "Optimal load flow for electrical power systems with multiterminal hvdc links," in *IEE Proceedings C-Generation, Transmission and Distribution*, vol. 137, pp. 139–145, IET, 1990.

[188] A. Lotfjou, M. Shahidehpour, Y. Fu, and Z. Li, "Security-constrained unit commitment with ac/dc transmission systems," *IEEE Transactions on power systems*, vol. 25, no. 1, pp. 531–542, 2009.

[189] G. Y. Yang, G. Hovland, R. Majumder, and Z. Y. Dong, "Tcsc allocation based on line flow based equations via mixed-integer programming," *IEEE Transactions on power systems*, vol. 22, no. 4, pp. 2262–2269, 2007.

[190] H. Zhang, V. Vittal, G. T. Heydt, and J. Quintero, "A mixed-integer linear programming approach for multi-stage security-constrained transmission expansion planning," *IEEE Transactions on Power Systems*, vol. 27, no. 2, pp. 1125–1133, 2011.

[191] N. Alguacil, A. L. Motto, and A. J. Conejo, "Transmission expansion planning: A mixed-integer lp approach," *IEEE Transactions on Power Systems*, vol. 18, no. 3, pp. 1070–1077, 2003.

[192] M. ApS, "Mosek optimization suite," 2017.

[193] R. D. Zimmerman, C. E. Murillo-Sánchez, and R. J. Thomas, "Matpower: Steady-state operations, planning, and analysis tools for power systems research and education," *IEEE Transactions on power systems*, vol. 26, no. 1, pp. 12–19, 2010.

[194] G. W. Stagg and A. H. El-Abiad, *Computer methods in power system analysis*. McGraw-Hill, 1968.

[195] P. Haugland, "It's time to connect: Technical description of hvdc light® technology," *ABB Techincal Report*, 2008.

[196] F. Shang, Y. Liu, F. Shang, H. Liu, L. Kong, and L. Jiao, "A unified scalable equivalent formulation for schatten quasi-norms," *Mathematics*, vol. 8, no. 8, p. 1325, 2020.

[197] S. Aziznejad and M. Unser, "Duality mapping for schatten matrix norms," *Numerical Functional Analysis and Optimization*, pp. 1–17, 2021.

[198] W. D. Rosehart, C. A. Cañizares, and A. Vannelli, "Sequential methods in solving economic power flow problems," in *CCECE'97. Canadian Conference on Electrical and Computer Engineering. Engineering Innovation: Voyage of Discovery. Conference Proceedings*, vol. 1, pp. 281–284, IEEE, 1997.

[199] J. Lavaei and S. H. Low, "Zero duality gap in optimal power flow problem," *IEEE Transactions on Power Systems*, vol. 27, no. 1, pp. 92–107, 2011.

[200] B. C. Lesieutre, D. K. Molzahn, A. R. Borden, and C. L. DeMarco, "Examining the limits of the application of semidefinite programming to power flow problems," in *2011 49th annual Allerton conference on communication, control, and computing (Allerton)*, pp. 1492–1499, IEEE, 2011.

[201] C. L. Borges and J. M. Alves, "Power system real time operation based on security constrained optimal power flow and distributed processing," in *2007 IEEE Lausanne Power Tech*, pp. 960–965, IEEE, 2007.

[202] E. Dall'Anese, H. Zhu, and G. B. Giannakis, "Distributed optimal power flow for smart microgrids," *IEEE Transactions on Smart Grid*, vol. 4, no. 3, pp. 1464–1475, 2013.

[203] T. Erseghe, "Distributed optimal power flow using admm," *IEEE transactions on power systems*, vol. 29, no. 5, pp. 2370–2380, 2014.

Publications

[**J3**] Alzahrani, A. M., Zohdy, M., & Yan, B. **"An Overview of Optimization Approaches for Operation of Hybrid Distributed Energy Systems with Photovoltaic and Diesel Turbine Generator."** Electric Power Systems Research, 191, 106877, 2021.

[**J2**] Alzahrani, Abdullah M. and Mohamed Zohdy. **"Real-Time Performance Assessment of Operating Photovoltaic (PV) Systems."** Energy and Power Engineering, Vol.12. No. 6. 2020.

[**J1**] Talla Omar, Abdullah Alzahrani, and Mohamed Zohdy. **"Clustering Approach for Analyzing the Student's Efficiency and Performance Based on Data."** Journal of Data Analysis and Information Processing, Vol.8 No.3, Aug 2020.

[**C5**] F. Alrefaei, A. Alzahrani, H. Song, M. Zohdy and S. Alrefaei, **"Cyber Physical Systems, a New Challenge and Security Issue for the Aviation,"** IEEE International IOT, Electronics and Mechatronics Conference (IEMTRONICS), pp. 1-5, 2021.

[**C4**] Albira, Mohamed E., Abdullah Alzahrani, and Mohamed Zohdy. **" Model Predictive Control of DC-DC Buck-Boost Converter with Various Resistive Load Values."** Global Congress on Electrical Engineering (GC-ElecEng), IEEE, 2020.

[**C3**] M. E. Albira, A. Alzahrani and M. Zohdy, **"Model Predictive Speed Control of DC-DC Buck Converter Driven DC-motor with Various Load Torque Values,"** IEEE International IOT, Electronics and Mechatronics Conference (IEMTRONICS), Vancouver, BC, Canada, pp. 1-6, 2020.

[**C2**] F. Alrefaei, A. Alzahrani, H. Song and M. Zohdy, **"Security of Cyber Physical Systems: Vulnerabilities, Attacks and Countermeasure,"** IEEE International IOT, Electronics and Mechatronics Conference (IEMTRONICS), Vancouver, BC, Canada, pp. 1-6, 2020.

[**C1**] Alzahrani, Abdullah M., Rui Liu, and Jason R. Kolodziej. **"Acoustic Assessment of an End Mill for Analysis of Tool Wear."** PHM Society Conference. Vol. 10. No. 1. 2018.